An Investigation into the Thermal Field Associated with Typical Automobile Engine-Bay Flow Fields

by

Andrew Fleming

Dissertation submitted to the Faculty of Engineering, University of Glasgow

For the Degree of Doctor of Philosophy

November 2005

Preface

The work described herein was carried out by the author in the Department of Aerospace Engineering at the University of Glasgow during the period December 1999 to September 2004.

The Dissertation is original in content except where otherwise stated.

Andrew Fleming
November, 2005.

TABLE OF CONTENTS

LIST OF FIGURES

LIST OF TABLES

ACKNOWLEDGEMENTS

First and foremost, I would like to thank my supervisor, Prof R.A.McD Galbraith for his supervision over the course of this project. His unstinting support of this work has made it considerably more enjoyable than it might have been.

I would also like to thank former Research Fellow, Jingbin Yang, who guided the small group, including myself, based at the Acre Road facility.

I owe a debt of gratitude to everyone within the technical support staff and especially to Robert Gilmour (Research Technologist)

Thanks are also due to the management and staff of Kelvin International Systems of East Kilbride staff. The project would not have existed without the company involvement.

I would also like to thank my fellow Researcher, Wan An Sheng, for his support, exchange of ideas and good company.

Abstract

Computational Fluid Dynamics (CFD) modelling has been widely used within the automotive environment for areas such as the enhancement of the external aerodynamic performance of automobiles and the optimisation of the combustion process. More recently, however, the study of vehicle thermal management systems (VTMS), an area which encompasses the cooling, air conditioning and underhood airflow of vehicles, has embraced the use of CFD in an attempt to refine designs. Additionally, with continuing emphasis being placed on noise, vibration and harshness (NVH), engine design has tended towards neater, more integrated packages with a minimum of mechanical ancillaries; such as brackets. One of the significant aspects of this design philosophy is that there is now a proliferation of electronics in modern vehicles. One of the solutions to increasingly complex wiring harnesses has been to decentralize and migrate control units to the engine and the powertrain. This development has had consequent effects on environmental factors related to the powertrain control unit (PCU) itself. As increasingly strict legislation limits the kind of design solutions which may be employed to overcome these effects, the underhood area has had to be researched thoroughly.

For the work described herein, a CFD package and associated pre- and post-processors was used to assess the underhood flow characteristics with a view to determine the optimum positioning of these component packages. A further goal arose from the opportunity to check if the CFD package would be suitable for a non-specialist operator to use.

To achieve these goals, the underhood volume of a vehicle was modelled both numerically and experimentally. The experiments were carried out using a physical instrumented model in the smooth controlled flow of the Department's Handley Page wind tunnel. This provided the analogue model for a generic car, against which the

numerical results could be compared. The numerical modelling was performed using the commercial CFD package FLUENT 5.5.

It was envisaged that the data gained from the two models could be used to enhance current design procedures and influence future design methodologies in engine compartment layout, with regard to the placement of electronic devices. It may also serve to validate the integration of data provided by simulation and experiment.

It must be noted that the work was essentially an assessment of the usefulness of the methodology. Albeit the comparisons between CFD and experiment appear to possess significant differences, this early work illustrates the potential of the procedure and suggests the "follow-on" research that is required.

Acronyms and Abbreviations

ACIS – Native file format used by AutoCAD. Used in the course of this work for exchange between CAD (Computer Aided Draughting) package and CFD (Computational Fluid Dynamics) preprocessor.

ANSYS – Finite element solver

BATHfp – Univrsity of Bath cooling system simulation program

DRAG4D - Nissan CFD Software

ECU – Engine Control Unit. Microprocessor-based unit for adaptive control of automotive engines

ICE - Abbreviation used herein for Internal Combustion Engine, in variants, SI (Spark Ignition) and CI (Compression Ignition)

LDV - Laser Doppler Velocimetry

NVH – Noise, Vibration and Harshness. Term applied in comfort testing of automobiles

PCU – Powertrain Control Unit. Microprocessor-based unit for adaptive control of any combination of automotive engine, gearbox and transmission systems

PIV - Particle Image Velocimetry

PMMA - Polymethyl methacrylate (acrylic glass e.g. Perspex)

RPM – Rapid Prototyping Module (Imageware CAD modelling package)

SAE - Society of Automotive Engineers. Standards and Papers quoted herein.

SPICE – Simulation Program Integrated Circuit Emphasis

STREAM - Software Cradle Company cartesian solver

VECTIS - Ricardo CFD software

VINE 3D - General Motors CFD software

VTMS - Vehicle Thermal Management Systems. All encompassing term used to describe control of thermal conditions in engine bay, coolant, and passenger cabin.

Nomenclature

HP	Horsepower
T	Torque (Nm) (ft-lbf)
T_a	Axle torque (Nm) (ft-lbf)
T_f	Flywheel torque (Nm) (ft-lbf)
L_d	Drivetrain Losses (Nm) (ft-lbf)
Φ_w	Wheel Circumference (ft)
R_{tc}	Torque converter ratio
R_{tgr}	Transmission gear ratio
R_{fgr}	Final gear ratio
ρ	Fluid density (kg m^{-3})
μ	Kinematic fluid viscosity (m^2s)
υ	Fluid velocity (ms^{-1})
P	Wetted area
D_n	Notional diameter (irregular shape)

1. Introductory

1.1. Motivation

This project was first discussed with Kelvin International Solutions Ltd. (KIS) (1999) and, in collaboration with them, it was intended to develop a methodology for the proper placement of the engine control unit (ECU) in the automobile underhood environment. The importance of the environment to the ECU is manifest in the strict emissions requirements. It was envisaged that such a control unit would be tested *in situ* within a current production automobile and separately in environmental chambers. The experimental facility, located at the former National Engineering Laboratory Engine Test Division, would have allowed for the study of power fluctuations in an engine under load during predetermined duty cycles.

Over the first year, problems encountered with the set-up of this facility and subsequent developments within the company dictated a radical restructuring of the project. Nevertheless, the motivating factors which originally drove the project remained valid and the research contained herein reflects the need to develop an independent, inexpensive and efficient method of providing useful data for the road vehicle underbonnet thermal environment. This has become a major area of interest because of current environmental legislation. In addition, the proliferation of electronic devices demanded by recent consumer trends also has a significant effect on design in the underbonnet region.

The advent of strict environmental legislation, in particular the Clean Air Acts in the U.S that were introduced by the 1970s, in response to growing concern over the increasing level of industrial pollutants in the atmosphere, necessitated significant developmental changes in engine technology (Frank *et al.* 1998). The Clean Air Act of 1990 effectively

imposed the use of computerised diagnostics on all subsequently produced road vehicles in the U.S. In Europe, legislation pertaining to vehicle emissions was progressively introduced in the form of increasingly stringent EURO emissions laws. This has, consequently, affected vehicle under bonnet design (Emmelman and Berneburg, 1990).

In addition, consumer-driven computer technology increased the workload of the engine control systems. In many industrial applications controllers tend to be basic 8-bit microprocessors. In the automotive industry, however, 32-bit Reduced Instruction Set Computing (RISC) based controllers are now used routinely to handle the increased throughput of data (Frank *et al.* 1998).

As a consequence of the constraints imposed by the above major considerations and, to a lesser extent, 'sound pollution' issues, the packaging of electronic components, and their associated mechanical components in the engine compartment, became tighter. This was because more electronic subsystems and fixtures were introduced to meet consumer demands or to satisfy legislation.

Finally, engine compartment research was rarely pursued outwith commercial organisations and usually only as part of a major vehicle development programme. It was considered beneficial, therefore, to develop a test rig where research could be carried out independently within the confines of an academic research department. The design of such a rig and the placement of instrumentation is dependent on the airflows and the thermal effects around the engine components. This was a significant goal of the present work and the basic methodologies were developed, albeit further work is required.

1.2. Aims and Objectives

The work contained herein concerns the use of computational fluid dynamic (CFD) software and wind tunnel testing in the development of thermal modelling of car underhood flows. The main aim of the work was to create a design methodology for assessing underbonnet thermal conditions, to assist the placement of powertrain control units in such a way as to avoid any adverse effects on their performance. These PCU systems are an increasingly important constituent of vehicles and may contribute up to 35% of the vehicle's cost (Frank *et al.* 1998). Current trends, where some of the PCU functions are migrated onto the engine and transmission (DeVos and Helton, 2000), are motivated by a need for efficiency in manufacture and lower costs. It becomes apparent, therefore, that the placement of electronic components in the engine bay is an important design consideration and may even be critical.

The all-embracing term Vehicle Thermal Management Systems (VTMS) has come into general use for a range of areas, the two most significant of these are:-

- passive cooling by harnessing the aerodynamic effects of the underhood geometry;
- thermal effects imposed on automotive electronics and any associated performance degradation.

To assist in the assessment of the underhood environment, CFD has become an important tool. As CFD evolved, its application areas expanded to encompass a number of automotive flows where complex geometries would previously have been too expensive to compute in terms of computational hardware and/or time.

This work, therefore, complements several studies, which, in the recent past, have been carried out within the burgeoning field of VTMS research. These are discussed in detail in section 1.3.

For the project considered herein, the initial design, the subsequent development of the physical engine compartment and the placement of instrumentation was guided by the use of an industrial CFD software package, FLUENT 5.5. Solid models were created with a Computer Aided Draughting (CAD) package, AutoCAD, and these were exported to the FLUENT preprocessor, GAMBIT, for CFD grid generation. The grids were subsequently refined on the basis of results gained by use of FLUENT. FLUENT was chosen to ascertain whether a general engineering practitioner with no specialisation in fluid dynamics could produce reasonable results with a general purpose CFD package. This research, and the models created for it, formed part of a series of projects rarely pursued outwith industry. The integrated design methodology is specifically aimed at simplifying problems and reducing cost.

Equally important to this work was the use of the University's large section low speed wind tunnel facilities. The Department has the rare advantage of access to these facilities which can be employed to test models at an appropriate scale. In this case, the engine compartment was to have been incorporated into a 30% scale car model and tested in the Department's 2.65m x 2.04m 'Argyll' wind tunnel. However, for reasons discussed later, it was tested outwith the car body in the Department's 2.13m x 1.61m Handley Page wind tunnel. Further details on these facilities can be found in appendix 8.

Although the thrust of much CFD research relegates wind tunnel testing to the acquisition of data suitable for validating results, the aim herein was to combine the two technologies into one methodology within the development process. Both CFD and Experimental Fluid Dynamics (EFD) have advantages and limitations and, by taking

cognisance of these factors, it was hoped that a seamless development of the methodlogy, both physical and numerical, could be achieved so that design refinement, between development phases, could be rapidly implemented.

Although the inclusion of the engine compartment within a complete car model, developed for aerodynamic studies (Campbell *et al.* 2002) was originally proposed, it was decided that, due primarily to computational hardware limitations, the generic engine compartment would be tested separately. Although it is generally accepted that problems of this type cannot be treated in isolation, the combined use of EFD and CFD allows them to be decomposed, to some extent, so that data obtained from one part of the experiment can be used to set up boundary conditions for another which can then be examined in greater detail.

1.3. Literature Review

In a contemporary review of automotive CFD, Dhaubhadel (1996) provided a comprehensive summary of work done in the field and clearly illustrated the then state of the art. A more recent review by Bauer (2001), dealing with the computerized design process at Daimler Chrysler, served to illustrate subsequent progress over the intervening period as have the proceedings of the five Vehicle Thermal Management Systems (VTMS) conferences between 1993 and 2001. These references represent the reporting of the main developments in automotive CFD.

This literature review is hereafter subdivided into six sections: -

- Fluid Dynamic Studies
- Cooling Studies
- Electronics - General Automotive
- Electronics - PCU Specific
- Material Properties and Thermal Recording Studies
- Other Computer Studies

1.3.1. Fluid Dynamic Studies

In addition to the 1996 review by Dhaubhadel, other work within the Ford Motor Corporation, was reviewed and documented by the same author. Dhaubhadel and Shih (1996), presented studies for the validation of CFD. The latter of these dealt with a project based around a physical model of a simplified engine compartment within a simplified generic car. This project, called BOXCAR (figure 1-1), was used for the analyses and assessment of CFD codes. This simplified geometry was chosen because, as the author stated, "complex geometries are prohibitively expensive".

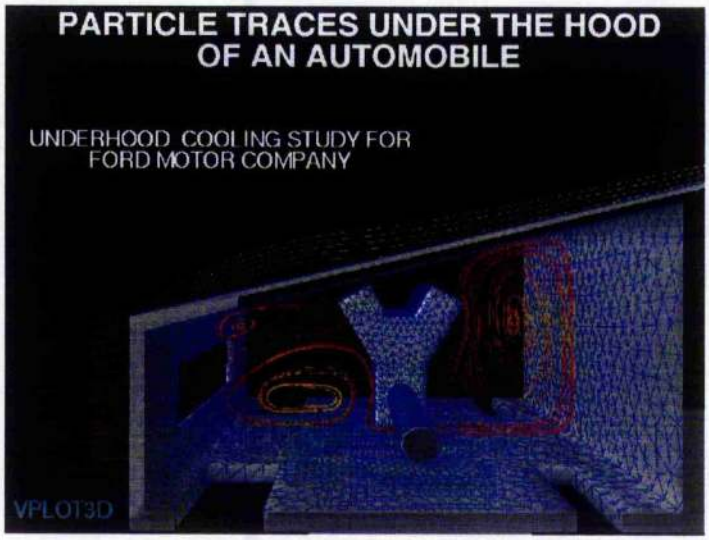

Figure 1-1 BOXCAR Project

This project also forms the basis of works by Paschal *et al.* (1996) and Shack *et al.* (1995). Both of these works were concerned with the experimental methods to acquire the appropriate data for CFD validation. It was noted, however, that despite the simplified generic engine compartment, the flows encountered were complex and highly three dimensional. This work was largely concerned with the velocity fields which were then subjected to experimental verification. There was, however, additional data from thermal studies, although the paper does not make clear if these were, or could have been, verified.

Both papers considered visualisation methods, in particular, particle image velocimetry (PIV) and laser doppler velocimetry (LDV) and reported good correlation between results obtained from these and the numerical analogues.

Earlier work, within Ford, dealt with the level of agreement between computational and experimental results (Hajiloo *et al.* 1990). This was found to be good for differing mesh densities. The paper served as background material to further work at Ford which specifically dealt with underhood airflow. Interestingly, that work used water tank

models to obtain the test data. The paper also discussed the factors that require consideration when using scale models as *per* Williams *et al.* (1991). Also at Ford, Li *et al.* (1993) presented experiments based on the ducting of underhood airflow, both under steady-state and transient conditions, and an unnamed method of representing this numerically. The work also made reference to the use of the EEC-IV[†] engine management module as a data gathering device in association with a datalogger. This is a particularly effective method of monitoring the ECU and would likely have been the preferred additional method for the present work had the project remained as originally envisaged. This type of monitoring should certainly be included for any future work which involves ECU placement.

Winnard *et al.* (1995) presented differing strategies for thermal management by underhood airflow control and investigated several operating conditions that may be experienced by a light truck including the case of power take-off to machinery such as farm implements. Although this is unlikely to be encountered in the operation of a car, an awareness of extreme and disparate duty cycles, such as these, is essential as many components are common throughout a vehicle range from a single manufacturer or associated group. It was concluded that, in typical operation, airflow management was sufficient but in extreme cases forced air cooling would be required.

The most recent work referenced from Ford, Ghani *et al.* (1999), dealt with water ingress and simulated environmental conditions (airborne moisture) by use of the commercial codes FLUENT and RAMPANT. A simple generic car geometry was used as a bluff body to validate results obtained in an environmental wind tunnel.

Research carried out by General Motors (GM) encompassed work by Opel and Pininfarina in Europe, Isuzu in Japan and Chevrolet/Pontiac in the US. Another

[†] EEC-IV is a standard engine control unit developed by Ford

significant division of GM involved was the computer services supplier, Electronic Data Systems (EDS). Aoki *et al.* (1990) dealt with the use of the 3D heat and flow analysis software package, STREAM, at GM Isuzu and gave a good description of numerical methods. More recently, however, Dohi *et al.* (1998) outlined the evolution of codes for CFD analysis and presented details of other packages, e.g StarCD, in addition to STREAM.

Focussing primarily on computer codes, work also emerged from the EDS division of GM. Ashmawey *et al.* (1993) described the lumped parameter method in CFD analysis. As it concerned the design of an actual production car, the 1993 Opel Vectra, he had to consider, due to stringent legislation, the practical implications on exhaust design of added underhood components (underbody cover, noise baffles, etc.). The study, while specific to this car, highlighted the tradeoffs in design when considering the positioning of components. Berneburg and Cogotti (1993) dealt with the effect of the drag coefficient (C_d) of underhood components and the effect that this had on the overall C_d of the vehicle. Experimental methods included the use of a newly designed test radiator and the control of underhood air vanes by stepper motor. Test data were obtained in the form of velocity fields by the used of LDV.

Emmelman and Berneburg (1990) discussed the impact of forthcoming legislation and presented the compromises involved in accommodating aerodynamic designs for low fuel consumption, environmental legislation and consumer driven trends in design.

The creation of a CFD model for a porous flow method using VINE-3D, one of the packages outlined in Ashmawey *et al.* (1993), was described by Han and Skynar (1992) together with a discussion on the selection of boundary conditions. Han *et al.* (1996) presented a more generalised discussion of computational versus experimental methods and concluded that, even in simple geometries, the CFD results benefit from denser

meshes but this increases the computational overhead. He also noted that 'the issue of turbulence models used for the computations is one that defies simple conclusions'. The complexity of the underhood geometry makes it difficult to decide on the most appropriate turbulence model.

As with General Motors, the package STREAM was also employed at Daihatsu along with other software tools to simulate 3D flow and heat transfer in an engine compartment (Katoh *et al.* 1991)

At Mercedes Benz, there were a number of studies carried out on in the field of CFD. The key area of interest to them was the computational platform since the work had its origins in the EUROPORT[1] CFD project. Bauer *et al.* (1995, 1996) dealt with the use of STAR-CD in underhood analyses and then addressed the scaleability of STAR-HPC over a number of processors using existing models. The work gave a good appraisal of the problems which can be encountered in using newly released codes on parallel systems. Reister and Ross (1997) dealt with the design of a cooling fan and emphasised the critical assumptions made in the development of a Multiple Reference Frame (MRF) model. The magazine Fluent News (Spring 1997) described an underhood thermal simulation carried out by Chrysler using Fluent/UNS in such a way so as to yield data for scalability on multi-processor platforms. The apparent similarity between this and the work of Bauer *et al.* (1996) suggests that the two activities might well be integrated since Daimler Benz and Chrysler have merged. This fan modelling is a useful area to consider as it was originally envisaged as part of the current project and should be included in any future work.

At Nissan, Minegishi *et al.* (1993) addressed the practicalities of the modelling process using the package DRAG4D but the observations made are applicable to other packages.

[1] EUROPORT – Research carried out by German High Performance Computing Centre

In this work, experiments were described that considered the collection of data in engine idle and shutoff conditions. Good agreement between numerical solutions and test data, at the majority of test positions, was obtained for all cases. Further work was carried out on an upwind differencing scheme that was used to consider the effects of flow around a vehicle and through its engine compartment (Ono 1992). They also created a test model, of a prototype vehicle, with simplified geometry. This was used to consider such details as the licence plate and it was concluded that these seemingly minor details tended to have a significant effect on the flow simulation. Joint work between Nissan and NEC was described on the NEC supercomputing applications website describing details of a full body aerodynamic simulation comprising 12,000,000 elements (figure 1-2). This work dates from 1998 and illustrated the contemporary state of the art at Nissan before the merger with Renault.

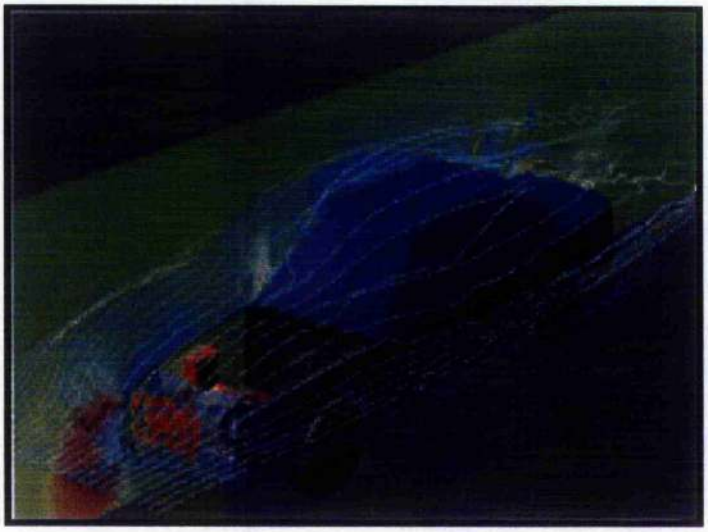

Figure 1-2 Nissan Full Body Simulation (ref. NEC)

Gilliéron *et al.* (1999) created a 2,300,000 element model, where the computational domain comprised the wind tunnel up to central pillar of a car. Results from this simulation were compared with results for actual car in Pininfarina wind tunnel. They concluded that the greatest errors found in a simplified model of an actual car were found in the most geometrically complex areas.

Shimonosono *et al.* (1993) described the use of an acrylic glass (PMMA) model to observe the effects of flow control devices. This was done in conjunction with a CAD modelled mesh of approximately 250,000 nodes. It was observed that temperatures were up to 10°C lower at the rear of the engine and concluded that thermal flow analysis was useful in engine compartment design, although it was stated, "in actuality, it is impossible to create a grid fine enough to reproduce an actual engine precisely". This reflects the complexity associated with the geometries in the underhood area and underlines the importance of simplified generic models when validating results.

Stevens *et al.* (1999) carried out work addressing the difficulties associated with improving underhood airflow prediction using the software codes VECTIS CFD and Imageware RPM (Rapid Prototyping Module). They also considered the interaction of a 1-D thermal model and a 3-D airflow model. The experimental technique used LDA and they provided a discussion of probe placement. This wide ranging study also considered the inclusion of louvres in the vehicle undertray to improve airflow while retaining sound deadening performance. They concluded that their numerical solutions were validated by LDA but added that accuracy would be improved when details such as the layout of the wiring loom and the behaviour of the unpowered fan were taken into account.

Software and experimental methods were described by Kataoka *et al.* (1991) for work considering the effects of different aerodynamic devices such as spoilers and underbody covers.

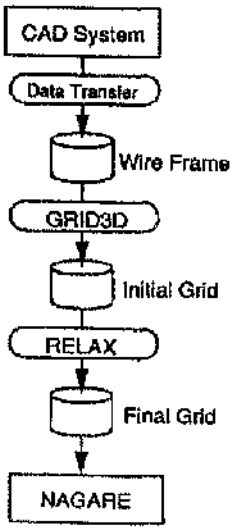

Figure 1-3 CAD Data Transfer to CFD Data (ref Katnoka 1991)

Foremost amongst the methods described was the use of a computational grid-generation system whereby the CAD model of a car body was converted, via two stage process, to a grid for use in a CFD code (figure 1-3). They concluded that the data derived from numerical simulations was satisfactory for practical use, that the complex shapes of aerodynamic devices could be modelled accurately and that by using a quick grid generating system, 'acrodynamic prediction by calculation becomes much faster than experiment'. This work was subsequently extended and reviewed by Sakai (1993).

Draper and Haidar (1999), in work carried out for Daewoo, investigated the effect of bumper design on the cooling of a van and presented a detailed appraisal of the software used, primarily STAR-CD.

At the University of Tokyo, the use of the 'SIMPLE' (Semi-Implicit Method for Pressure-Linked Equations) algorithm for the construction of simplified-shape models was explored in an attempt to significantly reduce CPU time (Taniguchi *et al.* 1991). Albeit modern computer power is far greater than that used in their study, it is still a relevant concern today. This is addressed in their findings where, although results almost

agree between numerically simulated and experimentally derived data, there is difficulty in simulating flow separation at small angular steps. They also noted that the Reynolds Stress Model may have to be adopted when dealing with strong vortices.

1.3.2. Cooling System Studies

Saunders and Udvary (1991), at the Royal Melbourne Institute of Technology, carried out a feasibility study which dealt with the main environmental conditions associated with thermal management, namely ram-air and heat soak. Particularly interesting in their paper was the use of a truncated car with an external coolant supply. This, they stated, was used to counteract blockage problems in their wind tunnel facility. They concluded that their experimental method was valid and would reduce the time for wind tunnel and heat soak testing. They also considered the number plate size and location and concluded that it was a significant factor in the cooling airflow; as was had been the case in the numerical simulations of Ono (1992).

Ishikawa *et al.* (1999) dealt with the determination of engine component temperatures and considered ways in which changes to component layout could be assessed, by computer modelling, and so improved. Similarly, Shibata *et al.* (1993) used a numerically simulated engine compartment to aid the design of a new cooling system.

Couetouse and Gentile (1992) at Renault dealt specifically with the cooling system using a useful experimental method that had remote data sensing. This study indicated that underhood airflow management significantly affects the cooling system and, if well conditioned, has associated performance benefits in terms of fuel efficiency.

Blisset and Austin (1999) used FLOWMASTER software to predict the thermal behaviour of individually customisable components and considered the effects of the cooling system fluids from startup. Directly relevant to the project herein is the description of the generation of a PTMU (PowerTrain Management Unit) component (i.e. PCU). An outcome of this work was a case study in the application of FLOWMASTER which they made available on the company's website. They concluded that this application would be of use to non-expert users when considering operating conditions dictated by legislation.

Ap *et al.* (1999), at Valeo, devised a simulated engine cooling model from which he was able to propose a new radiator cooling coefficient. The coefficient, which was found to be a useful parameter, was formulated in terms of the cooling system components. During his experiments he made use of micropropellors and fan shrouds. Also at Valeo, earlier work by Smith (1993) outlined the development of software for predicting cooling module performance using models of various cooling related components.

Sidders and Tilley (1997), University of Bath, modelled the cooling system through a 'lumped parameter' computer simulation using the BATHfp code. This method was described as using a library of conditions.

Jung *et al.* (1991), Korea Institute of Technology, investigated the detrimental effect on engine cooling from front end designs of modern vehicles and considered the selection of equations and velocity measuring points during their experiments. They concluded that, while a fast method for generating data, '2D computation may not be an efficient tool for the accurate prediction of flow field inside the engine compartment'.

1.3.3. Electronics Studies (General Automotive)

A report from Toyota by Igarishi (1986) on contemporary sensor technology lists a number of sensors which, although at the time were novel, are now widely used. For example, the particular focus of this work, which has influenced the aims of the present project, is the outlining of the extremes of inertial and thermal conditions encountered in automotive applications. Table 1-1 reproduced from this paper outlines the predicted requirements in sensor applications.

Purpose	Function	Objects of detection	Type of sensor to be used
Reliability	Self-diagnosis. Automatic detection of correction	Change with time Deterioration	Standard (time) + sensors, Memory + sensors
Safety	Detection of abnormality Self-diagnosis Detection of obstacles	Impossible to drive (functional deterioration or breakdown of major part.) Electromagnetic interference Road condition Object recognition	(Engine / Drive train – Overall), Tyre pressure, Brake pressure, Intensity of electrolysis, Ultrasound, laser, infrared, electro-magnetic wave
Lowering fuel consumption	Optimum A/F ratio control (ignition timing, exhaust gas), Lean combustion	Theoretical A/F ratio A/F ratio (real-time) Knocking Drive train	A/F, 02, NO~, CO Flow rate (air, fuel) Pressure (absolute, gauge, atmospheric) Knock, vibration, acceleration, torque Displacement, angle, Revolution
Comfort	Qualititative, display of ride, comfort, Sun-visor and interior temperature Humidity control Fatigue detection	Vibration and noise around seats, Width of vision, Amount of total sunlight Room environment, Relation between fatigue and physiological parameters	Speed, acceleration, hardness of seats, Amount of light, Skin temperature, Mean room temperature (multipoints) Humidity, dew-point Odor, pulse, blood pressure, breathing, oxygen concentration in blood

Table 1-1 Sensors required for automobiles in the future (from Igarishi 1986)

Similarly, Kobayashi (1996), at Nissan, presented an assessment of the properties of sensor materials. He concluded that the distinctive nature of sensor materials had to be considered in their selection when applied in diverse environmental conditions.

Matsuda (1991), also dealt with sensor properties, and presented a useful discussion of the harshness of the underhood environment and included not only thermal and mechanical factors but also the decline in functionality of sensors via the corrosive

effects of chemical processes. One of the conclusions outlined in this work was that passive heat management was not useful in heat soak conditions. This work is particularly relevant when one considers that Sumitomo Wiring submitted a United States patent (US5789704) in 1998 describing a housing for automotive electronic components specifically designed to deal with the harsh environmental conditions encountered in the engine compartment.

Kern and Ambros (1997) at Behr discussed the use of sensors and actuators to provide active engine cooling and presented actuator control strategies to effect a number of desired goals. These were mostly concerned with improving fuel consumption and enhancing the reliability of components. They concluded that active thermal management provides significant benefits particularly in commercial vehicles.

1.3.4. Electronics Studies (Powertrain Control Unit)

At Visteon, a subsidiary of Ford, work was carried out to evolve a methodology for the optimum placement of electronic components within a powertrain control unit, the EEC-IV, by bespoke software and commercially available code (Torossian and Lanphear 1990). Also at Visteon, Luettgen (1998) discussed the transient thermal analysis of power electronics and predicted the behaviour of heat sinks by reference to their thermal properties. The importance of the positioning of individual components within the PCU was addressed by Delphi Electronics (DeVos and Helton, 2000). This work outlined the typical underhood conditions that a powertrain control unit will be subject to, because of modern design considerations that are necessitating the migration of these units away from the bulkhead and onto the powertrain. The studies were concerned with such aspects of the underhood environment as temperature, NVH and moisture. Figure1-4,

reproduced from this paper, shows typical temperatures likely to be experienced in the engine compartment.

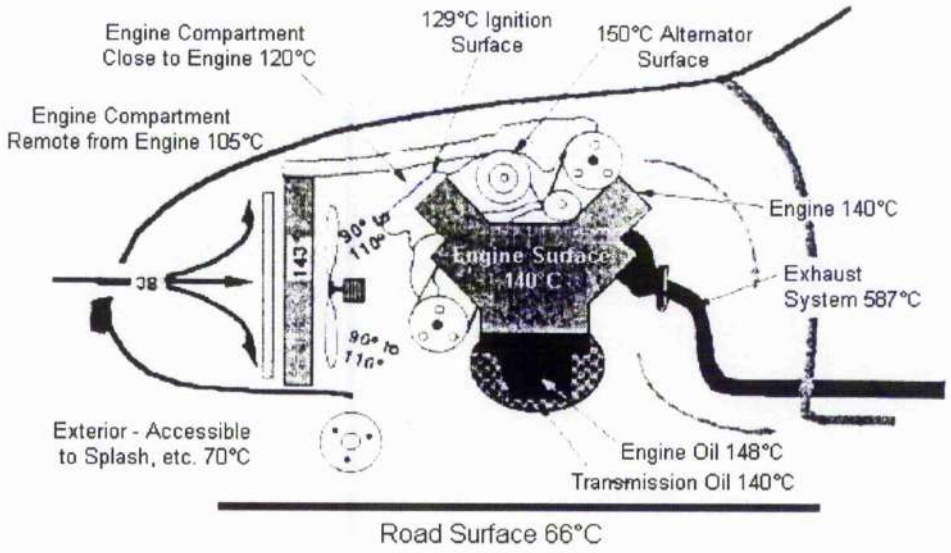

Figure 1-4 Typical Surface Temperatures (DeVos and Helton, 2000)

This diagram was also made available on the DuPont company website where it was used in a presentation illustrating the use of ceramic materials within the automotive industry. This additional source gave a broad overview of the hostile environments encountered in the underhood area, namely, 'temperature extremes, vibration, shock, exposure to dirt and contaminants, moisture, chemicals, radiation and gases.' In addition the hardware changes brought about by the following system changes are outlined.

- Tougher emission standards
- More complex diagnostics
- Direct injection
- Higher temperature operation
- Improved fuel economy
- Electromechanical evolving to solid state
- Functional/component integration
- Mechatronics (example: electromagnetic valve actuation)

Figure 1-5, also from DeVos and Helton (2000), shows two strategies for the placement of underhood powertrain control modules. The integrated strategy, where there is a single site selected for one overall controller is shown on the left of the figure. In contrast, the distributed strategy is shown on the right and clearly illustrates the migration of dedicated controllers to specific areas on the powertrain.

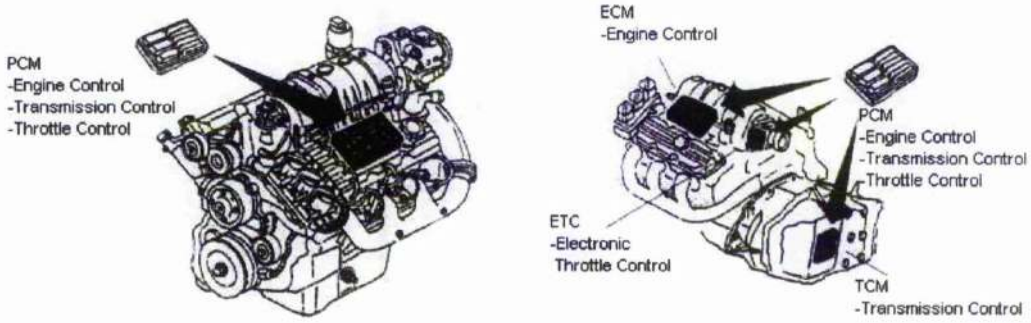

Figure 1-5 PCU Placement Strategies (De Vos and Helton, 2000)

The aforementioned information regarding the likely environmental operating conditions at specific points within the engine compartment were of use in the development of this project. The temperature rating of components was discussed with regard to cost factors when these are used in volume. Another significant issue which was addressed was the physical size of some uprated components. Other issues which may arise, due to the individual temperature rating of components within the PCU, were addressed and included the current carrying capacity of pin connections. As the main emphasis was on the PCU placement strategies themselves, the conclusion was that a hybrid distributed/integrated strategy would be the most beneficial. It was noted, however, that there was a significant design time overhead. Similarly, the temperature rating of individual components, comprising typical automotive electronics, was addressed within a review by Berger (2002). In that review much emphasis was placed on the uprating of components. Typically qualification of semiconductors based on junction temperatures had risen from 150°C in the 1980s to 175°C currently, with a further rise to 200°C envisaged. In this case, liquid cooling systems may be added to electronic modules.

Although it was noted that actual unit costs would be increased, this would be offset by the reduction in time of the expensive design process.

Agarwal and Gschwend (1997) investigated the thermal effects, both steady state and transient, on a powertrain control module. Their experiments provided data for the validation of a numerical simulation. The test technique included the use of infra-red (IR) sensing. Krishna (1997) referred to the environmental effects on a car audio system and described the experimental methods (thermal stickers were used in addition to more traditional thermocouples) and their correlation with cases simulated with the package, FLOTHERM. From a number of cases dealing with venting patterns and the use of forced and natural convection, they concluded that the package FLOTHERM could be used with confidence.

The review by Frank *et al.* (1998), also referred to in section 1.1 discussed the role of semiconductors in powertrain control and outlined the background to the subject matter in addition to presenting statistics regarding market growth. This work presented information regarding I/R measurement and data on the ZYTEK PCU design.

Brandt *et al.* (1993) dealt with power dissipation in a PCU and models were created using SPICE (Simulation Program Integrated Circuit Emphasis) and ANSYS. In addition, problems relating to air conditioning were outlined. Although this paper is concerned with the use of FEA (Finite Element Analysis) and power modelling, the vehicle test methods employ both environmental chambers and chassis dynamometer. As this was the initially proposed test method for the current project, and there are similarities between the data logging methods used in the initial tests, the experimental method they presented is highly relevant. Additionally, there is a good description of a traditional PCU placement and the severity of thermal conditions due to restricted

airflow. The summary suggests, however, that there are limitations in the thermal modelling methods available when considering packaging of the PCU

1.3.5. Material Properties and Thermal Recording Studies

Hartsock *et al.* (1997) were concerned with devising a standardised test procedure for evaluating heat shield materials and associated designs. They presented a discussion of the problems associated with the thermal properties of multi-modal materials used in instrumentation. Their experiments used a custom test rig featuring 'Fire Rods' (trade name for heating element) in a manner similar to the present project. They concluded that tests should be carried out for worst case emissivity and at higher temperatures similar to typical operating conditions. This is a significant conclusion especially for the present work which has strong similarities.

Pierson and Johnson (1993), although specifically concerned with the behaviour of automotive batteries, provided a good account of the procedures required for controlled temperature experiments that could be applied to any electronic system. Specifically, the use of environmental chambers for accurate analyses of the number of test cycles until component failure. A discussion regarding heat management during engine-off high temperature conditions was useful as it highlighted the effects of the hostile engine environment in the operating life of components. Again, as the paper is concerned with the longevity of the battery, there is a very specific focus, but the observations, regarding passive/active cooling methods and the financial cost of repositioning components, are applicable to any study concerned with engine compartment thermal mangement.

Selow *et al.* (1997) gave a contemporary review of techniques that could be employed in the construction of a virtual vehicle for thermal analysis. Using the system

FLOWMASTER an overview was given of the crucial parameters to be observed; subsystem interaction was also discussed. They concluded that it was feasible to model the thermal actions in vehicle sub-systems and planned to incorporate CFD into their work for modelling interior and underhood cabin flows. As they note "...[this] is seen to be of great importance due to the need for improving underhood thermal management."

Zhao *et al.* (1992) illustrated the use of I/R imaging for the Ricardo Hydra experimental cylinder head as a means of thermal sensing during the engine warm-up phase. Data were derived by computer analyses of the video images and were deemed to be 'invaluable in the development of engine heat-transfer and warm-up models'. There was some discussion of the problems associated with heat transfer to the silicon viewing window but as this study dealt with combustion temperatures in the range of 1000°C these problems would be mitigated in the study of underhood areas.

Gupta (1993), University of Michigan, Flint, reviewed the trends in materials used in automotive thermal management. He noted that as modern designs forced underhood temperatures to rise, there was not only a consequent risk of corrosion and oxidation of cast iron and ferrous components, but also the risks of softening, melting and flammability of plastic and elastomeric components. They concluded that to alleviate the need for more expensive production materials, both spark ignition (SI) and compression ignition (CI) engines would require thermal management to eliminate 'hot-spots'.

1.3.6. Other Material Reviewed

This section summarises work primarily associated with layout and packaging of underhood components. In addition, it contains detail regarding factors affecting decision-making during the design process.

Banerjee (1993), University of Illinois, presented an 'agent-based-systems' (ABS) method for the rapid analysis of underhood design with regard to component shape. It also discussed the information required for the weighting of solutions with regard to the interdependence of components, design for manufacture and assembly (DFMA) and the need for access during maintenance. Although this study did not specifically refer to underhood environmental conditions, it brought to light other issues pertaining to the placement of components and concluded that the ABS method offered rapid evaluation of component packaging in comparison to traditional manual methods.

Hyslop *et al.* (1999), University of Loughborough, presented a review of computer tools for the packaging of electro-mechanical systems and also noted that ABS methods were a powerful and flexible tool for data transfer between design tools. Although this paper was primarily concerned with military and aerospace products it is included in this review as it considers environmental problems more fully than Banerjee (1993) and includes parameters such as electromagnetic and radio frequency interference in addition to space constraints and thermal management. One of the conclusions to emerge from this review, however, was that the complexity of decoupling some solutions dictated that some systems could not be considered in isolation.

Rubin *et al.* (1997), University of Wisconsin Powertrain Control Research Lab, dealt with the hierarchy of components in computer models of the powertrain. They included examples of the use of simulated data being read by the ECU during the experimental phase. The use also of simulated data from the ECU to the engine was discussed and they concluded that the use of powertrain modelling as a 'hardware-in-the-loop' tool would reduce the design cycle cost.

In addition to the descriptions of work in the papers noted above, a number of other sources were used for background information. Primarily, articles and editorials from Automotive Engineering and Electronics Cooling magazines and a number of WWW based presentations noted below:-

- **Argonne National Laboratories**: web presentation contained a good deal of background material in the use of CFD for the development of Hybrid Electric Vehicles, where, arguably, cooling is even more crucial than in more traditional SI and CI engined vehicles.
- **Du Pont Industries**: Although primarily concerned with ceramic materials this site contained a good discussion of underhood conditions and concluded that thermal problems pose the greatest challenge.
- **Europort**: This site presented a good deal of background on Daimler Chrysler's involvement with the German supercomputing facility.
- **COMPAQ**: Similarly, the COMPAQ site includes some background into the use of the CFD packages Fluent and AVL-Fire by PSA Peugeot Citroën on high performance computers.

1.4. Conclusions

The studies described above provided the background for this research. The disparate nature of the disciplines outlined serves to illustrate the significance of the project.

Many papers amongst those reviewed illustrated the variety of experimental methods employed, either in the confirmation of CFD results or for the purposes of data gathering. As a whole, much of the literature reviewed, highlighted the practicalities of each experiment and the trade-offs that have to be accepted in the realisation of projects through the design phase and onto manufacturing.

An appreciation of various aspects outlined such as the economic factors involved in the product design cycle and the issues of manufacturability and serviceability is essential in research which hopes to be applicable to practical, 'real-world' situations.

In addition, the use of high performance, parallel architectures for CFD studies is becoming the accepted method when considering complex geometries. Finally, the increasing use of an algorithmic approach to the placement of components may herald an integrated approach to vehicle underhood design.

2. Experimental Investigations

2.1. Introduction

This section deals with the development of the experimental parts of the project from initial power and thermal tests on road cars at the premises of KIS Ltd. to the development of a model engine compartment and its associated instrumentation for wind tunnel testing.

The placement of the instrumentation shown in this chapter is described in section 3.5.4 and was based on the initial CFD investigations of section 3.5.3. It will be appreciated that there was simultaneous development of the experimental test rig and the subsequent CFD simulations.

2.2. Initial Investigations and Testing

During the period spent with KIS Ltd. at East Kilbride (October 2000 – July 2001), the process of recommissioning test equipment from the former National Engineering Laboratory's Engine Research Centre was undertaken so that full scale automotive testing could begin. This equipment had been decommissioned on a previous closure of the facility and, although the equipment around the chassis dynamometer remained *in-situ*, many other items had been disconnected and placed in storage.

This equipment consisted of gas analysers, thermocouple rigs and engine or chassis dynamometer that could either be used independently or in unison, depending on the desired test type. It was intended to use the gas analysis equipment and so institute an

integrated testing regime. This was not to be, however, because the only remaining member of the original NEL research group, whose specialism was in chemistry, and in particular the gas analysers, left. For the purposes of this study, therefore, only the thermocouple rig and chassis dynamometer were used simultaneously.

The initial experiments considered the power requirements during transient performance testing of the vehicle. To this end, the chassis dynamometer and thermocouple rig were employed to gather torque and temperature data. These data were collected in anticipation of the planned testing of *in situ* PCUs and of PCUs in environmental chambers.

2.2.1. Chassis Dynamometer

Figure 2-1, below, shows the chassis dynamometer room at KIS Ltd. The boom to the left of the door is part of the 16 channel thermocouple rig.

Figure 2-1 Chassis Dynamometer

The dynamometer was originally built to the specification of NEL and consisted of a Telma electric absorber employing a Consine Dynamics controller. During initial testing, this controller was found to intermittently select the failsafe mode. This had the unfortunate effect of leaving the rollers either in the raised or lowered position. As a consequence of this, the controller was subsequently decoupled, though still usable, and a second controller (Ricardo TA3000) was employed. This latter controller was used for torque measurement whilst the original controller was used only for roller positioning at the start of each test. By using this method the failsafe mode could not be activated.

As noted above, the chassis dynamometer was used for a number of tests and it was investigated as to whether it would be of use in evaluating transient power fluctuations. The power fluctuations of interest were those of the engine. In other words, the transient power available at the flywheel. The dynamometer, however, simply measures the power at the driving wheels. It is essential, therefore, to have a means by which flywheel torque could be derived from the that measured at the wheels.

Traditionally, UK and US automotive engineering states the measure of torque in ft/lbf, with the power, as HorsePower (HP), given by

$$HP = \frac{TN}{5252}$$

where T = torque (in ft/lbf) and N=revolutions per minute.

The dynamometer returned the HP of the wheel drive axle and hence the axle torque could be calculated from the equation above. Torque could then be converted from ft/lbf to Nm by a conversion factor of 1.356. To relate this torque to that available at the flywheel it is normal to use a semi-empirical formulation. Jones (1999) offers the following formula:

$$T_a = T_f R_{tc} R_{tgr} R_{fgr} + L_J$$

where T_a = axle torque and T_f = flywheel (or flexplate) torque, R_{tc} = torque converter effective torque multiplication (1 for manual), R_{tgr} = transmission gear ratio (e.g. 3 for a 3:1 ratio), R_{fgr} = final drive gear ratio and L_d= drivetrain torque losses due to friction in transmission, rear end, wheel bearings, torque converter slippage, etc.

The drivetrain losses, rather than having a discreet value as noted above, can be otherwise described as a proportion of the overall power and the following formula (Jones 1999) can be obtained.

$$T_f = (1+L_d)T_f R_{tc} R_{tgr} R_{fgr}$$

This can be arranged in terms of flywheel torque as

$$T_f = \left(\frac{T_a}{1+L_d}\right)\left(\frac{1}{R_{tc} R_{tgr} R_{fgr}}\right)$$

which is more in keeping with the SAE (Society of Automotive Engineers) standard for deriving flywheel torque from a known axle torque, wherein a constant of 85%is used to represent drivetrain losses in a rear wheel drive car with manual transmission.

The calculation method used at KIS Ltd. was similarly derived and a 15% efficiency co-efficient was used to give the following equation, in which the torque converter term is not included as all cars tested were manual transmission models.

$$T_f = 1.15\frac{T_a}{R_{tgr} R_{fgr}}$$

T_a, in turn, being derived from the torque measured at the rollers by way of the following formula.:

$$T_e = \frac{16.81 \Phi_w T_{rr} 60}{5280}$$

Where T_{rr} is torque at the rollers, Φ_w is the wheel circumference in feet and 16.81 is an empirical constant used to derive true road speed from roller rpm.

Initial tests with this equipment showed a good correlation with published torque figures over a wide range of vehicles tested. For the purposes of the research, however, it did not give a resolution which could adequately monitor performance fluctuations caused by the electronics. The reasons for this were threefold:

1. Wheel torque, in general, is considerably greater than flywheel torque and increases in lower gears. Typically, a midrange gear would be used on the chassis dynamometer to allow for a broader engine rpm range (this is simply because of an upper speed restriction of 100mph on the dynamometer). This requires the chassis dynamometer controller to be set to a fairly coarse resolution, in this case, 0.5lbft (0.678Nm) at the wheels.
2. Extended testing on the chassis dynamometer was not practical. The manual for this particular facility instructed that the maximum session time should be no more than 20 minutes; due to overheating in the retarder. In practice when vehicles were generating close to the maximum specified torque of 1250Nm, retarder efficiency was noticeably impaired as overheating occurred and, in these cases, test sessions had to be limited to less than 10 minutes.
3. Another problem that affected the chassis dynamometer was the fact that flywheel torque was calculated from wheel torque. There are a number of common standards used to assess the flywheel torque. A typical example being SAE J1349. There are a number of other methods in common use including those conforming to ISO (International Standards Organisation) and DIN (Deutsche Industrie Norm) standards. The common feature of these standards is the requirement of a reference air temperature and barometric pressure. Other

factors can include humidity and altitude. These factors do not simply affect the engine, they affect all fluids within the vehicle and the interaction between the tyre and the roller. The deformation of the tyre can also be accommodated by estimates and, more importantly, drivetrain efficiency is frequently represented by an estimated percentage. So, while results for flywheel torque are repeatable, they are fundamentally notional and not suited to examination of a device which will only produce small, but significant, fluctuations; except in the case of component failure.

This caused the author to conclude that the proposed methodology was tending to an ill-conditioned experiment. Nonetheless, work continued for a short while until the abovementioned chassis dynamometer was conclusively demonstrated as inappropriate for the intended research. Whilst a better engine dynamometer could have been used, the basic difficulties would have remained resulting in a complex and expensive undertaking. A few of these difficulties are discussed in more detail in Chapter 5.

2.2.2. Thermocouple Rig

Combined tests were carried out to gain torque and temperature values on a Morgan Plus 8. As the car belonged to client of KIS Ltd., testing which would have required alterations to the bonnet section was decided against. The system had the capacity to record 16 channels of data, however, only the temperatures at the following positions were recorded:-

1. sensor 1 Engine temperature front
2. sensor 2 Exhaust manifold right bank central
3. sensor 3 Engine temperature rear @ bulkhead
4. sensor 4 Exhaust temperature rear pipe right bank

Condition	Sensor number 1	2	3	4
no fan	61°C	550°C	75°C	202°C
fan @ 3ft	40°C	530°C	40°C	184°C
fan @15ft	37°C	540°C	51°C	202°C

Table 2-1 Recorded Temperatures for Morgan Plus 8

Typically, however, in production testing, a more thorough test would include measurement of the following areas:

- Oil temp at sump
- Oil temp at oil cooler
- Air temp at air intake / before turbo inlet
- Air temp at intake manifold
- Air temp in test cell (Ambient)
- Air temp before/after air cooler if fitted
- Exhaust temp at exhaust outlet pipe
- Exhaust temp at exhaust
- Fuel temp at fuel return line
- Water In (usually before water pump)
- Water out (after thermostat - returning to radiator / header tank)

Figure 2-2 shows temperature testing on a Morgan Plus 8. During this test, although not obvious from the figure, the car was being run on the chassis dynamometer with the rear wheels on the rollers.

Figure 2-2 Morgan Plus 8 Data Acquisition

It should be noted that the small fan shown here was not intended to provide accurate airflow, it was simply there to provide an air draught for cooling purposes.

2.3. Revised Approach to the Problem

A review of the project became necessary when access to a full scale vehicle and, more importantly, the facility's availability became problematic then unavailable. It was, therefore, decided that testing would continue within the University on a generic 30% scale model. It was hoped that thermal testing of PCUs in environmental chambers would be undertaken by KIS Ltd. and the results obtained from this could be incorporated into the wind tunnel experiments carried out on a new engine compartment. This also became impracticable due to extended contract negotiations and company restructuring.

The focus of the project, therefore, shifted to a consideration of the flow patterns and temperature profiles inside an engine compartment. The project eventually became one of assessing the ability of a commercial CFD package to predict the underbonnet environment and so its value to the design process and the placement of the PCU's components. This goal was achieved by designing, incrementally (as discussed in Chapter 3) a generic engine compartment, including an engine block and exhaust pipe modelling, and then testing it in a wind tunnel. The data collected would then be compared with the CFD prediction both preliminary, and adjusted to meet the new flow conditions of the wind tunnel. If the CFD could adequately predict the measured data then the entire flow field information would be available to guide the PCU placements.

2.3.1. Some Basic Considerations

The revised approach required the placement of a scaled car model and associated engine compartment within the Argyle wind tunnel. Of particular relevance was the engine compartment and its contents. This required careful consideration of the CFD limitations and the actual thermofluid dynamics of the internal flows.

The resultant engine compartment was designed to accomodate a generic engine block and exhausts. These last two components are illustrated by the CAD drawing in figure 2-3. The results of the earlier work, carried out at KIS Ltd., indicated that the temperatures of the engine block and exhausts should be broadly similar to those reported by other authors in chapter 1. That is, 400K and 800K, respectively.

Accordingly, the preliminary CFD simulations (chapter 3) were conducted using these temperatures and were used to guide the transducer placement.

Although, when the wind tunnel tests were conducted, the difficulties experienced in maintaining the above temperatures resulted in the use of 600K and 360K temperatures, it was considered that the predominant aspects of the flow would remain. As such, only the magnitudes of the temperature contours would alter. The transducer placement would still be acceptable.

As noted above, the work was to employ a 30% scale car model, with an instrumented engine compartment, mounted and tested in the Department's Argyle wind tunnel. Time and resource constraints, however, further curtailed the work to such an extent that only the engine compartment was mounted on the models chassis and tested in the Department's smaller Handley Page wind tunnel. A fortuitous consequence of this,

however, was that the engine compartment's insulation, to protect the model car body, would also act as an insulator from the internal to the external flow. For the numerical simulation no flow existed over the engine compartment.

It was assumed, initially, that the downpipe temperature would be the most critical but after further consideration it was decided that the cowl (figure 2-3) should also be monitored, as this was an area most likely to exhibit substantial variance.

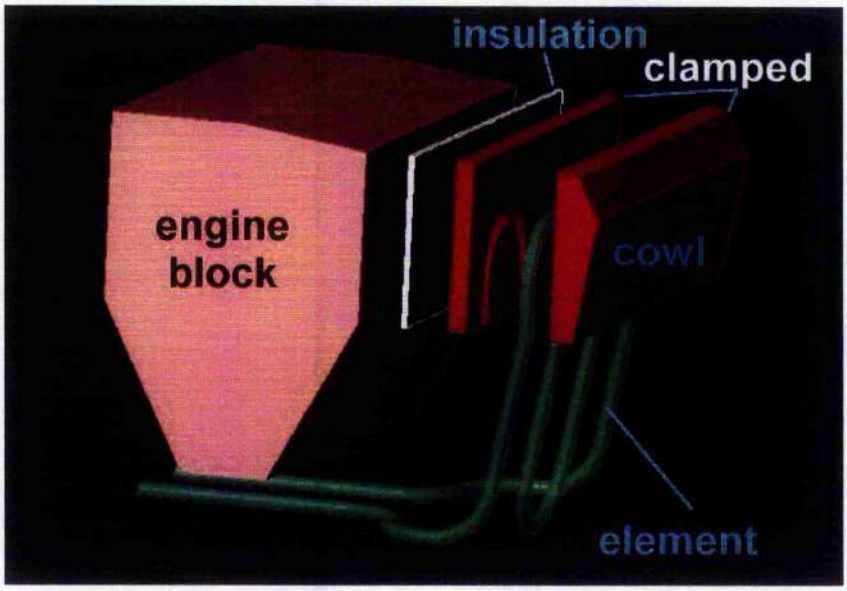

Figure 2-3 CAD 3D Representation of Engine Block (Exploded View)

2.4. Car Model

The car model, as originally envisaged (see appendix 3 for details), was to have included a realistic fibreglass front section to mount the engine compartment within. Although a model was constructed, with the help of the present author, and successfully tested in a different series of experiments (Sheng 2003, Bisset 2002), time constraints dictated that that the engine compartment be tested, mounted only on the car model's baseplate.

Taking into account the assumptions outlined above, however, the actual geometry of this model was considered not to be too significant.

2.4.1. Generic Engine Compartment

The design of the engine compartment (drawings are given in appendix 3) was based around the geometry used for the car model. The model itself comprised a foam body and it was envisaged that a front section in fibreglass would house the engine compartment.

Figure 2-4 Physical Model of Engine Compartment

The engine compartment model derived from the CAD models shown in the following chapter in figures 3-14 and 3-15 was fashioned from 6mm aluminium plate. Two views are presented here in figure 2-4. The cutaways shown in the panels were originally designed with a view to using acrylic glass panels to carry out thermal imaging (see section 5.4.1). To this end, the possibility of mounting an IR camera within the cowling

of the wind tunnel balance was investigated. Although acrylic glass is less opaque to the IR spectrum than conventional glass it was subsequently deemed inappropriate to use it in an experiment where it would have been not only a less than ideal viewing medium, but also a possible fire risk. As the same would also have been true for less IR opaque PMMA formulations and the fabrication of a panel in an IR transmissible glass such as silicon or germanium dioxide would have been prohibitively expensive, for the purposes of this research, it was deemed appropriate to use more conventional methods. The cutaways were thereafter used to mount replaceable instrumentation panels.

The engine compartment model was attached to an aluminium baseplate / chassis as shown in figure 2-5. In this figure, the front of the model is to the right hand side and the obvious cutaway represents the open outflow for the engine compartment. The car body, that would have been used, is shown in figure2-6 and the access for fixing the baseplate can be clearly seen along the lower outside edge, as can the cutaway for the connecting strut to the support gantry.

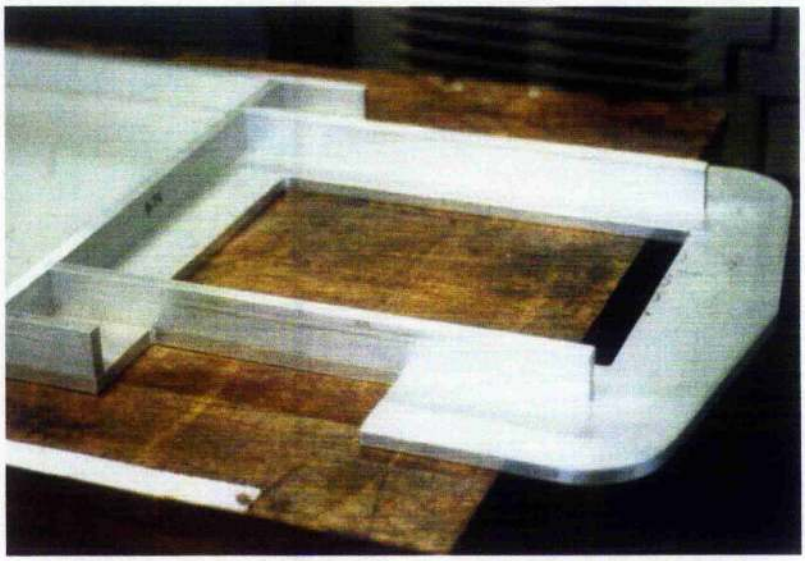

Figure 2-5 Car Chassis Showing Strengthening Ribs and Cutaway

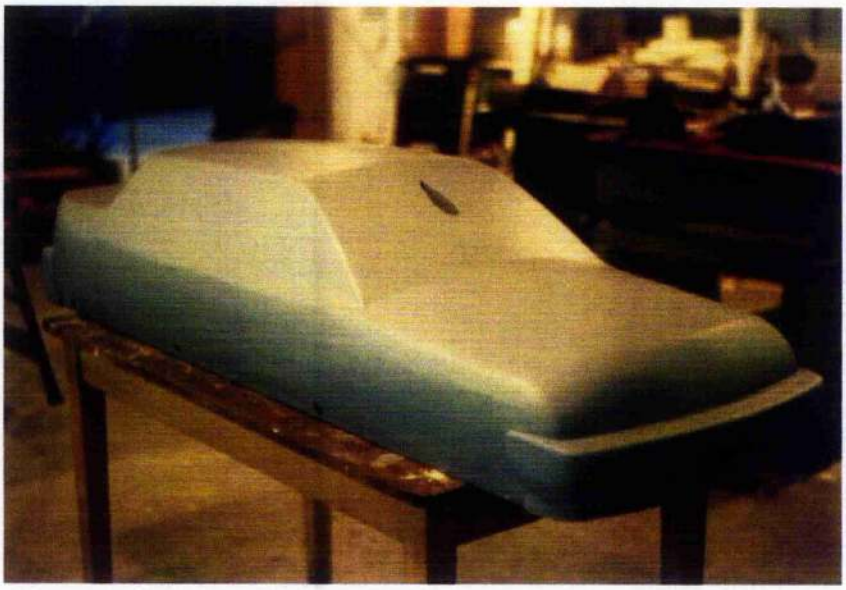

Figure 2-6 Car Body in Foam

The physical simulation of the exhaust heat source was by the use of a 2kW flexible heater fashioned into a realistic pattern as shown in green in figure 2-3. This was a similar method to that described by Hartsock (1997), although in that case the heater element was not open to the air. As the heater element has a diameter of 7.9 mm and this equates to around 26mm at the full scale, it was decided that enclosing the element as described in that research would bring it too far out of scale and would also cause manufacturing problems

Figure 2-7 illustrates the engine block, cowling and exhaust pipes mounted on the baseplate, all in place inside the wind tunnel working section. The block was heated by a single 1.5kW heating element and controlled thermostatically to 107°C (380K), reproducing the constant temperature boundary condition for this area which was used in the initial CFD investigations.

The possibility of uneven temperature contours was overcome by filling the block with granular material in a similar fashion to a storage heater thus providing a large constant temperature heat sink/source. This, however, required that the engine block be heated and brought up to temperature prior to the experiment taking place. The exhaust element was attached to the engine block as shown schematically in figure 2-3. This assembly was then mounted on the baseplate. This is clearly shown in figure 2-7.

5 K-type thermocouples (appendix 4) were used on the inner surfaces of the engine block to monitor temperature and provide feedback to an IR32 industrial temperature controller, which incorporated a compensated thermocouple cold junction.

K-type thermocouples were also used used on the cowl and downpipe to provide feedback for a similar controller.

Figure 2-7 Engine Block and Element *in situ* (without engine compartment)

2.4.2. Wind Tunnel

Although the companion series of experiments that concerned the external flow over and under the car models were carried out in the Argyll wind tunnel (Sheng 2003), the engine compartment specific experiments were carried out in the Handley Page wind tunnel. This was not as originally planned but occurred due to the constraints mentioned above. The differences between these two facilities are primarily size and the lack of a moving ground in the latter tunnel. Further details on these and other facilities are available in appendix 8. Fortunately, the work of Sheng (2003) clearly indicated that the lack of a moving ground would not be detrimental to the present authors work.

2.4.3. Thermal Instrumentation

The thermal instrumentation consisted of series of 31 thermistors arranged as shown in figure 2-8.

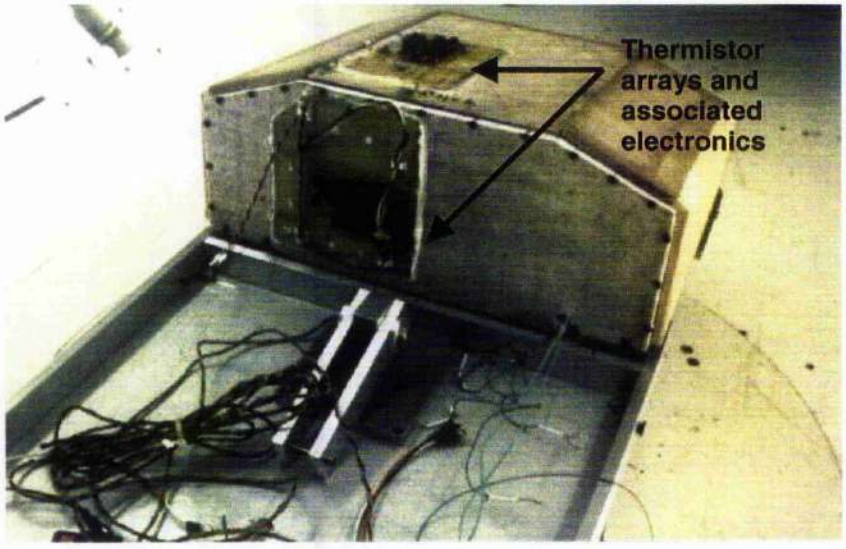

Figure 2-8 Thermistor Array and Circuitry

Their placement is not clear as the figure predominantly illustrates the position of the circuit boards and associated wiring. The thermistor positions can be more clearly seen in figure 2-9 as dark dots on the top and back of the engine compartment.

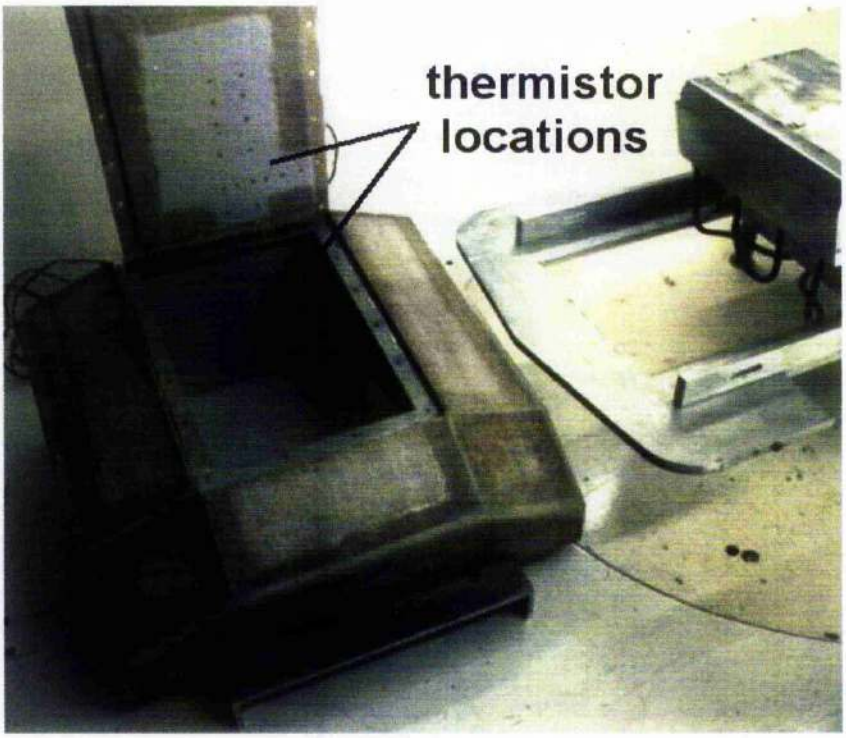

Figure 2-9 Sensor Positioning in Physical Model

The top panel sensors are more discernible than the rear panel. The front section of the engine block is also shown in this figure but its mounted configuration on the baseplate is more clearly seen in figure 2-7.

A clearer indication of positioning is given in figures 2.11, 2.12 and 2.13 and tables 2.2 and 2.3. The detail and reasoning behind the transducer location is based on initial CFD investigations for geometry based on the drawings for this model and is dealt with in sections 3.53 and 3.5.4 of the following chapter. The following chapter 3 deals primarily

with the development of the CFD work for this project. It will be appreciated that after the initial CFD work was used to guide the placement of the transducers that, subsequently, there was simultaneous development of both the experimental rig and the further, more detailed, CFD work.

sensor number	co-ordinate(mm) x	y	z	sensor number	co-ordinate(mm) x	y	z
back 01	491	155	-152	back 09	491	105	-152
back 02	491	205	-152	back 10	491	80	-152
back 03	491	225	-152	back 11	491	65	-152
back 04	491	155	-130	back 12	491	50	-152
back 05	491	155	-110	back 13	491	80	-130
back 06	491	155	-70	back 14	491	80	-110
back 07	491	155	0	back 15	491	80	-70
back 08	491	80	0				

Table 2-2 Rear Sensor Positions

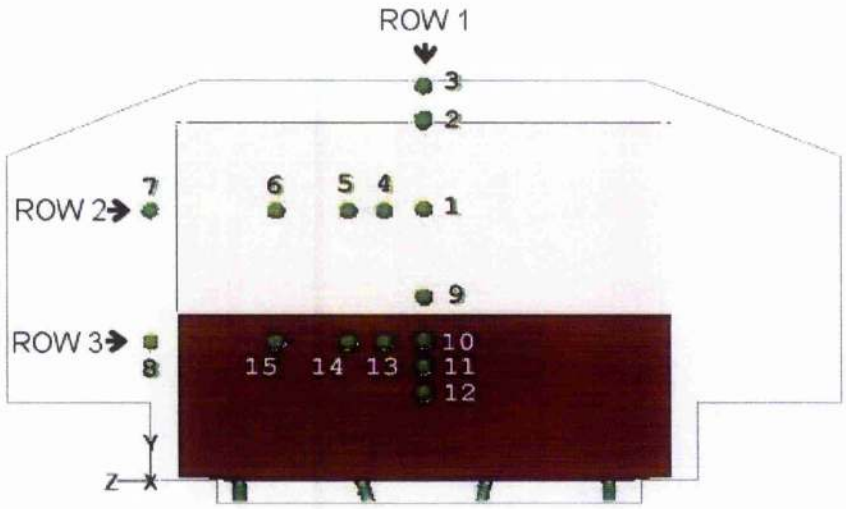

Figure 2-10 Orthogonal View (looking forward) of Rear Sensors Numbered and Showing Engine Block Position

sensor number	co-ordinate(mm) x	y	z	sensor number	co-ordinate(mm) x	y	z
top 01	370	213.8	-118	top 09	415	219.6	-152
top 02	370	213.8	-152	top 10	450	223.9	-152
top 03	330	208.8	-152	top 11	415	219.6	-137
top 04	330	208.8	-118	top 12	415	219.6	-118
top 05	300	205	-152	top 13	450	223.9	-118
top 06	275	202.4	-152	top 14	415	219.6	-105
top 07	300	205	-118	top 15	415	219.6	-85
top 08	275	202.4	-118	top 16	415	219.6	-63

Table 2-3 Top Sensor Positions

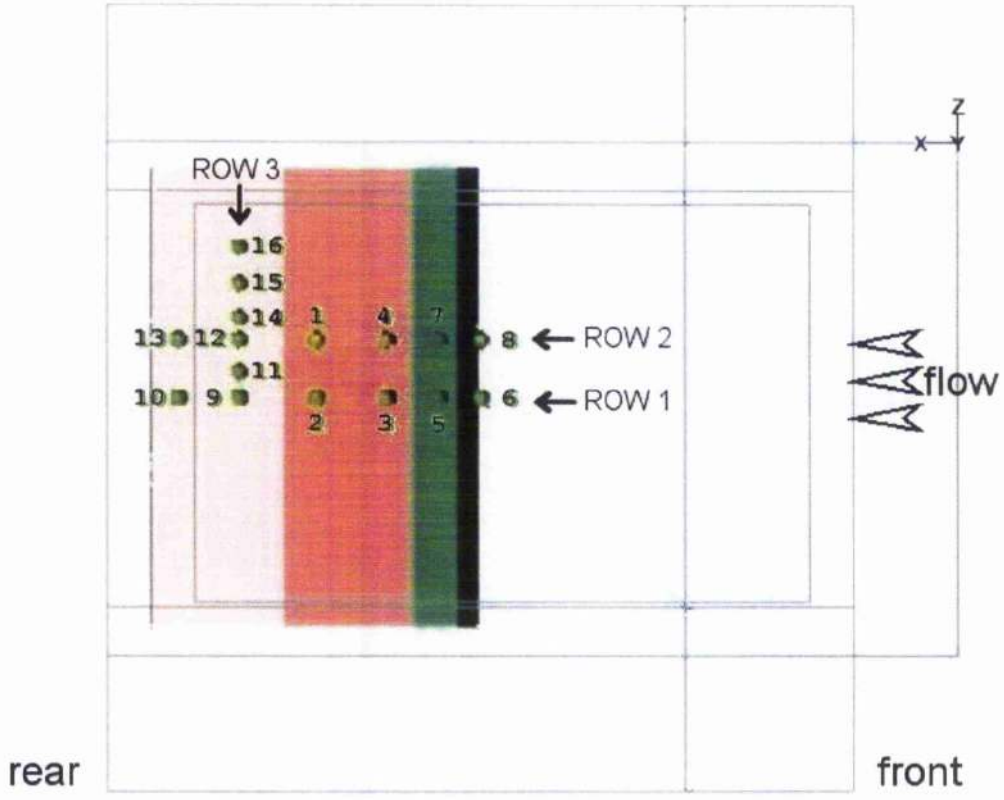

Figure 2-11 Orthogonal View of Top Sensors Numbered and Showing Engine Block Position

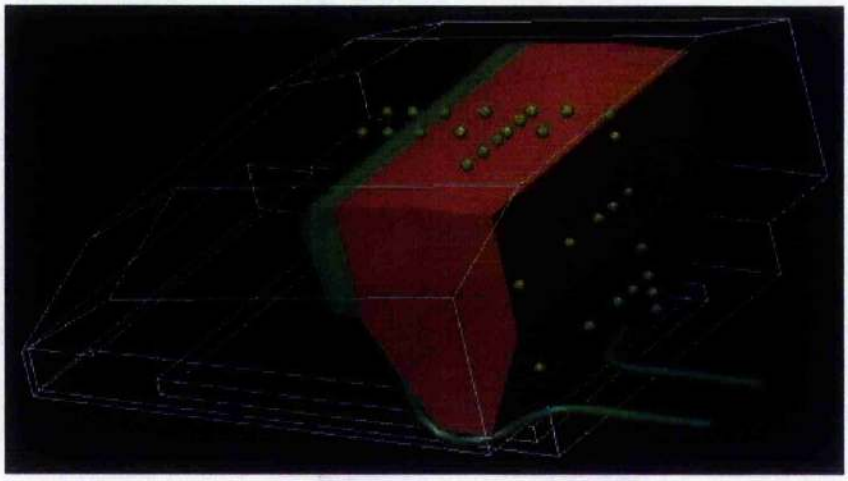

Figure 2-12 3D View of Sensor Positions

G-type thermistors (appendix 4) were chosen because of their low cost, availability and accuracy within the temperature range anticipated. Data were acquired using LabView (appendix 6) routines. Correction co-efficients for the thermocouples were included within these routines and were verified by experiment. Data acquired in this manner was then saved in Excel format for comparison with results obtained from the CFD simulations.

As noted in section 2.4.1, K-type thermocouples were used to provide feedback for the control of both heat sources although as wind tunnel velocity increased it was found that the flexible heating element cooled to such an extent that power was effectively constant at the maximum level in these cases. The values recorded from the thermocouples at the top of the engine block, the cowl and the downpipe were also saved to file.

As noted in the previous chapter, the full body was not available for this experiment and so only the engine compartment mounted on the baseplate was used as shown below in figure 2-13.

Figure 2-13 Engine Compartment and Baseplate

The whole configuration was then mounted in the Handley Page wind tunnel, as shown in figure 2-14, where the geometric blockage was 4.1%. (i.e model's frontal area as a percentage of the tunnel's working section's cross-sectional area)

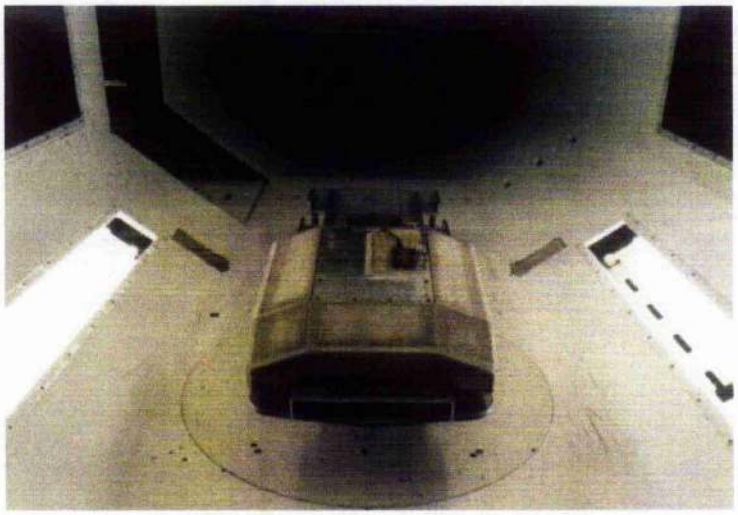

Figure 2-14 Model in Handley Page Wind Tunnel

2.5. Experimental Method

2.5.1. Wind Tunnel Procedure

Before each test, the engine block and exhausts were monitored to ensure that the desired temperature had been achieved. Readings from thermocouples and thermistors were taken for a range of airspeeds of $5ms^{-1}$ to $20ms^{-1}$ at $2.5ms^{-1}$ increments. These represented full scale speeds from 18 to 72 km/h assuming that the kinematic viscosity of air for both the full scale car and model were the same.

When airspeed had stabilised, temperatures for the thermocouples located at the downpipe, cowl and engine block locations were visually monitored and recorded manually. Airspeed was also recorded manually. A picture of the instrumentation used to monitor the experiment is given in Figure 2-15.

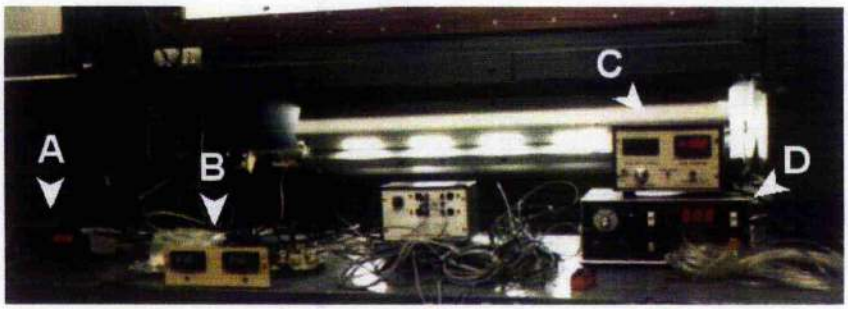

Figure 2-15 Monitoring Instrumentation

In this figure (A) denotes a switchable meter used to monitor the thermocouples within the engine block so that any temperature differentials could be noted and (B) shows the paired IR32 controllers used for the control of the heating elements used to represent the engine block and downpipes. These instruments are shown below in greater detail in figure 2-16. (C) indicates wind tunnel temperature and (D) indicates wind tunnel speed

via pressure readings within the tunnel. Output from (B) was recorded automatically to file, (C) and (D) were manually recorded and readings from (A) were used only to monitor and confirm the state of the engine block temperatures.

Figure 2-16 Temperature Controllers

Thermistor readings were recorded automatically as described in section 2.5.2.

2.5.2. Data Collection

Again, when the airspeed had stabilised, the Labview data acquisition program logged the thermistor data across 16 channels at 100Hz for 1 second. Separate files of data were created for the top and rear groups of sensors. A schematic of the control and data acquisition for the experiment is shown below in figure 2-17.

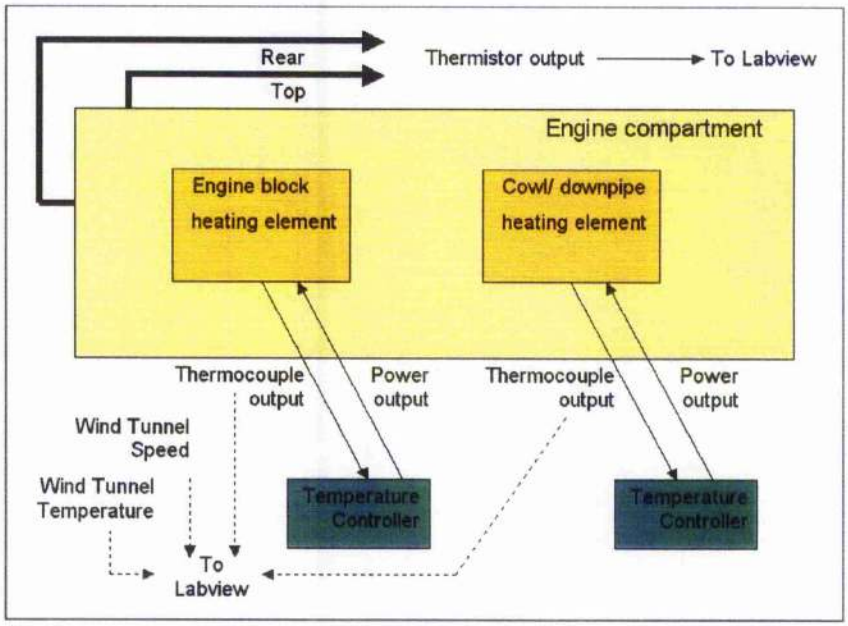

Figure 2-17 Schematic of Experiment

The manually recorded data for airspeed temperatures data for engine block, manifold and downpipe temperatures were saved to file along with the

2.5.3. Data Processing

Data files were imported into Excel for data reduction. Data were visually checked for anomalies and, for each sensor, an average reading of the 100 samples was used. Only 6 readings from 21700 were more than 0.5°C different to the adjacent reading and none of the recorded data showed more than 2.1°C variance.

To illustrate this, consider the two longitudinal banks and one lateral bank of sensors on the top surface as illustrated in figure 2-11 for a flow speed of $5ms^{-1}$. Figures 2-18 to 2-20 demonstrate the consistent nature of the data; the legend represents the sensor

number. These illustrate the thermistor readings for the $5ms^{-1}$ case. This case has been chosen to illustrate the worst single data 'spike' and this, when averaged out, was deemed to be insignificant. For the sensors chosen, their precise location is unimportant as the data are intended to show the nature of the data recorded.

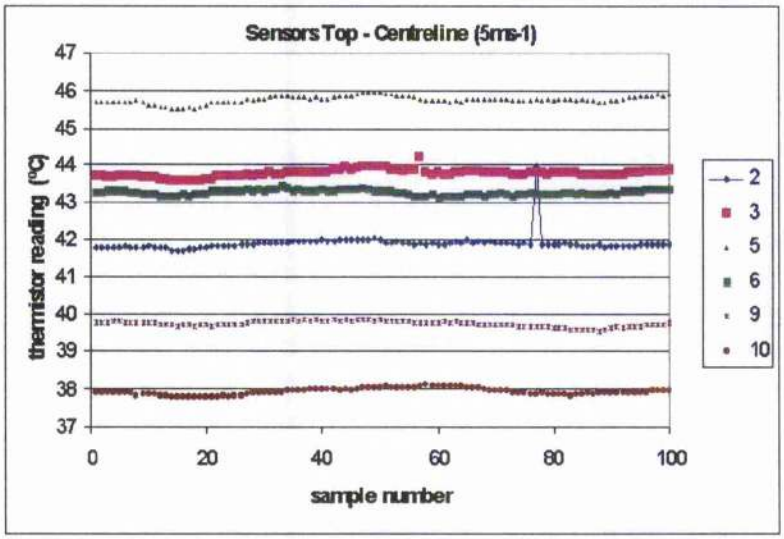

Figure 2-18 Thermistor Raw Data - $5ms^{-1}$ - Top Centreline

Similar data were recorded for the other upper surface sensors thermistors as depicted in figures 2-19 and 2-20. Once again there are no gross temperature fluctuations which would invalidate the averaging process and subsequent discussions.

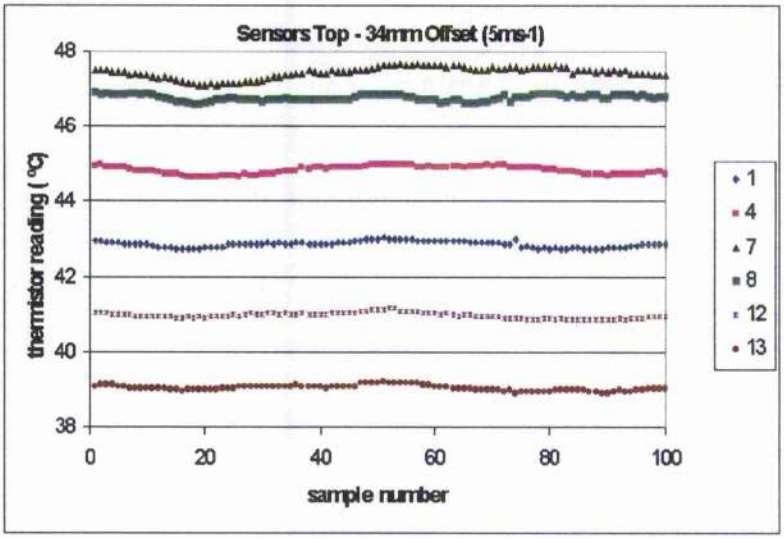

Figure 2-19 Thermistor Raw Data - 5ms^{-1} - Top Offset 34mm

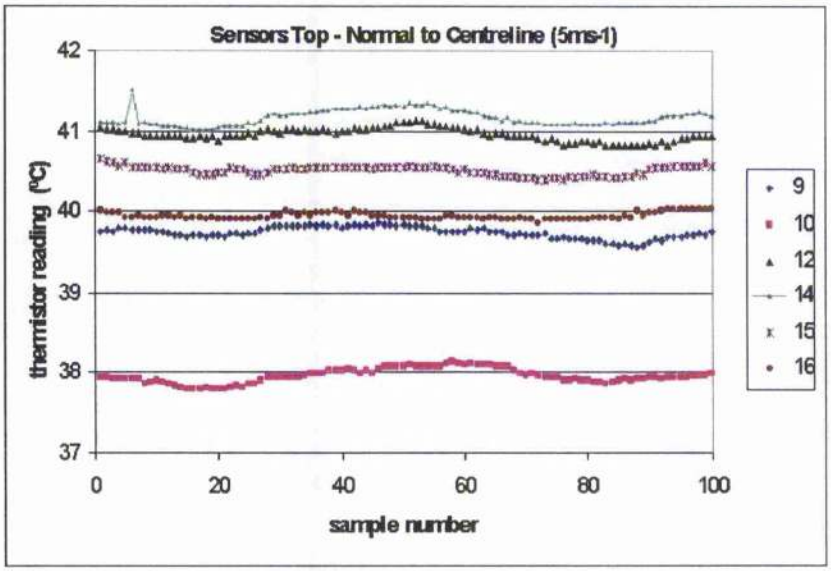

Figure 2-20 Thermistor Raw Data - 5ms^{-1} - Top Lateral

2.6. Experimental Results

Experimental data presented in this section were derived from reduction of raw data as described in section 2.5.3.

2.6.1. Rear Surface of Engine Compartment

This section presents the measured data taken from the thermistors on the rear face of the engine compartment. Whilst the distribution of, and primary row locations, are illustrated in figures 2-10 and 2-11, their precise locations (tables 2.2 and 2.3) are again given in tables 2-4 to 2-6 for ease of reading. Each table is for a specific row of sensors and their associated numbering is shown.

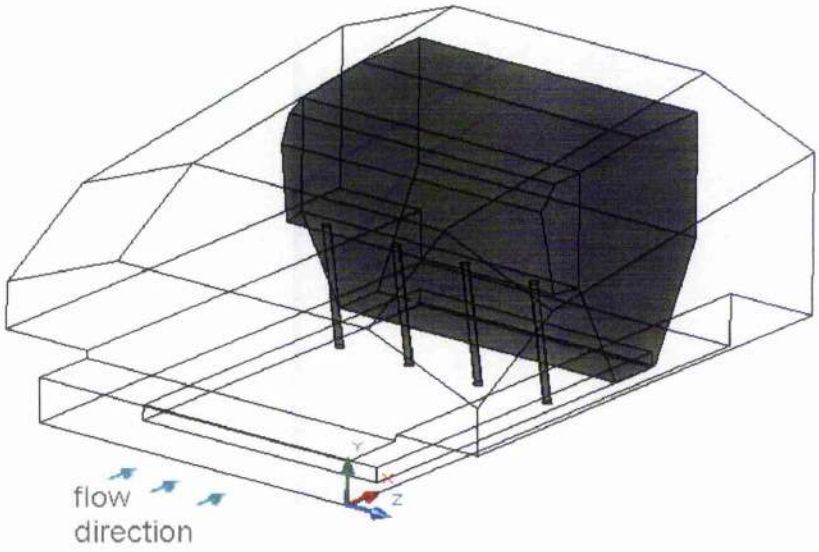

Figure 2-21 Wireframe of CAD Model Showing Data Origin and Flow Direction

The co-ordinate system origin is located at the bottom left of the entrance to the engine compartment and for clarity it is illustrated above in figure 2-21.

Whilst the following tables contain the quantitative data in numeric form, they are presented graphically in figures 2-23 to 2-25. To assist with the visualisation of the sensor positions, the schematic in figure 2-22 is used hereafter. As this represents the sensor positions as viewed from the rear of the engine compartment, the axes are offset for clarity.

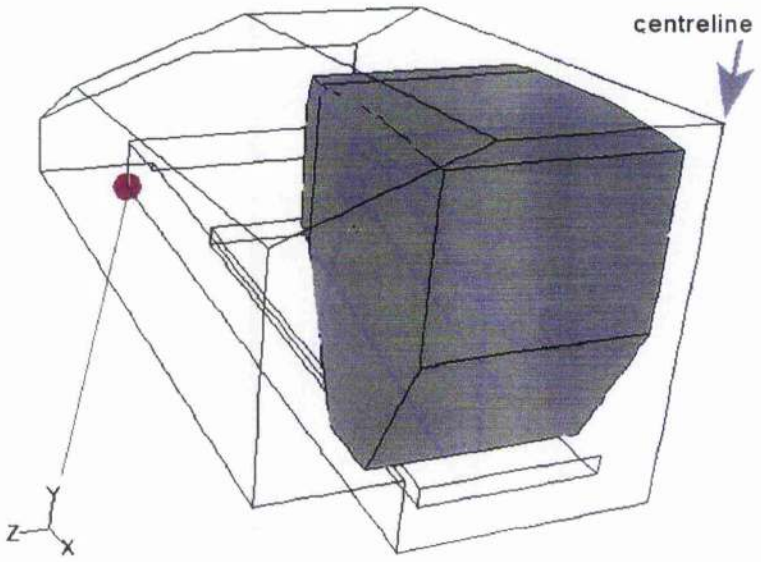

Figure 2-22 Schematic Showing Offset Axes

The data are most interesting for they indicate well defined but different trends. For example, for all three rows of sensors, as the tunnel speed increases the temperatures fall; as is to be expected. Also noticeable is the decrease in temperature at the very top of the rear panel. This suggests that there may be some form of stagnant flow in the region into which the hot air from the manifold does not penetrate. The overall variation, however, appears to be smooth.

Sensor number	Co-ordinate(mm)			temperature (K) at varying velocities ($5ms^{-1}$ to $20ms^{-1}$)						
	x	y	z	$5.0ms^{-1}$	$7.5ms^{-1}$	$10.0ms^{-1}$	$12.5ms^{-1}$	$15.0ms^{-1}$	$17.5ms^{-1}$	$20.0ms^{-1}$
back 12	491	50	-152	312.3	311.1	309.8	308.5	307.2	305.9	304.9
back 11	491	65	-152	312.3	310.7	309.6	308.2	307.1	305.7	304.9
back 10	491	80	-152	312.4	311.0	309.9	308.7	307.6	306.2	305.4
back 9	491	105	-152	313.7	312.5	311.4	310.2	308.8	307.4	306.5
back 1	491	155	-152	314.0	313.9	313.3	312.5	311.3	309.9	308.8
back 2	491	205	-152	314.7	315.0	314.7	313.9	312.7	311.4	310.2
back 3	491	225	-152	312.0	313.0	313.2	312.8	311.9	310.8	309.7

Table 2-4 Results (Rear Sensors: row 1 – Vertical)

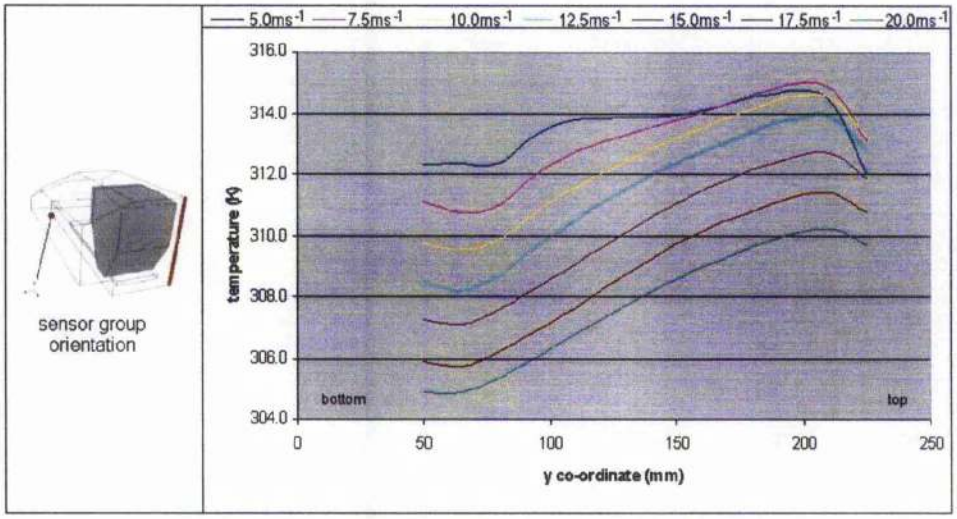

Figure 2-23 Results (Rear Sensors: row 1 – Vertical)

Figure 2-23 referred to the vertical line of sensors on the model centreline. Figures 2-24 and 2-25, however, refer to data associated with the horizontal variation at position of y=155mm and 80mm respectively.

sensor number	co-ordinate(mm)			temperature (K) at varying velocities ($5ms^{-1}$ to $20ms^{-1}$)						
	x	y	z	$5.0ms^{-1}$	$7.5ms^{-1}$	$10.0ms^{-1}$	$12.5ms^{-1}$	$15.0ms^{-1}$	$17.5ms^{-1}$	$20.0ms^{-1}$
back 1	491	155	-152	314.0	313.9	313.3	312.5	311.3	309.9	308.8
back 4	491	155	-130	314.2	313.9	313.0	312.0	310.7	309.4	308.2
back 5	491	155	-110	314.3	313.8	312.8	311.7	310.4	309.0	307.9
back 6	491	155	-70	313.5	312.7	311.6	310.5	309.3	307.9	307.0
back 7	491	155	0	309.3	308.0	306.8	305.8	304.8	303.7	303.1

Table 2-5 Results (Rear Sensors: row 2– Horizontal at y=155mm)

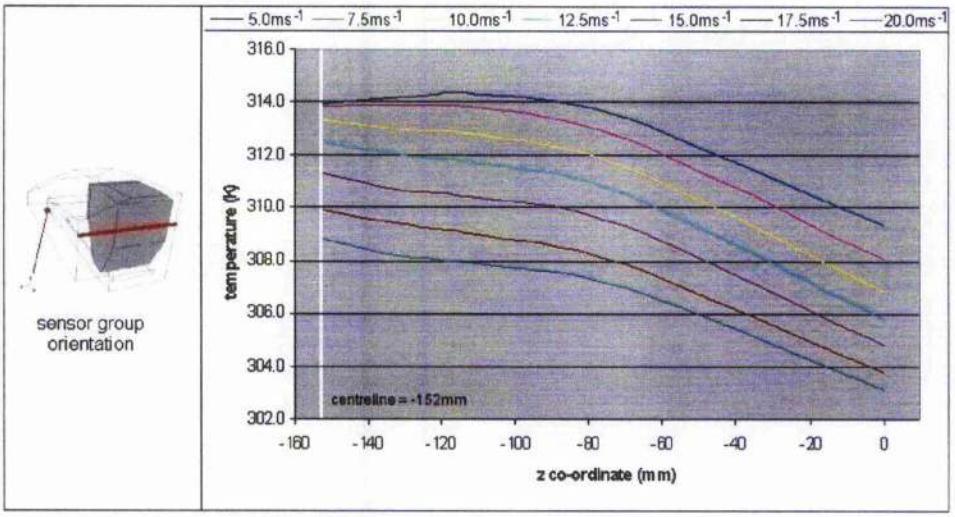

Figure 2-24 Results (Rear Sensors: row 2 – Horizontal at y=155mm)

sensor number	co-ordinate(mm)			temperature (K) at varying velocities ($5ms^{-1}$ to $20ms^{-1}$)						
	x	y	z	$5.0ms^{-1}$	$7.5ms^{-1}$	$10.0ms^{-1}$	$12.5ms^{-1}$	$15.0ms^{-1}$	$17.5ms^{-1}$	$20.0ms^{-1}$
Back 10	491	80	-152	312.4	311.0	309.9	308.7	307.6	306.2	305.4
Back 13	491	80	-130	310.6	309.3	308.2	307.1	306.0	304.8	304.0
Back 14	491	80	-110	308.9	308.0	307.0	306.0	305.0	303.9	303.2
Back 15	491	80	-70	307.1	306.3	305.4	304.5	303.6	302.7	302.1
back 8	491	80	0	304.1	303.1	302.4	301.7	301.1	300.5	300.1

Table 2-6 Results (Rear Sensors: row 3 – Horizontal at y=80mm)

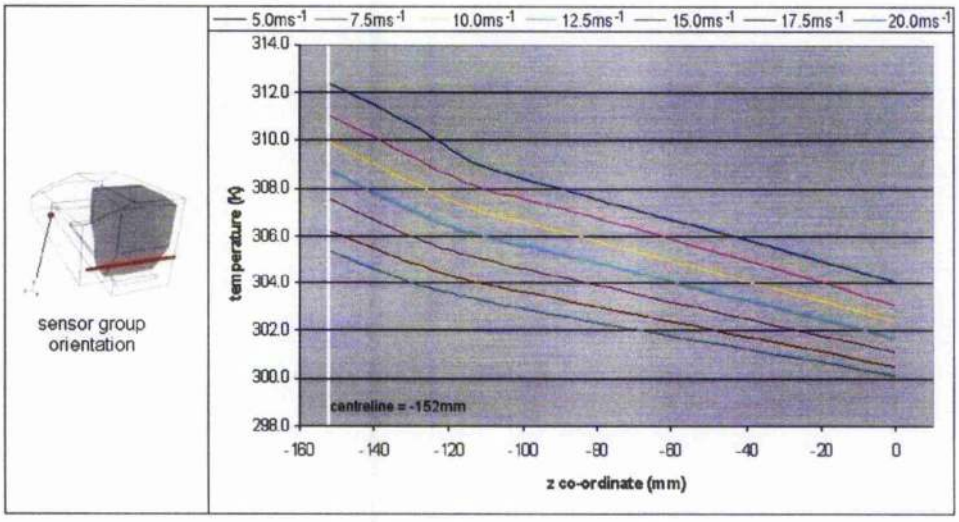

Figure 2-25 Results (Rear Sensors: row 3 - Horizontal at y=80mm

Once again there is obvious monotonic variation associated with the sensor location from z=-152mm to z=0mm. The most noticeable difference between the two rows, however, is that at y=155mm the temperatures exhibit a slower spatial reduction between z=-152mm and z=-110mm compared to that out to z=0mm; whilst at y=80mm the drop off is fairly consistent over the entire range of z values. Both plots/rows, like the vertical row (figure 2-23) exhibit the obvious, and understandable, temperature reduction with increased tunnel speed.

It may be observed that, aside from small differences to the temperature profile for the 5 and 7.5ms-1 cases, the general trend shows regular cooling at the higher velocities; as may be expected. Also there is obvious smooth gradation between sensors.

In common with the previous set of results for the vertical row of sensors, these figures demonstrate a regular cooling pattern as the velocity increases with only a slight deviation for the 5ms-1 case.

2.6.2. Top Surface of Engine Compartment

As was shown in figure 2-11 the sensors were placed on two longitudinal rows and one lateral row. Of the two longitudinal rows one was on the centreline of the model (z=-152mm) and the other offset by 34mm (z=-118mm). The lateral row was positioned at x=415mm. The locations of the individual transducers in these rows are given in tables 2-7 to 2-9. The sensor number corresponds to that on figure 2-11.

Table 2-7 to 2-9 also include the averaged measured data from each of the transducers at all the chosen tunnel speeds. These measured data are presented in graphical form in figure 2-26 to 2-28. Both the longitudinal sensor rows display similar trends in as much as the temperature decreases as the flow progresses toward the rear. Once again the temperature drops with increasing tunnel speed. The initial rise in temperature is accentuated at the lower speeds.

sensor number	co-ordinate(mm)			temperature (K) at varying velocities (5ms^{-1} to 20ms^{-1})						
	x	y	z	5.0ms^{-1}	7.5ms^{-1}	10.0ms^{-1}	12.5ms^{-1}	15.0ms^{-1}	17.5ms^{-1}	20.0ms^{-1}
top 6	275	202.4	-152	327.1	323.0	322.9	323.8	322.4	320.2	318.6
top 5	300	205.0	-152	331.1	328.8	327.5	325.7	323.7	321.1	319.4
top 3	330	208.8	-152	327.4	327.1	326.2	324.9	323.0	320.6	318.9
top 2	370	213.8	-152	324.2	324.4	323.9	322.7	320.8	318.8	317.2
top 9	415	219.6	-152	321.1	321.0	320.4	319.2	317.7	315.9	314.4
Top 10	450	223.9	-152	318.5	317.9	317.1	316.0	314.5	312.9	311.7

Table 2-7 Table of Results (Top Sensors: row 1 – Centreline)

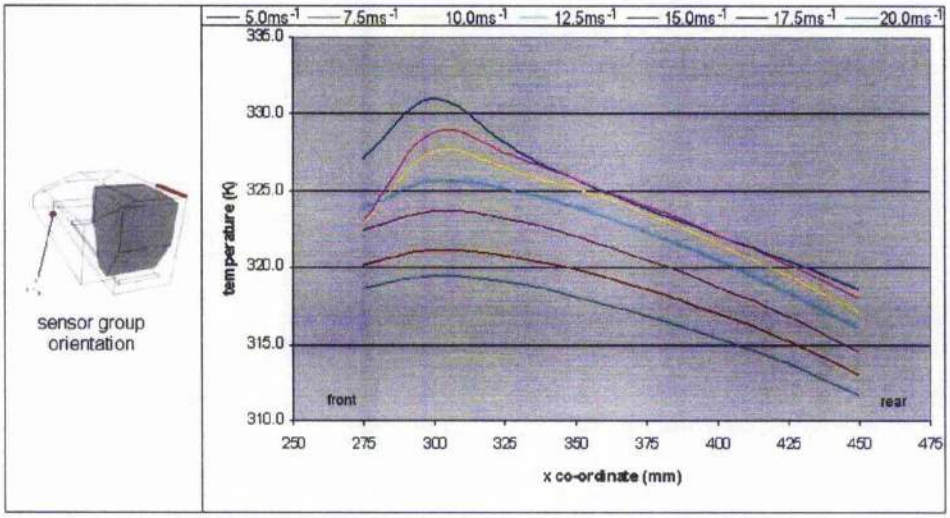

Figure 2-26 Results (Top Sensors: row 1 – Centreline)

sensor	co-ordinate(mm)			temperature (K) at varying velocities (5ms^{-1} to 20ms^{-1})						
number	x	y	z	5.0ms^{-1}	7.5ms^{-1}	10.0ms^{-1}	12.5ms^{-1}	15.0ms^{-1}	17.5ms^{-1}	20.0ms^{-1}
top 8	275	202.4	-118	332.3	325.6	325.5	326.0	324.2	321.3	319.5
top 7	300	205.0	-118	333.2	330.4	328.4	326.4	324.1	321.2	319.1
top 4	330	208.8	-118	328.3	327.7	326.4	324.8	322.7	320.1	318.2
top 1	370	213.8	-118	324.9	325.3	324.1	322.8	320.8	318.3	316.6
top 12	415	219.6	-118	322.2	322.2	320.9	320.0	318.0	315.8	314.4
top 13	450	223.9	-118	319.2	318.6	317.3	316.3	314.7	313.0	311.6

Table 2-8 Results (Top Sensors: row 2 – 34mm Offset from Centreline)

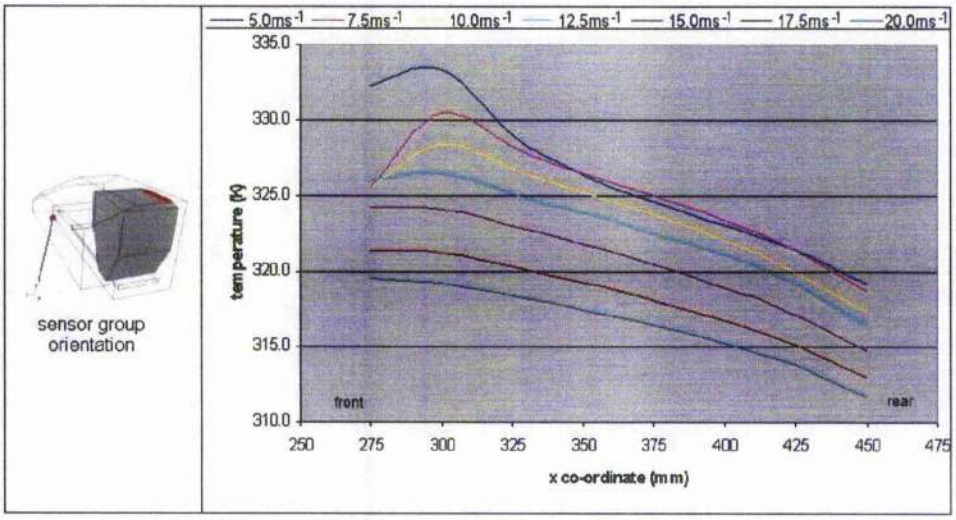

Figure 2-27 Results (Top Sensors: row 2 – 34mm Offset from Centreline)

In figure 2-27, at the points in line with the exhaust downpipe, one would have expected slightly higher temperatures. At the lower speeds this is certainly the case but the temperature diminishes as the tunnel speed increases. For the transverse series of transducers (row 3, table 2-9, figure 2-28) the above trend is obvious and particularly so for the highest tunnel speed.

Sensor Number	co-ordinate(mm)			temperature (K) at varying velocities ($5ms^{-1}$ to $20ms^{-1}$)						
	x	y	z	$5.0ms^{-1}$	$7.5ms^{-1}$	$10.0ms^{-1}$	$12.5ms^{-1}$	$15.0ms^{-1}$	$17.5ms^{-1}$	$20.0ms^{-1}$
Top 9	415	219.6	-152	321.1	321.0	320.4	319.2	317.7	315.9	314.4
Top 11	415	219.6	-137	320.8	321.0	320.3	319.1	317.7	315.8	314.3
Top 12	415	219.6	-118	322.2	322.2	320.9	320.0	318.0	315.8	314.4
Top 14	415	219.6	-105	322.5	322.4	320.9	319.7	317.8	315.6	314.1
Top 15	415	219.6	-85	322.1	321.8	320.0	318.7	316.8	314.4	313.1
Top 16	415	219.6	-63	320.3	319.8	317.7	316.4	314.4	312.1	311.0

Table 2-9 Results (Top Sensors: row 3 – Normal to Centreline at x=415mm)

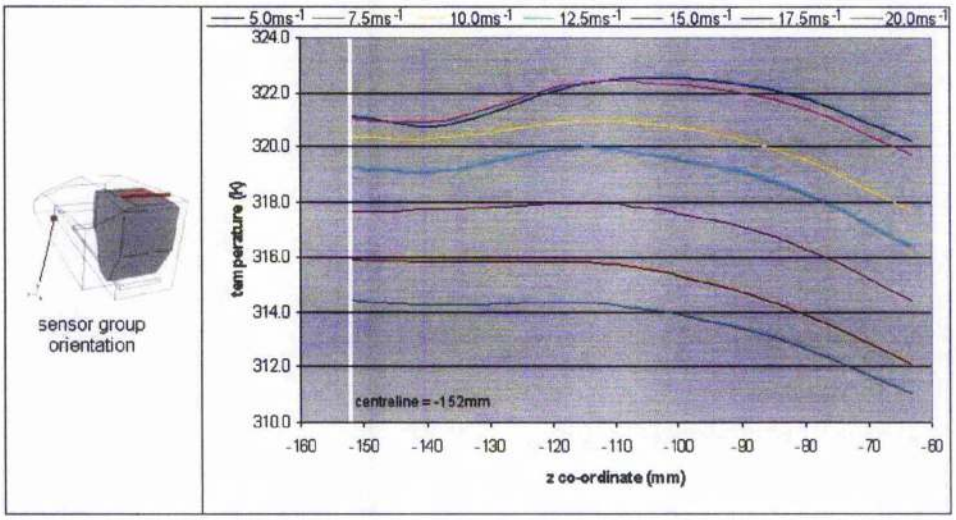

Figure 2-28 Results (Top Sensors: row 3 – Normal to Centreline at x=415mm)

As with the vertical row of sensors at the rear, there appears to be slightly different characteristics in the temperature profile for the lower velocities which are eliminated as the velocity increases to produce a more regular cooling effect. Once again, the temperature distribution, for increasing speed, predominantly reduces. At the lower speed there is a clear enhancement of the temperature drop at the most forward transducers.

This set of results shows similar results for the two lower velocity cases (5 and 7.5ms^{-1}) which, in fact, overlap at points. A more regular cooling profile emerges as the velocities increase.

Again, despite the configuration of this row of sensors being normal to those in the previous two cases, the 5 and 7.5ms^{-1} cases produce similar results.

2.7. Concluding Remarks

Overall the various compromises have resulted in an experiment far simpler than at first envisaged. There was no thermal imaging, no external car body and it was carried out in a smaller wind tunnel. Nonetheless, the instrumentation used and the entire rig performed well, resulting in well behaved and believable data.

It is unfortunate that the engine block and exhausts temperature could not be the same for all tunnel speeds. Perhaps improvement could be made here. Nonetheless, the resulting data and trends are such that they can be compared to with CFD predictions. These comparisons are described in Chapter 4.

3. CFD Simulation

3.1. Introduction and Background

As will have already been noted from chapter 2, the initial aim of the project was to model an actual car. With regard to the CFD simulation, this was, from the early tests refined to the modelling of a model car and engine compartment within a wind tunnel. Whilst the car and the wind tunnel working section was to be modelled by Sheng (2003), the engine compartment was originally envisaged to run within the model and be a complementary component. Had the project progressed as originally envisaged, after using an actual car had been abandoned, this work would have been a complementary and necessary contribution.

Whilst reading this chapter, it is hoped that the reader will follow, what may seem unnecessary work, through to the simple generic engine compartment that was eventually modelled and wind tunnel tested.

Nonetheless, the initial aim of assessing CFD for powertrain control module position remained intact. This was through an experiment, described in chapter 2, and the associated CFD modelling (using the commercial package FLUENT 5.5) which is the subject of the present chapter. Both the CFD and the physical wind tunnel modelling were to be complementary in that they were both analogues of the same flow state. As alluded to above, this would have involved full wind tunnel CFD modelling of a model car including an engine compartment. This was not possible during the present work.

Another major feature of the work was to assess the use of a CFD package by a non-specialist in fluids; as the author is. This was an important activity since the commercially available codes are regularly used by non-specialists in industry; in a

similar way to Finite Element codes are used for stress analysis. Although the author is a non-specialist, a brief description of the process is provided including reasons for particular choices of, for example, the turbulence model.

3.1.1. Initial Modelling

Early tests with FLUENT 5.5 considered the flow around typical but relevant shapes, the purpose of which was twofold. First, a familiarisation process and, second, an assessment of what the limitations of the facilities would be. This led to the development of a computer model based on work done by Ford during the 'BOXCAR' project (Dhaubhadel and Shih, 1996) where a basic 'Y' configuration was taken as the engine shape and no other components were included. This was as the present work started and then, gradually, complexity was added. Such was the complexity achieved that the engine compartment shape was from a photogrammetric study of an actual car transferred into a computer aided draughting (CAD) package. Once completed, an attempt was made to run the Fluent program. It seemed that this would take far too long (up to and in excess of a week) even if it did actually converge, and so a generic approach was adopted.

As resources such as computer overheads and time constraints impinged, the complexity of the model was reduced in stages until a grid which gave a solution within a reasonable time (<18 hours) was created. The final arrangement of the engine compartment resulted from a compromise between computing power and the need to have a realisable wind tunnel model. Accordingly a number of features, including some of the engine components and inner wing profiles, were discarded. Hence, both the CFD and wind tunnel model were mutually interactional.

A further limitation occurred when a large cell count resulted in a significant increase in time taken for gambit to generate the mesh (<20 minutes to >2 hours). The computers used for this project within the University were IRIX 6.5 based SGI O2s running on a shared user system. A typical hardware profile for these would be a 180MHz MIPS R5000 CPU with 256Mb of RAM.

It was empirically concluded that, when the cell count was limited to between 150000 – 180000 cells, acceptable generation times were achievable. For cell counts more than 190000, the unacceptable increase in execution time was attributed to computer memory allocation problems. This was concluded after many failed jobs, attempting to use larger cell counts, reported errors of this type.

3.1.2. Modelling Constraints

In all engine compartments, the hot elements radiate heat. Whenever one wishes to compute or model a physical flow field then, dependent on the complexity and nature of the problem, modelling constraints are always required.

The inlet of the model used was 0.304x0.039 (see appendix 3), giving an inlet area of 0.0011586, from this P (wetted area) is derived as:

$$P = 0.686\text{m}$$

Dn (notional diameter of a irregular shape) as:

$$D_n = \frac{4\times 0.011856}{0.686} = 0.069\text{m}$$

Transition to turbulent flow is at

$$R_e(D_n) \approx 2000$$

or

$$\frac{\rho \upsilon D_n}{\mu} = 2000$$

thus

$$\upsilon = \frac{2000 \times 1.8 \times 10^{-5}}{1.225 \times 0.069} = 0.43 \text{ms}^{-1}$$

so flow is turbulent at 0.43ms^{-1}. As this is the case, a turbulence model was required for the simulation. The choice of turbulence model is dealt with in section 3.2.3.

Although the inclusion of thermal radiation models was considered for the present work, they were eventually not incorporated. The main reason for this was the results from a series of tests which showed that the more complex the radiation model, the greater the overhead in computer time. Although this is to be expected, testing using a grid with a simple geometry was found to take less than seven hours to converge without a radiation model but that the same setup including a radiation model would take over 3 days to converge. It should be noted here that these runs were for very simple flows such as an isolated heated pipe.

3.1.3. Engine Compartment Model Considered

The physical rig to be modelled (see section 2.4.1) consisted of a generic engine compartment fabricated in aluminium. It had been designed in AutoCAD and so was available for export to GAMBIT (the FLUENT preprocessor). The engine block had a steady temperature of 380K (107°C) and the manifold (replicated in the rig by a high temperature flexible element) varied between temperatures of 420K(147°C) and 630K(357°C) dependent on the airflow velocity. These temperatures do not replicate those of the car initially tested (see section 2.4.3) as this would have been difficult to reproduce safely and consistently in this model.

The data obtained through this simulation, however, was used to guide the positioning of the temperature transducers. Simulation indicated that the variation in underbonnet pressures across a range of gauge pressures at the outlet would be very low and so no attempt was made to measure these.

This allowed resources, both in terms of project budget and fabrication time, to be focused on the acquisition of temperature data. Output from FLUENT was postprocessed to highlight given ranges so that detailed examination of temperature contours would be used to determine the position and type of the temperature probes. A range of 295K(22°C) to 360K(87°C) suggested the use of thermistors. By the same process, pressure and velocity contours were examined but were deemed to be of little significance in the placement of the thermistors.

3.1.4. Summary of Results

This chapter considers how the generic underhood model can be computed using FLUENT; even when used by a non-specialist. The quality of the computed data is such that it was used to revise, and hence guide, the placement of the transducers in the wind tunnel model.

3.2. Packages Used

This section deals with the software packages used to carry out the creation of meshes for the CFD simulation, the simulation itself and feedback into the design process derived from preliminary results. It covers a number of approaches explored before a final methodology was chosen.

Throughout the early part of the project, consideration was given to the package which would be used thereafter and a process of CFD familiarization was carried out using AVL-Fire and FLUENT under the auspices of Kelvin International Systems (KIS Ltd.) of East Kilbride. FLUENT was chosen as the package for expediting the project as it is widely used throughout industry and was, at the time, available both within the University and onsite at East Kilbride.

In addition, AutoCAD was employed for the initial geometry creation since it was found to be considerably easier to make changes to the geometry than with GAMBIT. This approach, however, caused some problems which are described later in this chapter.

3.2.1. CFD Preprocessor

The native preprocessor used for the Fluent suite was GAMBIT 1.2. Although it is a very powerful package, the performance on the shared-user system computers within the Aerospace Engineering department was limited in comparison to the dedicated machines available at KIS Ltd. Developing a model in this environment was difficult and, at times, dictated that model geometry had to be manually entered as the graphical editing interface did not respond in realtime. It was decided to create the basic geometry outwith the package in a dedicated CAD package and import it for mesh generation. GAMBIT was used, therefore, to define regions and boundaries and to create a mesh in the MSH mesh format for use with the FLUENT solver.

3.2.2. CAD Package

Typically, in problems where there is a simple, well-defined geometry, it is enough to use the preprocessor supplied with the CFD package. It quickly became apparent with this model, however, that 3D CAD modelling and the export of the geometry for meshing would have to be undertaken to provide the rapid creation of models required when making geometric changes. Even allowing for some problems which resulted in the creation of very small gaps (approx 10-30 μm) in the geometry that held up the grid generation, it was felt that generating these models in the native preprocessor would have been more time consuming.

AutoCAD was chosen as it was readily available within the university and has industry-wide acceptance. Some problems which arose with data exchange in various file formats may have been more easily handled by other packages. After discussion with other

experienced CAD users, no definitive answer as to whether or not this would have been the case, was discernable.

3.2.3. CFD Solver

Fluent is a general purpose RANS (Reynolds Averaged Navier-Stokes) based CFD solver. It typically uses unstructured grids created in TGRID and GAMBIT and can be used in 2D or 3D, single or double precision modes. For the purposes of this study the 3D single precision option was chosen. Further information on the preparation of cases in Fluent is given in appendix 7.

3.2.3.1 Segregated Solver

The FLUENT solver can be utilised in both segregated and coupled modes.

Typically the evolution of the segregated solver came about through low speed incompressible problems and the coupled solver by high-speed compressible problems. Currently, both models have evolved to a point where either can be used to solve both types of problem but the advantage of the segregated mode, for low speed incompressible flows, is that the memory requirement is between 1.5 and 2 times less than that for coupled mode applications. As noted earlier, memory and processor use throughout the project was a prime consideration and so the segregated solver was chosen.

3.2.3.2 Viscous Model (Turbulence Model)

The basic equations used for turbulent flow require a closure hypothesis; more commonly known as a turbulence model. Turbulence modelling is a specialist field and

so the author has simply employed that which is widely used in industry. That is the 2 equation k-epsilon model. Whilst other models are available, and would, in future, make useful comparisons, none was used.

Turbulence models are highly empirical and are required to model a wide range of flows. Close to solid surfaces, however, special treatment is required. This is because the nature of turbulence varies rapidly as walls are approached and also because of the nature of the flow immediately adjacent to the surface. For example, large re-circulations or boundary layer type flow. With the above in mind, and with restricted time, the author simply employed the standard wall functions available. Like the turbulence model, however, future work should consider these in more detail.

3.2.3.3 Materials

The default materials for this work were air for the fluid, and aluminium for a solid. These were chosen because the engine compartment and the engine block are largely fashioned in aluminium although the downpipes themselves are incolloy (iron, nickel, copper alloy) and there is some use of steel in the cowl.

3.2.3.4 Radiation modelling

Although some radiation modelling would have been beneficial, the processor demands for this option were particularly heavy and so mitigated against such a refinement. Some preliminary tests to assess the viability of using radiation modelling were carried out by considering a model of a solid heated sphere within a cuboid of fluid. These tests were not conclusive with results differing widely for the different models available. Convergence also took between 4 and 6 times longer than for no radiation modelling. Extrapolating this figure to the more complex engine compartment geometry, which

itself could take upwards of 18 hours to converge without radiation modelling, meant that results may have taken upwards of 4 days to complete. For these reasons, radiation modelling was not included in this study although it should be considered in any future work. A possible improvement was the introduction of the Surface to Surface (S2S) model in FLUENT 6. S2S radiation modelling is considerably faster than the widely used Discrete Transfer Radiation Modelling (DTRM) and has been used elsewhere for underhood solutions (FLUENT 2001).

3.3. Preliminary Work

Preliminary work was carried out in conjunction with KIS Ltd. at their offices in East Kilbride. The main thrust of the project, at this stage, was to have been based on the power testing of PCU modules *in situ* and to this end a number of avenues were explored during the process of CFD familiarisation. The creation of a stylised engine compartment, based on a Morgan Plus 8 car (section 2.2) and engine block was undertaken using GAMBIT and resulted in the mesh illustrated in figure 3-1.

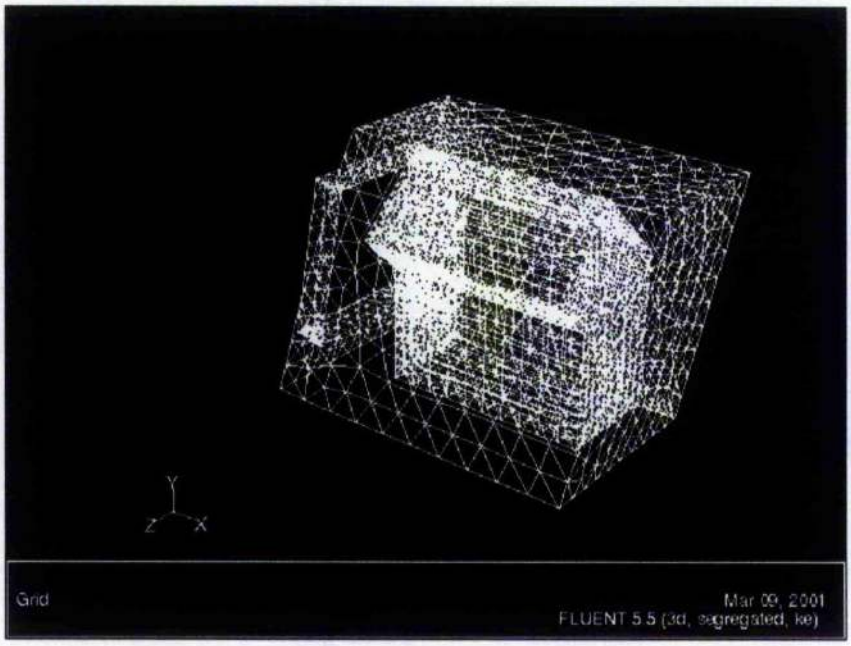

Figure 3-1 Geometry for Basic Engine Compartment Shape

What this figure shows is only the internal surfaces of the mesh and on the surface of the engine block. The front of the compartment is to the left where one may observe the air intake simply by the lack of surface elements. Similarly the bottom of the compartment is open. It should also be noted that only half of the compartment has been meshed as permitted by the assumption of symmetry along the longitudinal or x-axis.

At this time there was no particular emphasis on absolute results as there was no specific data to compare against, but the options available for setting boundary conditions were explored. Solutions for the case shown in figure 3-2 were obtained using the boundary conditions detailed below.

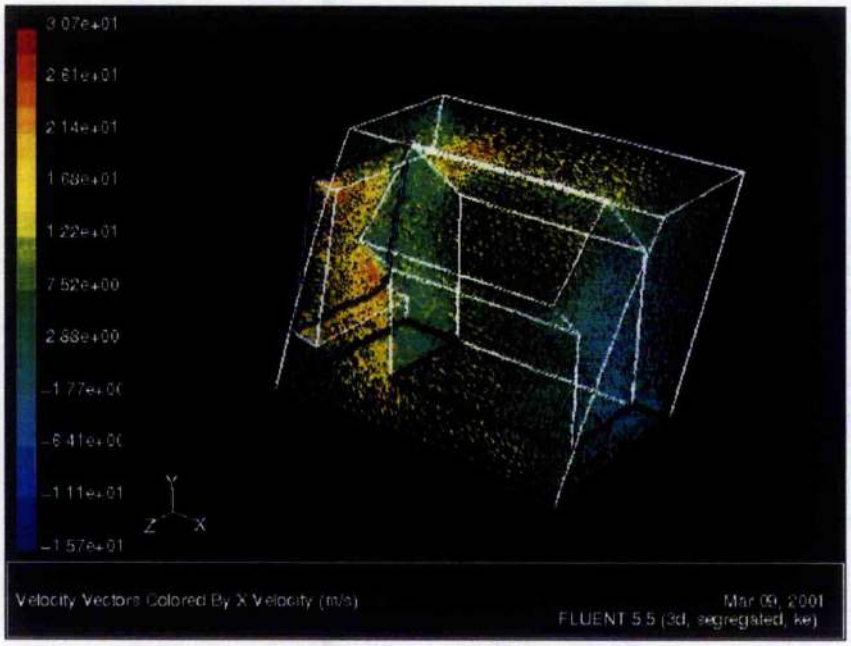

Figure 3-2 Velocity Vectors (x velocity component)

Figure 3-2 is densely detailed, which hampers rapid assessment, but has been included to provide a qualitative illustration of the computed x component of velocity. It may, therefore, be observed that as expected, all the red and yellow coloured vectors (positive u) are at the front of the engine and the reversed flow (blue vectors) at the rear.

In this particular case, the boundary conditions were

1. Manifold at 600K
2. Engine block at 400K
3. Freestream at 300K
4. X Velocity at Inlet 35ms^{-1}

Three of these are illustrated in figure 3-3 in which the hot manifold area is taken to be at constant temperature and the uniform velocity inflow and constant pressure outflow are highlighted in blue

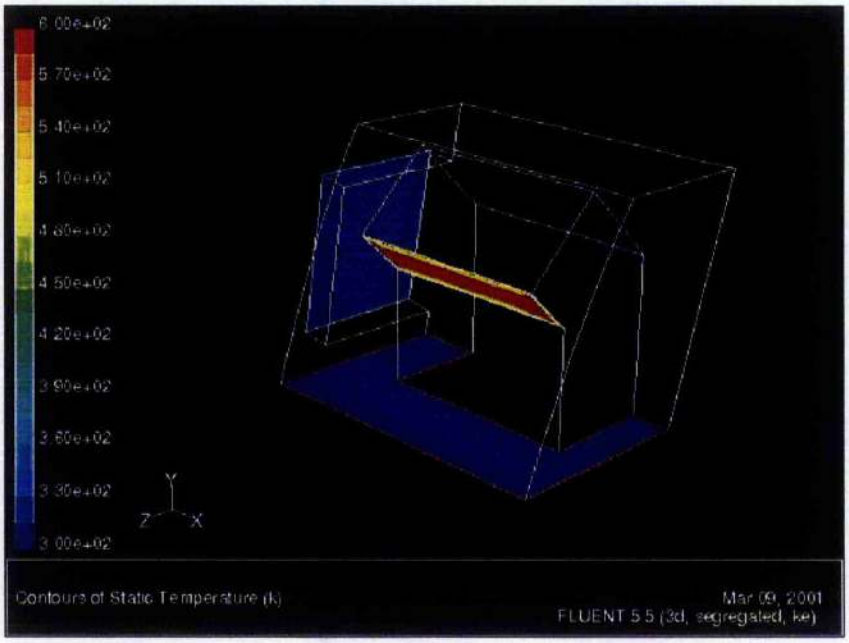

Figure 3-3 Initial tests using energy enabled solver

The engine block modelled above has been significantly simplified. The author, however, had available scale drawings of the Rover V8 engine used in the Morgan. These were scanned in and an AutoCAD basic three dimensional model digitised model created in ACIS format (figure 3-4)

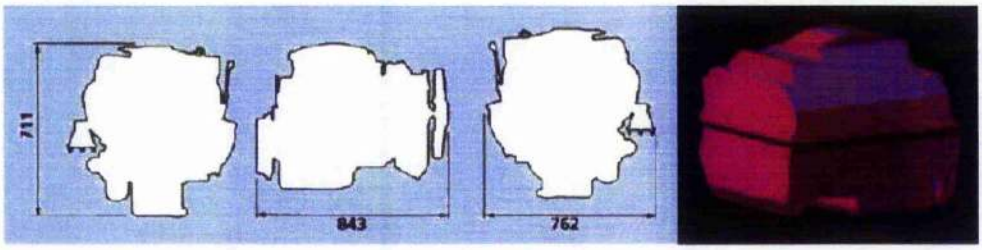

Figure 3-4 Engine Model Created from V8 Extents

The main purpose of this was to assess (for later use) the ACIS format for input to the mesh creating GAMBIT pre-processor.

Accordingly the AutoCAD file was imported into GAMBIT and a mesh bounded by a cuboid was successfully generated. The suitability of this procedure was tested by running the FLUENT code to ensure that it would converge to a reasonable conclusion. The boundary conditions were simply those of uniform flow at the upstream and tangential flow on the longitudinal surfaces. The exit was defined as a pressure outlet.

The ensuing predictions are illustrated in figure 3-5 and this is included simply to show that, as expected from the problem setup, the flow accelerates around the engine and slows down as it exits the computational domain. The figure depicts contours of velocity magnitude at various transverse sections. In this case, the X velocity was set at $60ms^{-1}$ and no temperature conditions were defined.

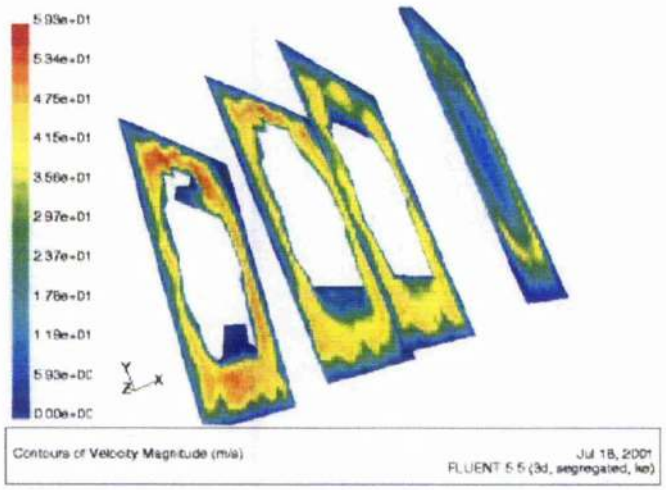

Figure 3-5 Fluid Flow round V8 Model

The intention was that, due to the success of the procedure, the engine could be incorporated into a very accurate model of the Morgan's engine compartment. The Morgan Car Company seemed, at first, to be very enthusiastic; but the necessary drawings were not passed on. Presumably, company confidentiality intervened.

Additionally, it became apparent at this time, though, that there would not be unrestricted access to the Morgan and that the planned testing of *in situ* PCUs for a client of KIS Ltd. was subject to contract negotiations and the likely delay would impinge severely on the project. The decision was taken to develop a generic car model within the University. This in turn would be constructed as a physical model for the acquisition of experimental data.

As both the physical and CFD work was proceeding together and, as mentioned in Chapter 2, the final model was a simplified generic compartment tested in isolation, the work leading up to that final choice is described here. This is because the geometry was so closely linked to the FLUENT modelling and meshing.

Having forsaken the KIS Ltd. Facilities with fixed geometry vehicles, the author was free to adapt geometries to the restrictions of both CFD and wind tunnel requirements.

3.4. First Approach (Eagle Talon Model)

With the demise of the Morgan work, the project became that of producing a wind tunnel model of a car that included an instrumented engine compartment. The question to answer was, of course, what car. As will be anticipated, the initial desires were gradually simplified and, although the engine compartment was made and tested, it was not inserted into the car model. Nonetheless, much effort was expended designing the complete model and this was done in two stages. First, a model of a production car and then a generic design.

The model details were sourced in DXF format from Kaizen Tuning, a company specializing in the race preparation of the Eagle Talon / Mitsubishi Eclipse and which had created the model for publicity purposes. The extremely detailed model was created by photogrammetry and consists of the entire bodywork, minus the engine block, in 66 DXF format files. On request, they gave their permission to use the model for the project (SINGH 2001).

3.4.1. Creating Solid Geometry

The front end geometry was assembled from the DXF files as shown in figure 3-6.

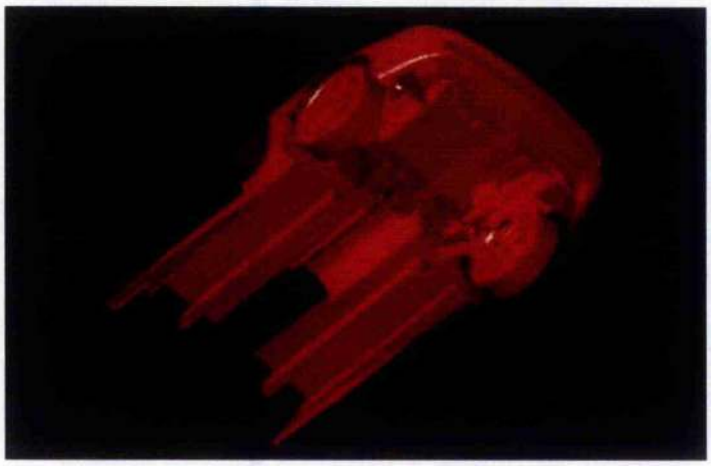

Figure 3-6 Eagle Talon Front End Geometry.

One of the problems encountered was that the model, although complete, consisted only of surface geometry and there were no solid objects which could be exported to GAMBIT. This lack of 3D data involved the processing of the data in the following manner.

Any surfaces that were capable of extrusion were extruded to a depth of 0.003m creating a group of solids. This process produced extremely large and unwieldy files, typically

>50MB. Sections through this created geometry were taken at 0.025m intervals, except at the nose and air intake where the intervals were taken at 0.01m (figure 3-7) Thereafter, the sections were extruded and edited by Boolean operations to give the closest possible approximation to the original geometry in solid form.

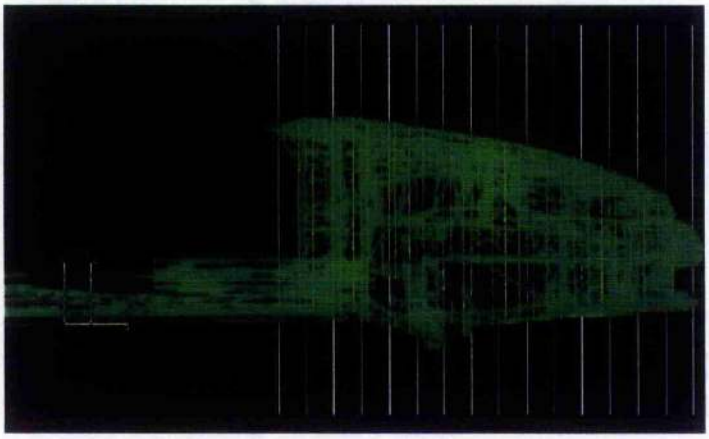

Figure 3-7 Sample Sections from Geometry (white lines)

The geometry was only created as far as the A-Pillar (figure 3-8) because, as noted in Srinavasan *et al.* (2000), the effect of including the entire car geometry affects the front-end cooling by less than 0.5%. As may be seen in figure 3-8, there were numerous sections used. Although a rather cluttered figure, it does depict clearly the overall intensity of the sectioning.

This procedure was extremely labour intensive and time-consuming. It was abandoned when the practicalities of creating a physical scale model based on this geometry were examined. The level of detail would also have required a very fine mesh to have been created and the processor overheads in solving a fine mesh would have been excessive.

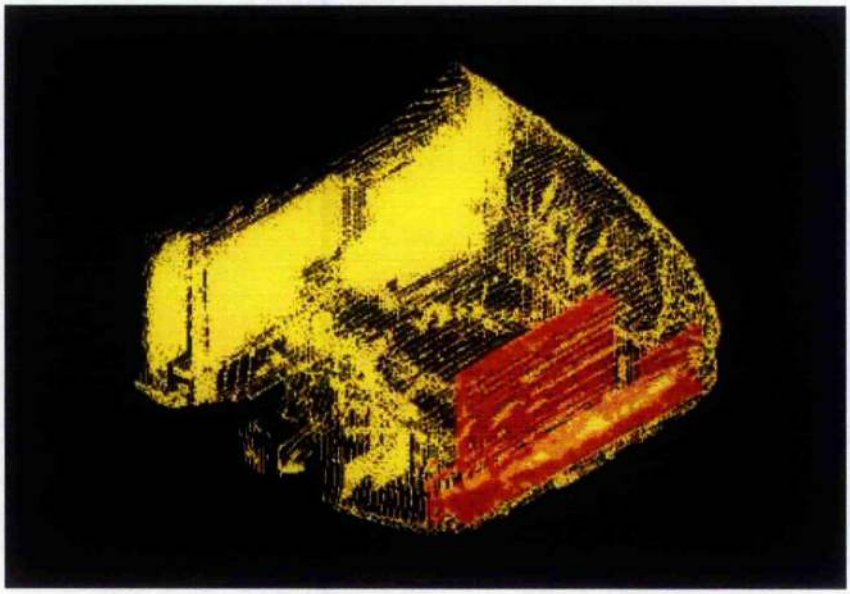

Figure 3-8 Sliced Geometry with Original Radiator

At this point, the image processing software package Surfdriver was investigated and attempts were made to extrude the sections from bitmaps generated by AutoCAD. This, however, was found to be an equally laborious method, exacerbated by the limitations of the trial version of the software.

3.4.2. Initial CFD Modelling based on Eagle Talon

Having obtained the geometry of the engine compartment and placed within it an engine block based on the Rover V8, a radiator and simplified fan. A CFD model was then created

For the initial simulations only the radiator was included and this was modelled as a solid. The intention at this stage was to refine the model later, with the radiator being set as a porous material and the fan model employed. The boundary conditions were defined as before in the simplified Morgan engine compartment model.

A typical prediction (figure 3-9) illustrates the static pressures within the simplified compartment. Again, the figure is a little cluttered but shows static pressure as a vector field throughout the engine compartment and contours of the same data at three specific sections within the compartment. It is included simply to illustrate, however, that the process had been successful with a converged solution. The convergence history for this case is shown in figure 3-10. It should be noted that in this case there were no thermal conditions set and that convergence has taken place in a much shorter time than the cases described later.

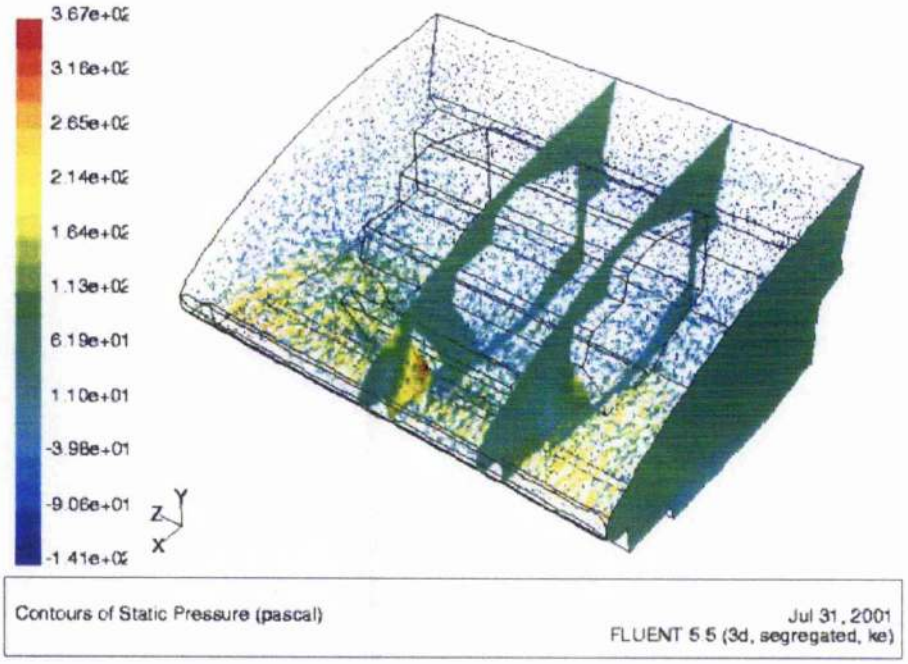

Figure 3-9 Static Pressure Results for Simplified Talon Geometry

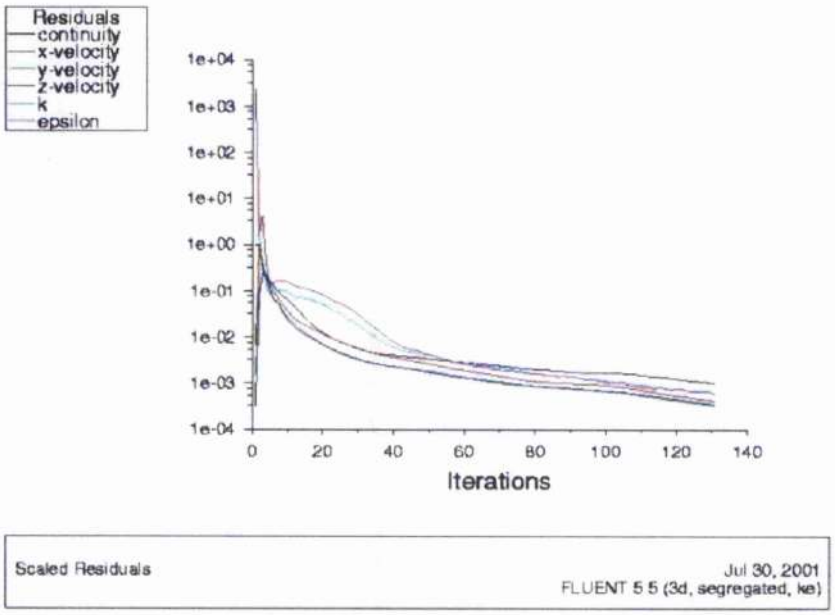

Figure 3-10 Convergence History for Simplified Talon Geometry

Overall the whole model was somewhat unwieldy and the use of the Talon model was abandoned for a car body shape already available in FLUENT tutorials (see figure3-11)

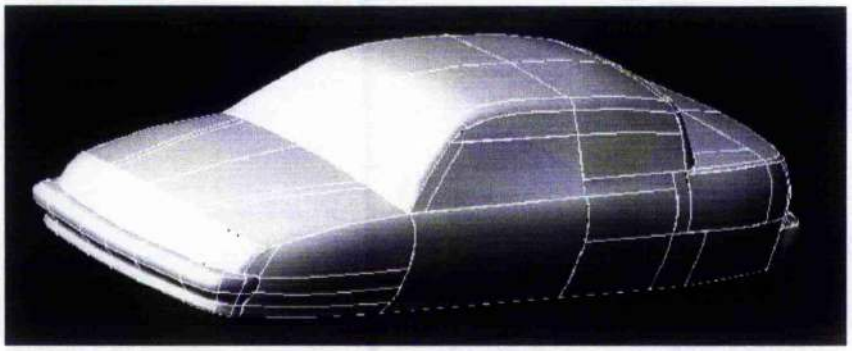

Figure 3-11 Sedan Geometry from FLUENT Tutorial Exercise

It had been hoped to retain the then current engine compartment model in a simplified form. One of the reasons for this was that when the drawings were imported to GAMBIT the CAD model proved to be very difficult to mesh.

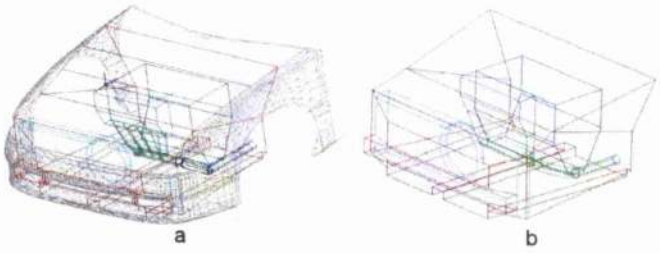

Figure 3-12 Angular Engine Compartment

Initially, this was thought to be a problem with the now very angular geometry as illustrated in figure 3-12b. Figure 3-12a shows the outer shape of the Eagle Talon with the outline of the engine compartment drawn in dark red. That compartment is shown more clearly in figure 3-12b. Consequently, a more rounded version was created (figure 3-13).

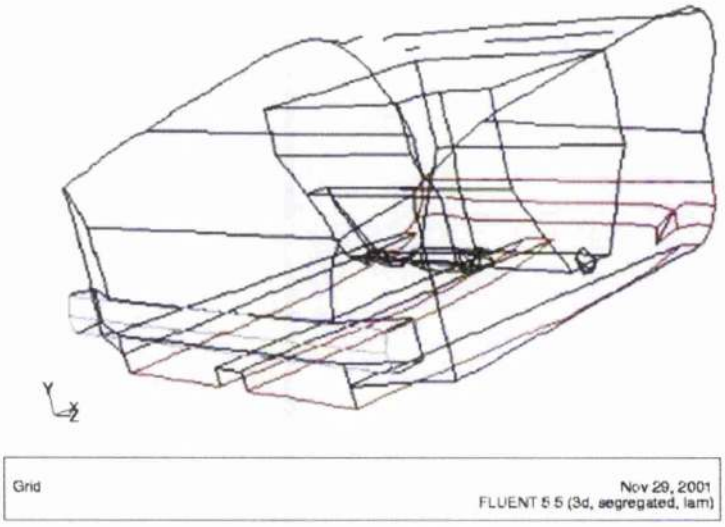

Figure 3-13 Rounded Geometry

This latter assumption proved to be incorrect as the problem was eventually traced to very small anomalies in the CAD geometry. Although there is an option in GAMBIT for cleaning up anomalies when importing the geometry into GAMBIT (and this was utilised), objects extruded along an arc and joined by Boolean operation could

occasionally be found to be unconnected at various points. On inspection, there were found to be gaps of less than 20 microns between sections of the downpipe geometry. These went undetected by the geometry cleaning routine as this scans for edges rather than gaps. This created miniscule spaces which GAMBIT attempted to mesh unsuccessfully and which caused a large number of errors. The difficulty was resolved by either creating small sections of geometry to fill the gaps or extruding the geometry further using a complementary geometry to remove the excess with a further Boolean operation.

3.5. Second Approach (Generic Model)

As noted in the previous section, the development of the model based on the third party geometry was abandoned due to the manner in which the given data had to be processed and the availability of a suitable vehicle geometry readily available in a FLUENT tutorial exercise (figure 3-11). On the basis of other concurrent projects within the department, namely an undergraduate study on vehicle drag (Bisset 2002) and a PhD study into wind tunnel effects which required a reasonably large model (Sheng 2003), the decision was taken to make a scale model based on the geometry from the FLUENT suite's tutorial exercises. Original drawings from Bisset's project are reproduced in appendix 2.

At this stage it was still intended to embed the engine compartment within the overall car model and test it in the Argyll wind tunnel. Accordingly, the author was fully involved in all aspects of the model design. That design would dictate the overall shape of the final engine compartment (as may be seen in appendix 3)

3.5.1. CAD Modelling

It was quickly established that the engine block could be placed within the new model but that the compartment would have to change radically. Figure 3-14 shows the arrangement of the engine compartment geometry as it was to be mounted on the model's baseplate.

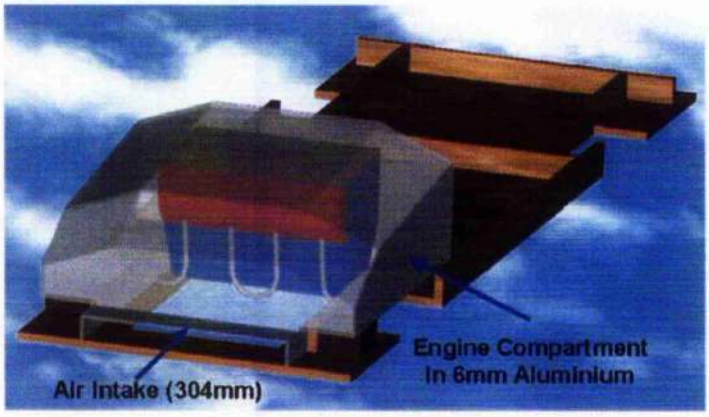

Figure 3-14 CAD Model of Engine Mounted on Baseplate

The intended configuration of the engine compartment within the bodywork can be seen in figure 3-15 where the CAD design of the engine compartment is placed within the original geometry imported from GAMBIT into AutoCAD.

Figure 3-15 Engine Compartment within Bodywork

3.5.2. Initial Results – Truncated Region

Since the engine compartment did not require to be a scale model of a real car's compartment, it could be executed far faster than a more complex shape. In addition, the current work used a symmetric model which again simplified mesh generation. In addition, two computational volumes were used and are depicted in figure 3-16.

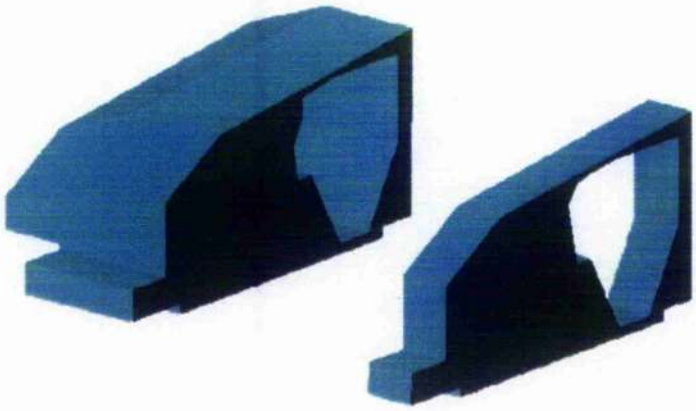

Figure 3-16 Full and Truncated Fluid Regions Derived from CAD Geometry

Shown on the left of this figure is a half section of the engine compartment. This was used for all the main calculations. To the right is a second, truncated volume employed during initial exploratory work. The computational domain is shown in blue. Although the downpipes are not shown in the figure, they were included in the domain, as may be seen in figure 3.18

The preliminary work considered the truncated domain and typical surface meshing by GAMBIT may be seen in figure 3.16. The inlet is coloured blue and had boundary conditions of

- X velocity of $15ms^{-1}$;
- Freestream temperature of 300K.

The red surface is the flow exit to atmosphere and gauge pressure was set to 0.0Pa, ie case was atmospheric pressure only. Along the side walls (yellow) the boundary was set as a symmetry. It will be appreciated that this does not create a truly three dimensional case as there is no flow around the sides of the engine block. This option was used simply to extend the fluid region to model a more realistic flow at the downpipe region than would have been the case with a single section. The remaining surfaces were treated as solids with a constant temperatures. It may also be noted that these initial tests on the truncated section contained a single downpipe (exhaust).

This allowed a series of cases to be explored while refinements were carried out in the meshing of the full fluid region.

Figure 3-17 Relative Mesh Density

Figure 3-17shows a typical mesh refinement. In this case, the density of the unadapted mesh at the symmetry of the truncated region (≅58000 cells) used for the initial investigations described is represented in figure 3-17a. The adapted mesh of the engine compartment (≅170000 cells) used for later work is shown as figure 3-17b.

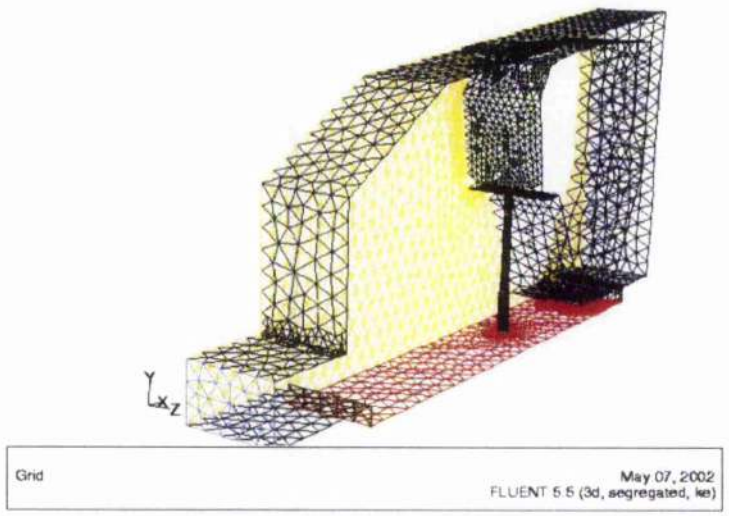

Figure 3-18 Mesh of Truncated Fluid Region

Figure 3-19 illustrates the resultant velocity magnitude contours in the x-y plane for a case using the truncated fluid region at a freestream velocity of $15ms^{-1}$ with boundary conditions as noted above. There is clearly a large jet that passes through the grille and subsequently impinges on the engine wall. A large re-circulation can be observed in the upper part of the compartment.

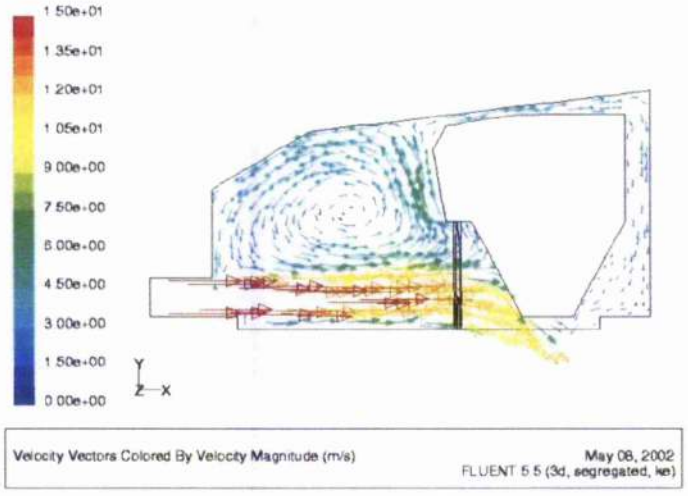

Figure 3-19 Velocity Magnitude (Range : 0-15ms^{-1})

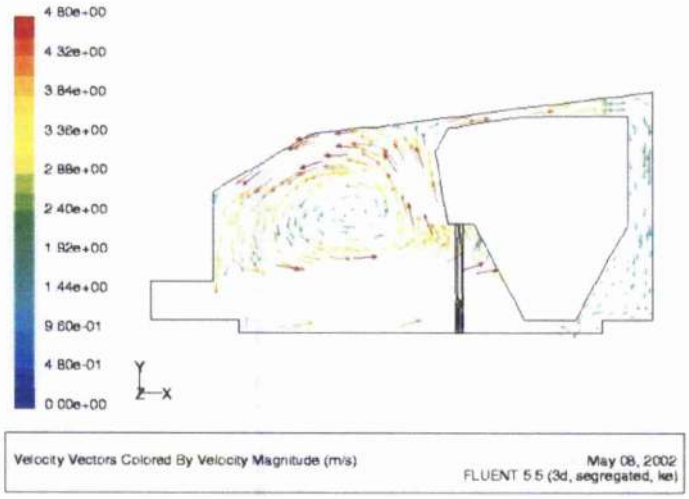

Figure 3-20 Velocity Magnitude (Range : 0 to 4.8ms^{-1})

In an attempt to highlight greater detail outside in the area behind the engine block, fig 3.18 shows the same data as the previous figure but with velocity vectors values now limited to those within the range 0 to 4.8ms^{-1}.

The large re-circulation alluded to above is now most prominent since the main jet like structure is outside the contour range and simply appears as a white area. Additionally, there may be observed a distinct flow over the top of the engine block and down. This could be an important observation since the bulkhead of the engine compartment is a common location for electronics.

Whilst informative, however, for this particular work, no temperature profiles were calculated. These were done using the geometry created for half of the engine compartment.

3.5.3. Initial Results – Engine Compartment

Further development of the mesh with the fluid region representing half of the engine compartment included the addition of the temperature data. The simulation in FLUENT was undertaken for a range of speeds with the temperatures of the engine elements set as:

- free stream = 300K
- engine block = 400K
- manifold =700K
- downpipes = 800K

based on tests done on the Morgan and from data found in a number a number of studies described in chapter 1.

These were the standard wall functions advised and used by FLUENT. Essentially, they model the heat transfer from the surface to or from it into or out of the fluid. The validity of this method is governed by the fluid conductivity and, when the mesh is not resolved down to the wall, accuracy of the wall function. In figure 3-21, the predicted temperature contours (in 3 dimensions) on the compartment surfaces can be clearly seen. In this case, the downpipes and manifold were set to the temperatures noted above. As the range set for data output was 300 to 400 K, it can be clearly seen that these heated surfaces are outwith the range by the absence of temperature data.

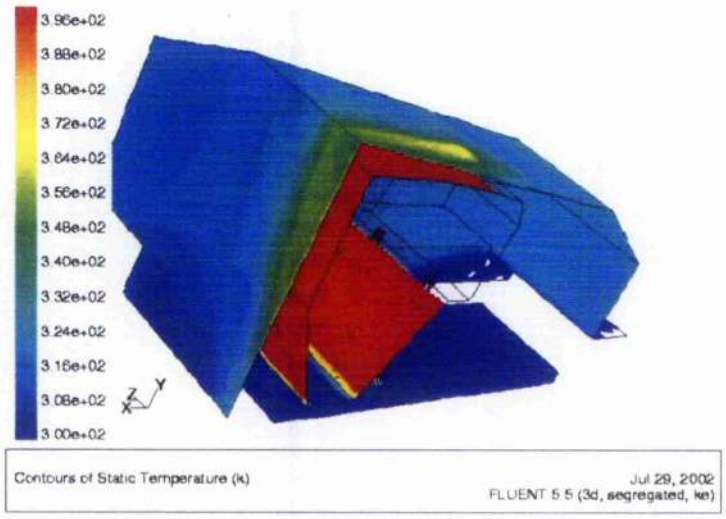

Figure 3-21 Temperature Contours Derived from FLUENT

3.5.4. Deriving Sensor Position from Temperature Contour Output

The initial findings clearly indicated that the FLUENT solver, with the associated computational grid, converged to what appeared to be a reasonable prediction. This was assumed since the flow exhibited plumes of hot fluid, from the downpipes, travelling up and over the engine block. This is clearly illustrated in figure 3-22 and shows temperature contour data on the upper surface of the fluid region.

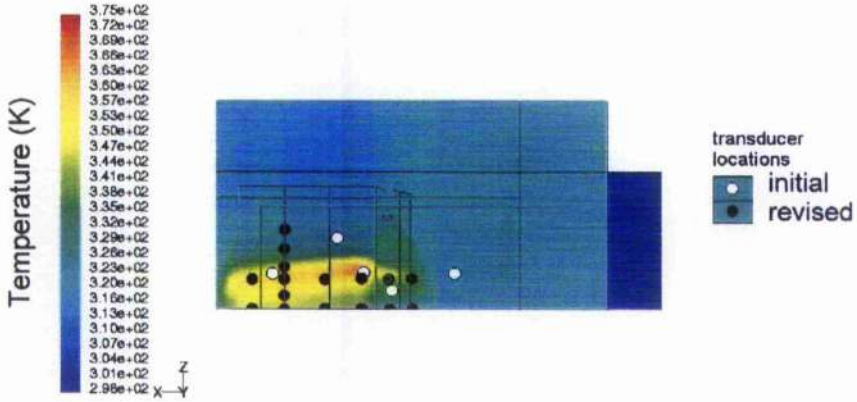

Figure 3-22 Illustration of Hot Plume from Downpipes

Figure 3-22 contains a number of sizeable dots both white and black. The white dots represent the originally proposed transducer locations (see appendix 5). The black dots were the revised locations. Clearly the CFD had been of much help in the experiment design and the number of sensors was increased (for the back and top plates) from 9 to 31. The position and numbering of the sensors is illustrated clearly in the previous chapter in figure 2-11.

Figure 3-23 illustrates the temperature contours of the fluid at the back plate and the new sensor locations. It can be seen that the choice of sensor location has been made to capture the salient features of the flow.

There is a row of sensors on the top plane offset by 34mm (z=-118mm) from the centreline which is in line with an exhaust downpipe. Sensors were not placed in line with the downpipe offset at 102mm (z=-50mm) as placement would have proved problematical due to their being at the edge of the viewing panel. On the basis of the initial results, which show a well-defined plume close to the centreline this, was not considered at the time to be a significant omission.

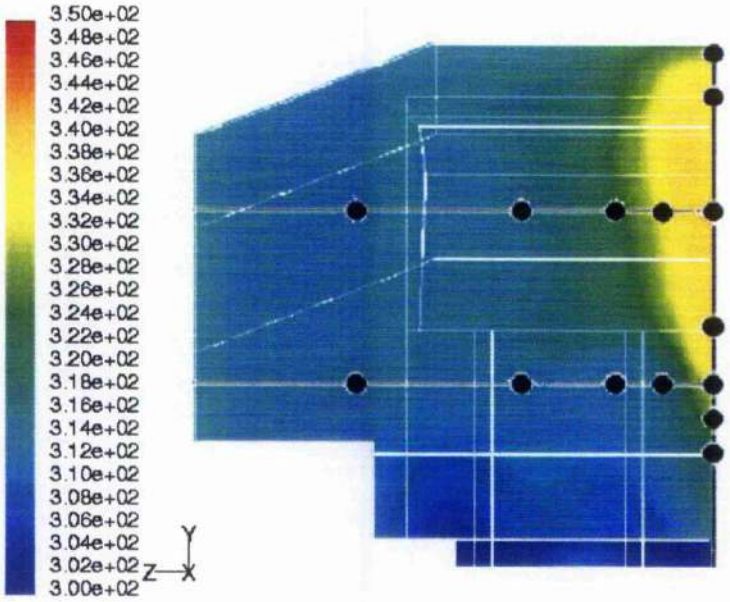

Figure 3-23 Rear Sensor Positions

Again, referring to a figure from the previous chapter, figure 2-10, shows both the layout and numbering of the sensors.

Sensor availability had been finalised before the positions at the rear of the engine compartment were considered and a rectilinear arrangement similar to that of the top sensors was adopted. Placement of a row of sensors vertically and a row of sensors horizontally (at a height of 155mm) were again selected to highlight salient features of the flow.

A second row of sensors at a height of 80mm was also added where the temperature appears to be fairly consistent across the majority of positions. It can be seen in figure 3-23 that only 15 sensor positions are employed. This was due to the originally proposed position being fouled by the strut balance mounting. To overcome this, a resistor was placed in the circuit to mimic the thermistor.

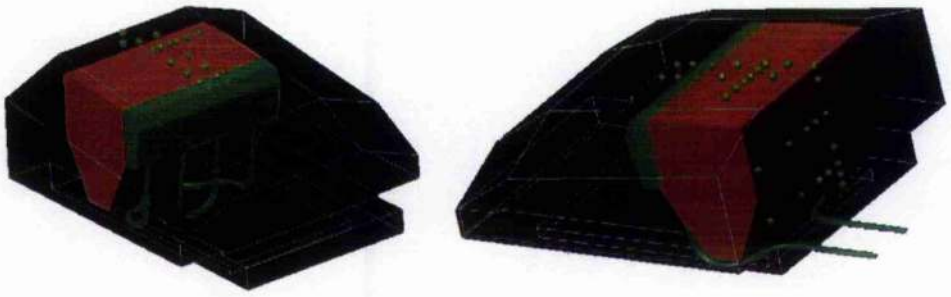

Figure 3-24 CAD 3D Views of Sensor Positions

Figure 3-24 is output from a CAD drawing of the engine compartment model and illustrates the position of the sensors, as guided by the CFD results, in relation to the fluid region and the engine block. The size of the sensors is exaggerated for clarity.

As noted above, initial sensor placement was derived from a modelled case using the approximate range of temperatures encountered on a real car model. It soon became apparent that it would be difficult to raise the experimental rig to these temperatures, and more importantly, sustain them for the course of the experiment. Figures 3-25 to 3-27 show the comparison between results from a FLUENT model using the envisaged car temperatures (hot) and the subsequently lowered engine block and manifold temperatures (initial) which more closely mimic the safe temperatures achievable in the experimental rig. These data confirmed that the sensor placements were satisfactory and that similar trends were obtained for various tunnel speeds.

From left to right in figures 3-25 to 3-27, the sensor banks are as follows:-

- Back : vertical at symmetry line, ie row 1 figure 2-10 starting at b12
- Back : horizontal at y = 155mm, ie row 2 figure 2-10 starting at b01
- Back : horizontal at y = 80mm, ie row 3 figure 2-10 starting at b10
- Top longitudinal at symmetry line, ie row 1 figure 2-11 starting at t06
- Top longitudinal at z=-118mm, ie row 2 figure 2-11 starting at t08
- Top normal to symmetry line at x=415mm, ie row 3 figure 2-11 starting at t09

For clarity, the corresponding sensor banks are indicated on figure 3-25 but not thereafter on figures 3-26 and 3-27.

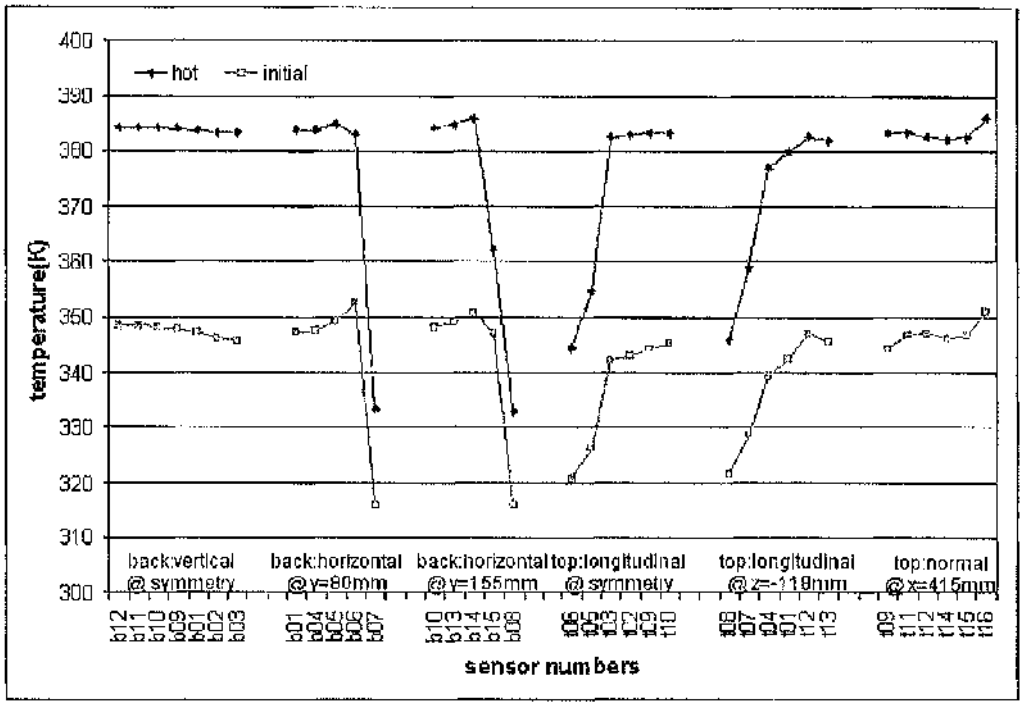

Figure 3-25 Computed Results across Sensor Banks using Hot and Initial Temperatures for 5ms^{-1}

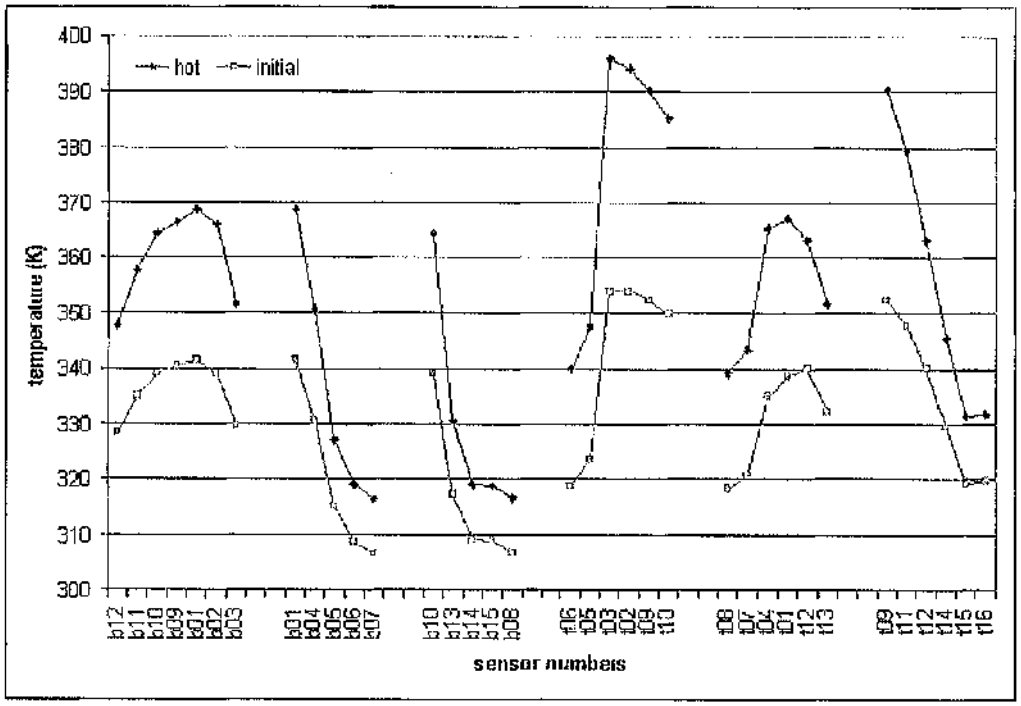

Figure 3-26 Computed Results across Sensor Banks using Hot and Initial Temperatures for 12.5ms^{-1}

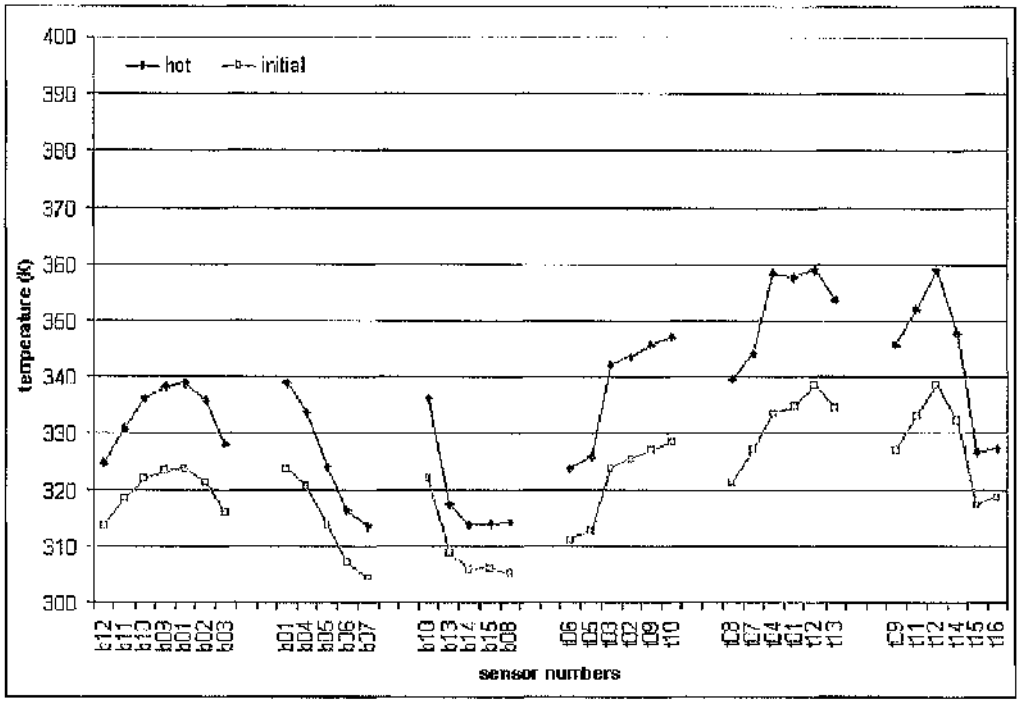

Figure 3-27 Computed Results across Sensor Banks using Hot and Initial Temperatures for 20ms^{-1}

One of the results of this set of simulations is the notably higher temperatures generated for the bank of sensors on the top symmetry line for the case at 12.5ms^{-1}.

It is also noticeable that the general trend is decreasing temperature with increasing speed. These particular data have been presented to re-assure the reader that the CFD clearly indicated that the final positioning of the sensors was acceptable for the lower temperatures of the experiment. The comprehensive predictions, with boundary conditions corresponding to the experiment are contained in table 3-1 to 3-6 and shown from figure 3-28 to figure 3-33. These show predictions for cases between 5 and 20ms^{-1}. These are presented in a similar fashion to the initial computed results. Temperatures are presented in Kelvin.

The convention of showing the sensor positions with offset axes is carried forward from figure 2-22.

Sensor	Position (mm)			Velocity (ms^{-1})						
Number	X	y	z	5	7.5	10	12.5	15	17.5	20
b12	491	50	-152	348.5	335.9	331.8	328.3	321.0	322.0	313.7
b11	491	65	-152	348.5	339.6	338.9	334.9	328.5	329.1	318.3
b10	491	80	-152	348.1	339.3	339.1	339.2	334.7	334.0	322.0
b09	491	105	-152	347.8	339.1	339.0	340.3	336.9	335.5	323.3
b01	491	155	-152	347.1	338.6	338.6	341.3	338.2	335.3	323.8
b02	491	205	-152	346.0	337.9	337.7	338.9	337.5	333.8	321.3
b03	491	225	-152	345.5	338.1	337.0	329.7	336.5	332.7	316.1

Table 3-1 Computed Results for Back Sensors (vertical centred) at Varying Velocities

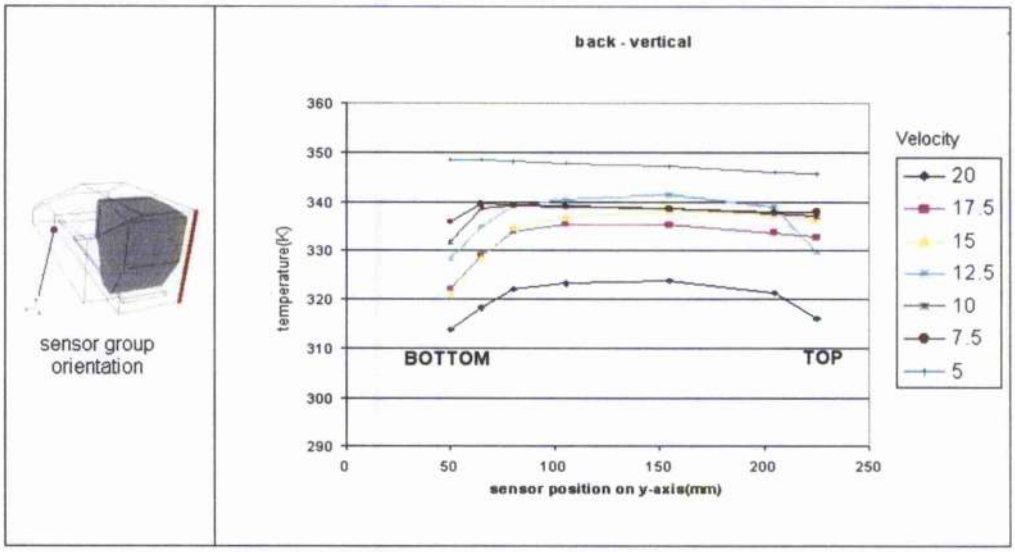

Figure 3-28 Computed Results for Back Sensors (vertical centred) at Varying Velocities

In figure 3-28, it is evident that not only, as mentioned before, the temperature drops with tunnel speed but also that the flow cools as it approaches the base of the model.

Sensor	Position (mm)			Velocity (ms^{-1})						
Number	x	y	z	5	7.5	10	12.5	15	17.5	20
b01	491	155	-152	347.1	338.6	338.6	341.3	338.2	335.3	323.8
b04	491	155	-130	347.4	338.9	339.0	330.7	327.1	332.0	320.5
b05	491	155	-110	349.3	340.1	338.4	315.0	316.4	317.1	313.8
b06	491	155	-70	352.5	341.9	318.5	308.7	308.8	308.6	307.1
b07	491	155	0	315.9	312.2	309.1	306.5	305.8	305.3	304.6

Table 3-2 Computed Results for Back Sensors (y=155mm) at Varying Velocities

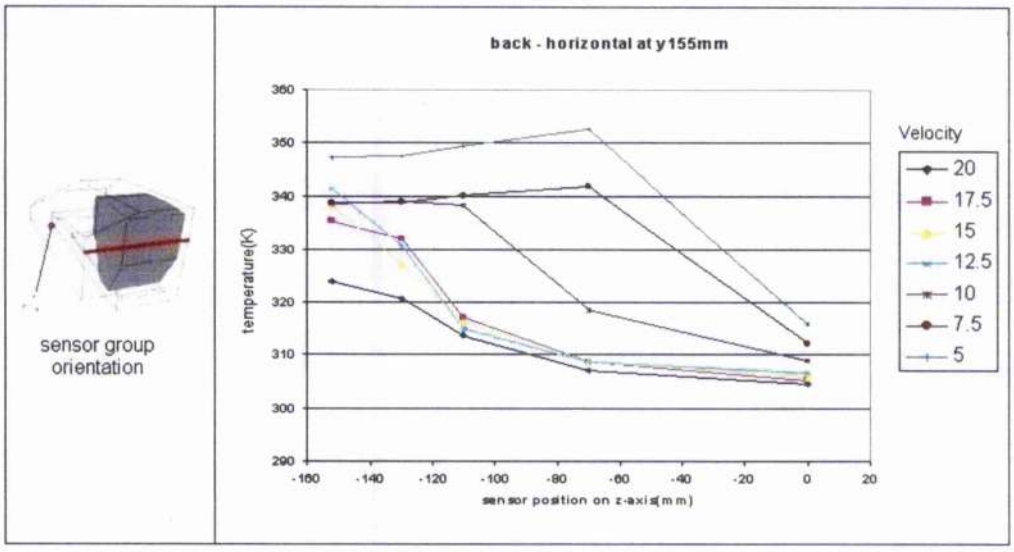

Figure 3-29 Computed Results for Back Sensors (y=155mm) at Varying Velocities

Sensor	Position (mm)			Velocity (ms^{-1})						
Number	x	y	z	5	7.5	10	12.5	15	17.5	20
b10	491	80	-152	348.1	339.3	339.1	339.2	334.7	334.0	322.0
b13	491	80	-130	349.1	340.0	332.1	317.1	312.3	311.9	308.8
b14	491	80	-110	350.8	339.3	322.8	309.1	308.0	307.4	305.9
b15	491	80	-70	347.0	339.8	322.2	308.8	307.6	305.8	306.0
b08	491	80	0	315.9	312.5	308.9	306.8	306.2	305.8	305.1

Table 3-3 Computed Results for Back Sensors (y=80mm) at Varying Velocities

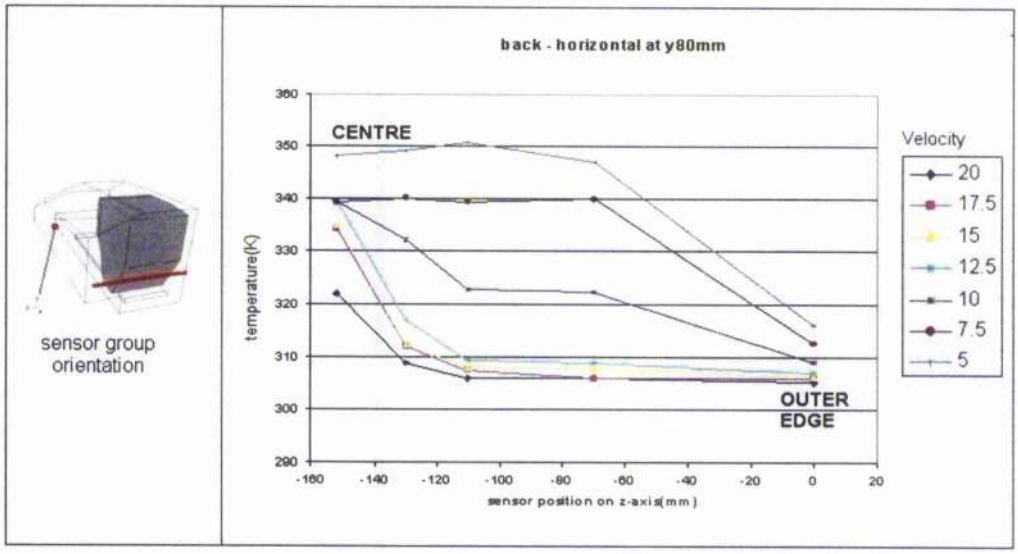

Figure 3-30 Computed Results for Back Sensors (y=80mm) at Varying Velocities

Figures 3-29 and 3-30 are more interesting for they are the two horizontal rows on the rear panel, at differing heights, and exhibit similar trends. More important, however, is the clear change at $10ms^{-1}$ where the inner parts temperature fell off rapidly rather than being held constant, to a first order. There is a definitive change in flow patterns and these can be observed more effectively in figure 3-34.

Sensor	Position (mm)			Velocity (ms^{-1})						
Number	x	y	z	5	7.5	10	12.5	15	17.5	20
t06	275	202.4	-152	320.7	316.1	315.8	318.7	312.8	310.7	311.1
t05	300	205.0	-152	326.1	320.8	319.7	323.6	315.0	312.4	312.6
t03	330	208.8	-152	342.1	334.1	334.8	353.9	328.4	324.9	323.7
t02	370	213.8	-152	342.9	335.2	335.8	353.8	330.3	326.7	325.3
t09	415	219.6	-152	344.3	336.3	336.7	352.4	332.6	328.8	326.9
t10	450	223.9	-152	345.1	337.0	337.4	349.9	335.0	331.2	328.3

Table 3-4 Computed Results for Top Sensors (Centreline) at Varying Velocities

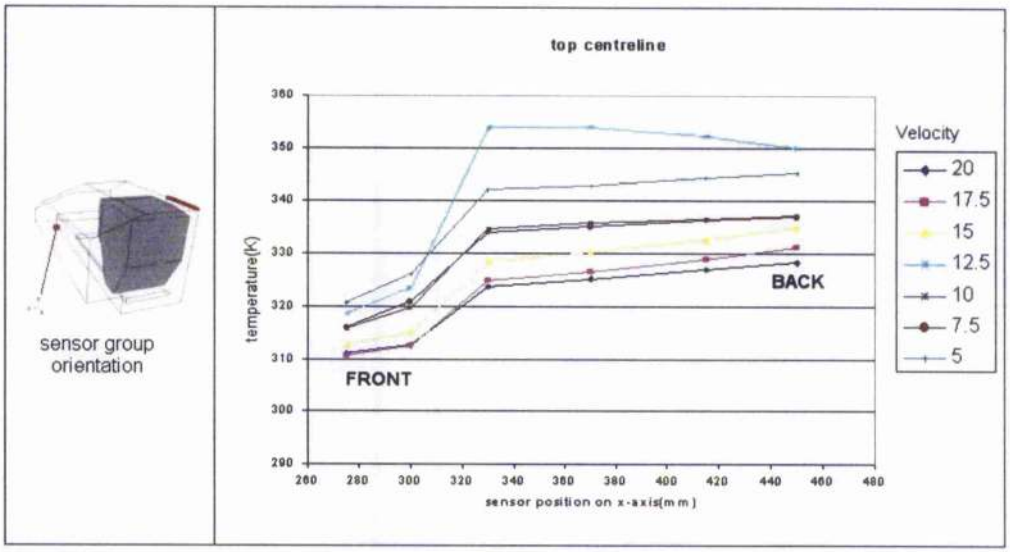

Figure 3-31 Computed Results for Top Sensors (Centreline) at Varying Velocities

Sensor	Position (mm)			Velocity (ms^{-1})						
Number	x	y	Z	5	7.5	10	12.5	15	17.5	20
t08	275	202.4	-118	321.6	316.7	316.7	318.2	319.0	316.8	321.3
t07	300	205.0	-118	328.6	322.9	322.0	320.6	326.4	324.1	327.2
t04	330	208.8	-118	339.2	332.3	332.7	335.0	342.7	338.8	333.5
t01	370	213.8	-118	342.4	335.0	335.8	338.7	340.0	338.1	334.6
t12	415	219.6	-118	347.0	339.4	340.3	340.0	341.2	339.5	338.7
t13	450	223.9	-118	345.5	337.2	338.1	332.3	335.0	333.6	334.3

Table 3-5 Computed Results for Top Sensors (offset at z=34mm) at Varying Velocities

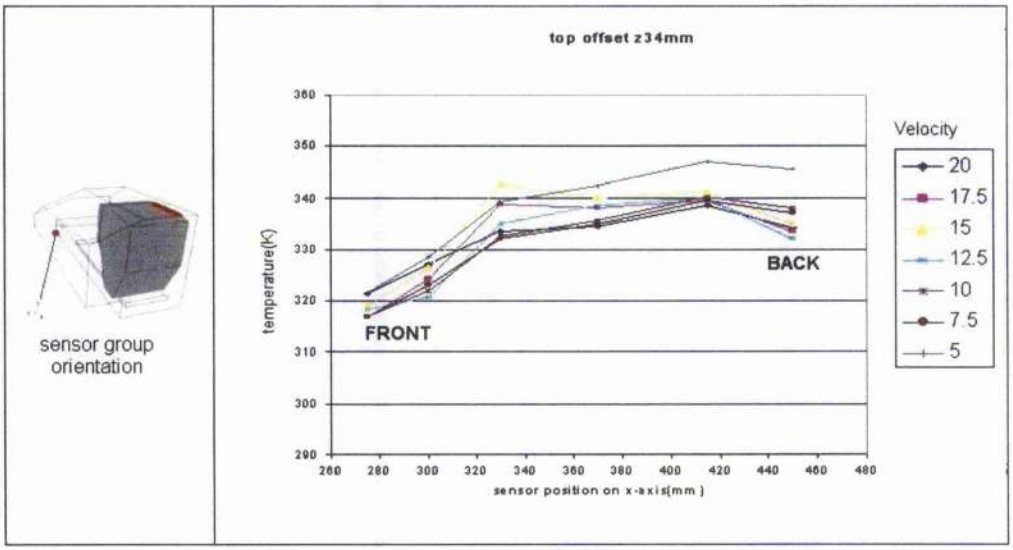

Figure 3-32 Computed Results for Top Sensors (offset at z=34mm) at Varying Velocities

Unlike the backplate, both the top longitudinal rows exhibit the same trends for all speeds. That of temperatures increasing along the x axis. This is hardly surprising as the fluid is convecting over a hot engine.

Sensor	Position (mm)			Velocity (ms^{-1})						
Number	x	y	z	5	7.5	10	12.5	15	17.5	20
T09	415	219.6	-152	344.3	336.3	336.7	352.4	332.6	328.8	326.9
T11	415	219.6	-137	346.8	339.5	339.9	347.7	341.3	337.9	333.0
T12	415	219.6	-118	347.0	339.4	340.3	340.0	341.2	339.5	338.7
T14	415	219.6	-105	346.0	337.6	338.7	329.4	330.7	329.9	332.2
T15	415	219.6	-85	346.6	337.4	338.8	319.2	320.0	320.0	317.3
T16	415	219.6	-63	350.9	341.4	333.1	319.7	319.9	319.9	318.7

Table 3-6 Computed Results for Top Sensors (Normal at x=415mm) at Varying Velocities

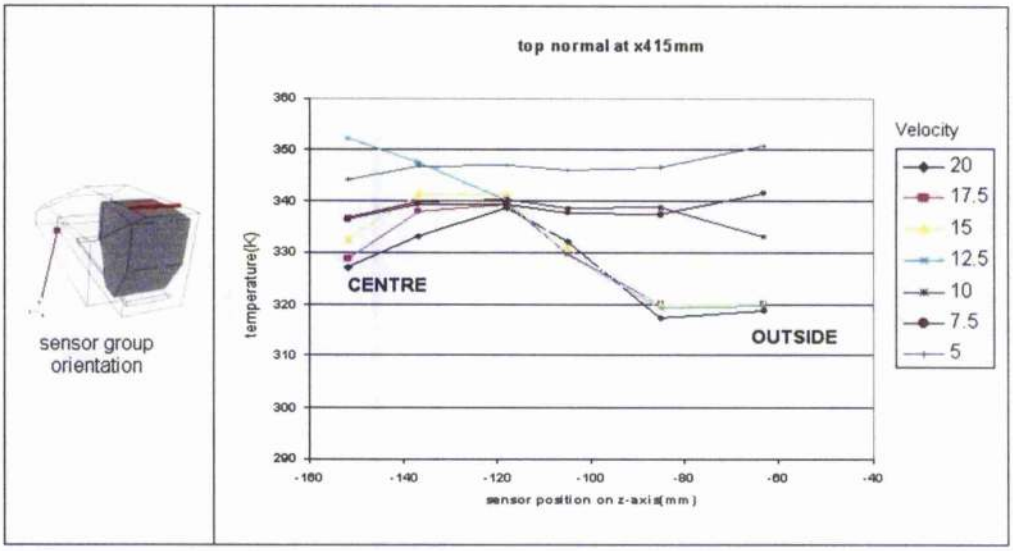

Figure 3-33 Computed Results for Top Sensors (Normal at x=415mm) at Varying Velocities

Figure 3-33 displays the prediction of the lateral temperatures and, like the corresponding profiles for the rear wall, displays a significant change in form from low to higher speeds. Here, however, the change in flow state occurs at $12.5ms^{-1}$. This is characterised by a rise in the centreline temperatures well above all others and then, for the higher speeds, a rise at the outside and a decrease at the centre to almost level profiles.

3.6. DISCUSSION

From the computed data, there appears to be a broadly consistent cooling trend for the sensors at the back of the engine compartment. It is notable, however, that there is no clearly discernible trend for the longitudinally placed sensors and two distinct trends for the laterally placed sensors, with a transition occurring at 12.5ms^{-1}. This is shown clearly in figure 3-34, in which the formation of the plume behind the downpipe at the 34mm (z=-118mm) offset is apparent. At 10ms^{-1} and below, the formation of this plume is not apparent and there appears to be significant activity behind the downpipe offset at 102mm (z=-50mm). This region was not chosen for monitoring, however, as the original design (ie including a viewing panel) militated against placing sensors in this region.

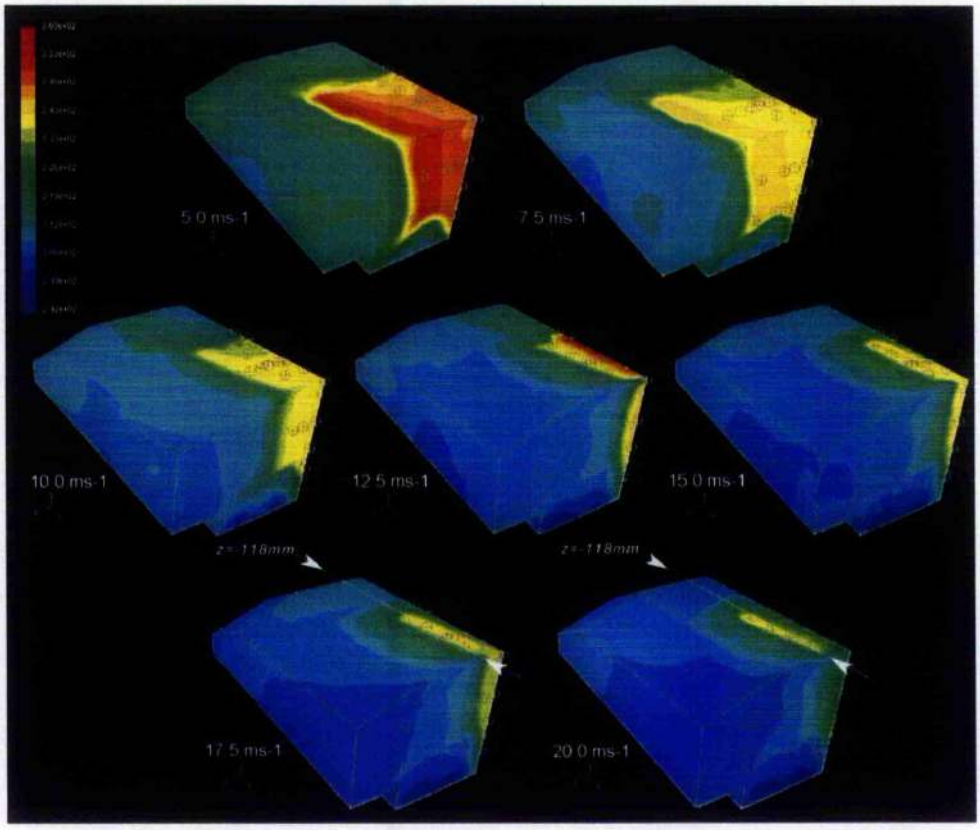

Figure 3-34 Effect of Increasing Speeds on Thermal Field

Note that the plume at the 34mm offset from the centreline (z=-118mm, shown in figure for 17.5ms^{-1} and 20ms^{-1} cases) only develops at the higher speeds. Sensor placement at the rear appears to be reasonably accurate, although more sensors would be beneficial at the top of the engine compartment. As noted earlier in this section, the inclusion of a viewing panel made it difficult to site sensors even at the 102mm offset (z=-50mm) of the second downpipe, although from the results at this early stage it would appear that this would be beneficial (see section 5.4.2)

3.7. CONCLUSIONS

This chapter has indicated the various "steps and turns" that the author has made to finally formulate an engine compartment that was successfully meshed and used by FLUENT to predict the flow within it. The data obtained were used to guide the placement of sensors within the physical engine compartment.

On further investigation, the number of sensors at the rear were found to be sufficient but for the top sensors, more configurations would be required. These initial pre-experiment temperature settings, against which initial measured data were compared were chosen as freestream=295K, engine block=400K manifold =500K and downpipes = 600K. Due to the envisaged difficulties in maintaining the higher temperatures typically associated with a car engine compartment while using the experimental rig, and the consequent risks involved in using such high temperatures within the wind tunnel.

4. Comparison with Measured and Simulated Results

4.1. Introduction

Experimental data presented in this section were derived from reduction of raw data as described in section 2.5.3.

This chapter presents the comparisons between the measured and the predicted temperatures on the surfaces of the engine compartment. It may be recalled (section 2.4.3) that the final placement of the thermistors was guided by the predictions of the suitably configured FLUENT CFD package. That configuration required a few initial values to be chosen such as free stream temperatures together with those of the engine block, manifold and down-pipe temperatures. As an estimate of what these should be the author was guided by the earlier work on the Morgan (section 2.2.2) carried out at the premises of KIS.

When the wind tunnel experiments were carried out, these initial temperatures were higher than those in the wind tunnel and so a new revised set of FLUENT predictions was made. The revised values were taken from that which was measured and also included atmospheric temperature, etc.. In other words, the revised calculations mimicked the experiments.

This chapter presents a comparison of both the initial and revised predictions with the data measured during the wind-tunnel experiments.

The initial and revised temperatures are given below in table 4.1

	Freestream	Engine Block	Manifold	Downpipe
Initial (All Cases)	295.0K	380K	520K	600K
Revised 5.0ms^{-1}	294.5K	379K	537K	621K
Revised 12.5ms^{-1}	294.4K	387K	542K	501K
Revised 20.0ms^{-1}	294.7K	383K	524K	421K

Table 4-1 Initial and Revised Temperatures

From the presented data, it is clear that the large disagreement between the initial predictions and the measured data has been greatly reduced. This is particularly so for the back-plate data where the revised data are in good agreement with with the measurements. The comparable agreement for the top surface is much poorer and indeed displays anomalies that will require further investigation as part of any continued improvements.

4.2. Comparisons of Temperature on Rear Surface

In this section, the convention of showing the sensor positions with offset axes is carried forward from figure 2-22.

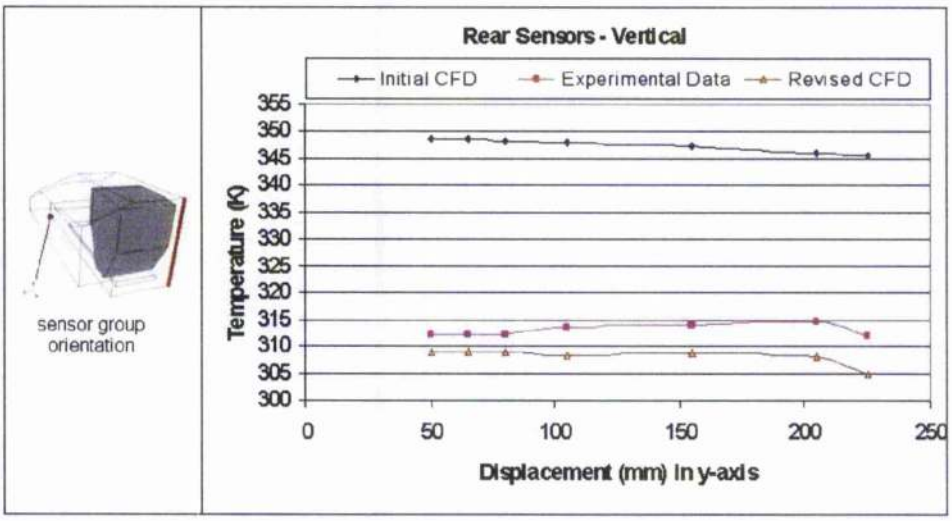

Figure 4-1 Measured and Simulated Data at Rear (Vertical) at $5ms^{-1}$

In the case shown in figure4-1, at $5ms^{-1}$, values from the initial simulation are much higher than the measured data, albeit there is a downward trend. Between the actual measured data and the revised simulation there is a more pronounced similarity, both in terms of temperature and trend and indeed may be said to be in reasonable agreement.

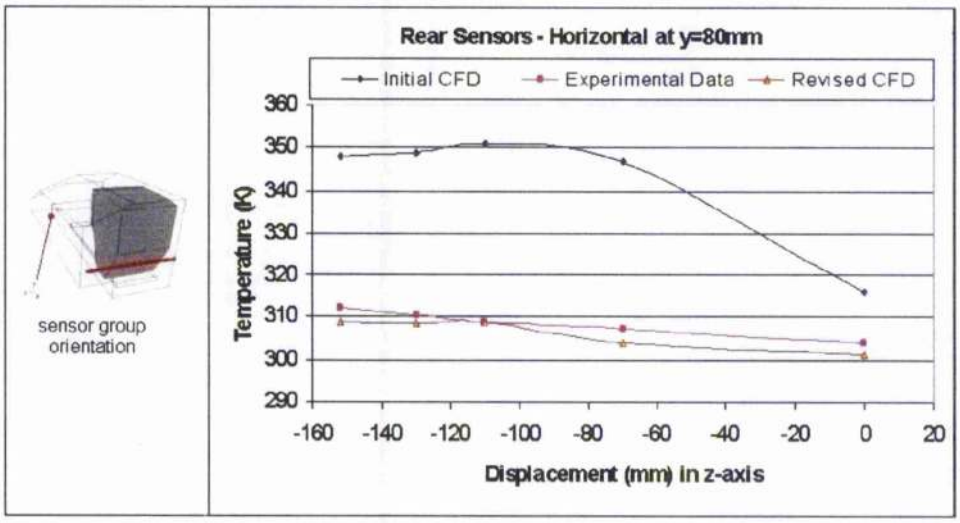

Figure 4-2 Measured and Simulated Data at Rear (Horizontal at y80) at 5ms^{-1}

Again, values from the initial simulation are much higher than the measured data and the downward trend away from the centre of the engine compartment is very pronounced. The actual measured data and the revised simulation are in good agreement. Perhaps a perplexing trend, however, is the greatly reduced variation in the revised prediction. A relatively small difference in the initial temperature has resulted in a much flatter profile.

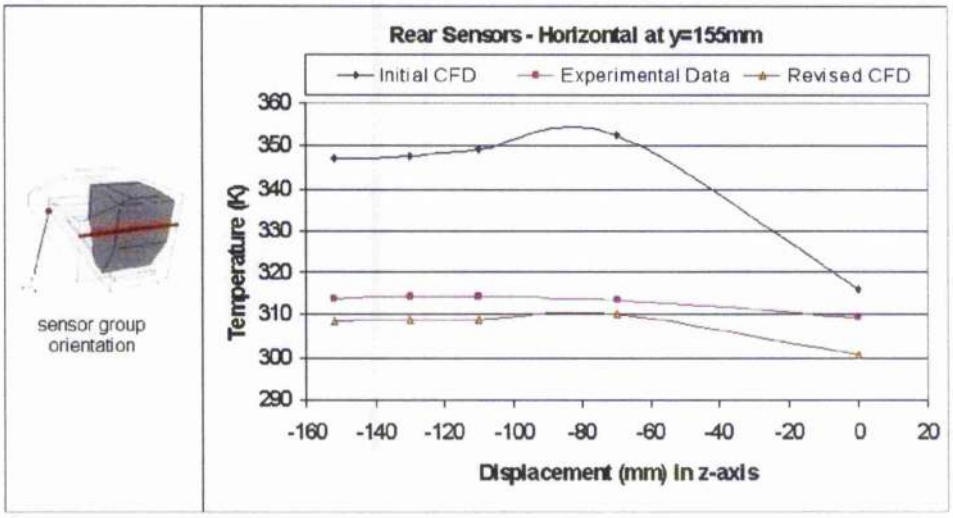

Figure 4-3 Measured and Simulated Data at Rear (Horizontal at y155) at 5ms^{-1}

The differences between the two simulations and the measured data are of a similar order to the previous data for rear sensors at $5ms^{-1}$.

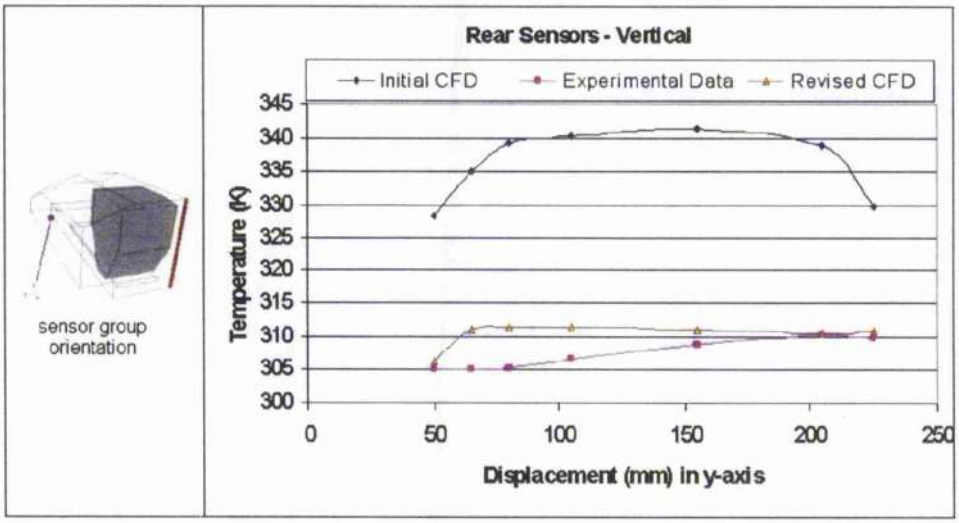

Figure 4-4 Measured and Simulated Data at Rear (Vertical) at $12.5ms^{-1}$

Initial values have a pronounced 'rise and fall' moving from front to back in the engine compartment. Revised values show a similar rise but no corresponding fall. Measured data are very close at both ends of the sensor bank but show a steady increase and thus diverge significantly from the revised data. Nonetheless, the temperature data are in much better agreement with the measured data than those of the initial values.

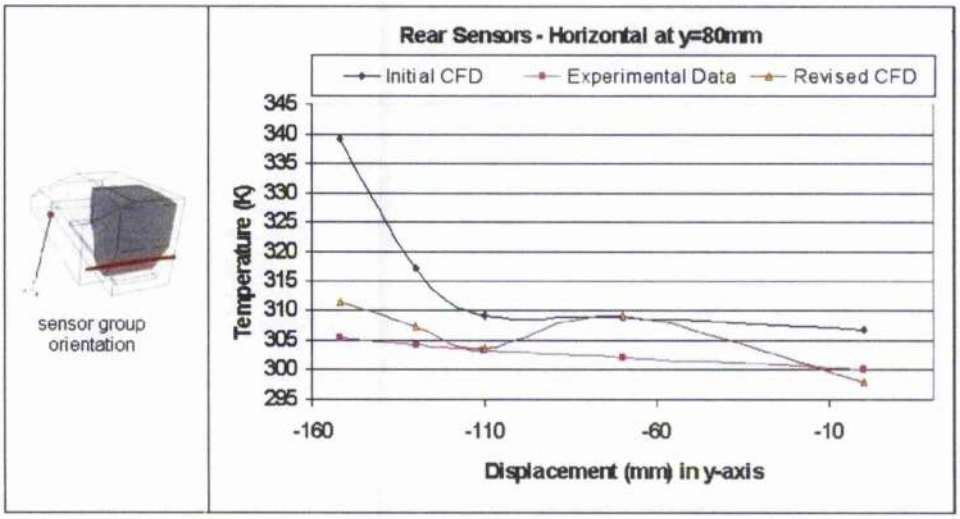

Figure 4-5 Measured and Simulated Data at Rear (Horizontal at y80) at 12.5ms^{-1}

Here there is very little similarity between trends for revised and initial values although there is a general downward trend. Measured data again shows a steady change over the length of the sensor bank and temperatures are similar to that of the revised simulation, apart from a divergence at z=–70mm (sensor B06). This divergence also occurs, for this sensor bank, in the 20ms^{-1} case.

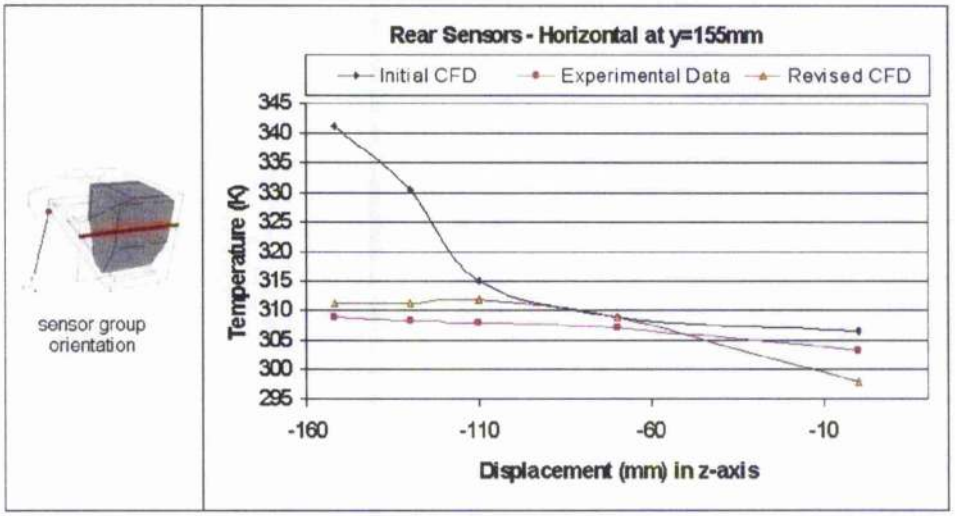

Figure 4-6 Measured and Simulated Data at Rear (Horizontal at y155) at 12.5ms^{-1}

Again, there is a steep downward trend for the initial data. There is a less pronounced downward trend for the revised data, although it must be noted that this is steeper than that of the measured data and, hence, has a higher temperature at the centre of the engine compartment and a lower value towards the outer edge. The agreement between the measured and revised prediction remains good.

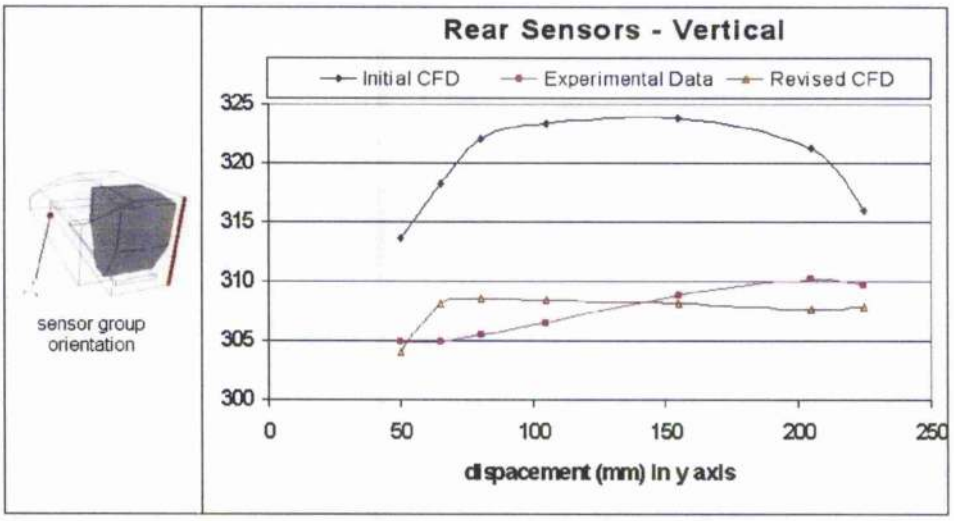

Figure 4-7 Measured and Simulated Data at Rear (Vertical) at 20ms^{-1}

Temperature range for revised data is within the range for observed data but there is little similarity in trend. This may be due to the choice of turbulence model which will affect the flow prediction when the flow is swirling. Note the similarity between all three cases and the corresponding ones for 12.5ms^{-1}. Once again, there appears to be a large sensitivity of FLUENT to the stated temperature inputs.

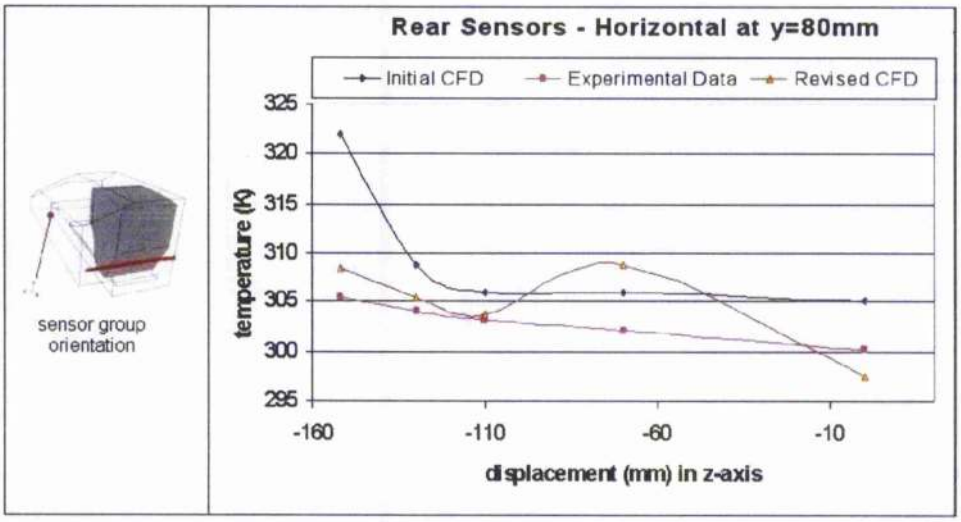

Figure 4-8 Measured and Simulated Data at Rear (Horizontal at y80) at 20ms^{-1}

Again, trends for all three sets of data is markedly similar to results for the 12.5ms^{-1} case. Revised data similar trend and temperature range discrepancies around z=-70mm.

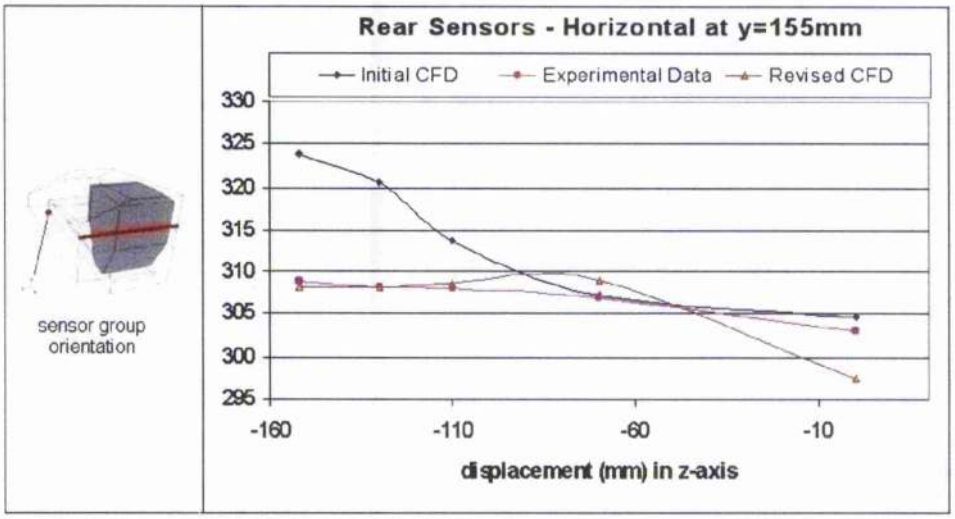

Figure 4-9 Measured and Simulated Data at Rear (Horizontal at y155) at 20ms^{-1}

Uncharacteristically, the initial, actual and the revised data all exhibit good agreement at about 50mm from the edge of the compartment. The revised and the measured profiles

are in reasonable agreement. Revised data exhibits a similar divergence from measured data at z=-70mm to the sensor bank at z=80mm for both 12.5ms^{-1} and 20ms^{-1} cases.

4.3. Top Surface of Engine Compartment

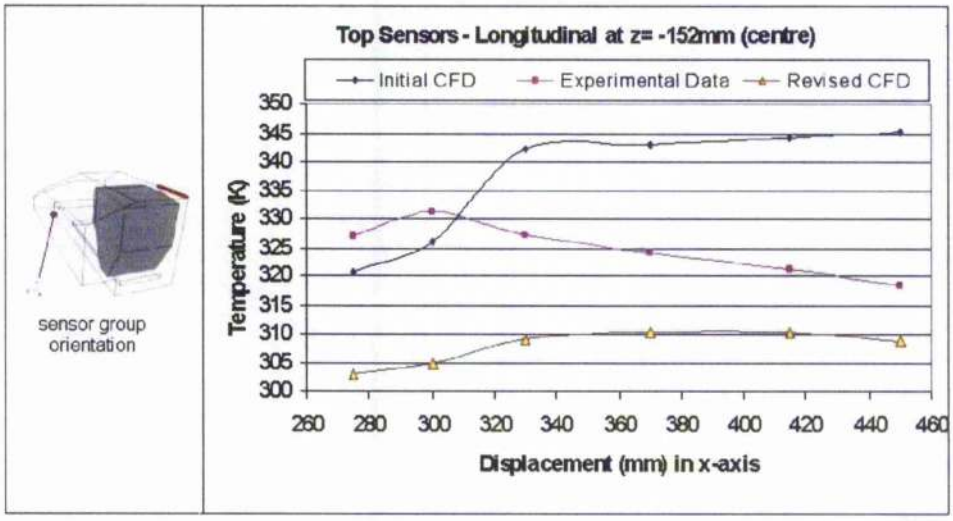

Figure 4-10 Measured and Simulated Data at Top (Centre) at 5ms^{-1}

Initial and revised data show a slight correlation, but the degree of change in the revised data from the initial is much less then that observed for the rear of the compartment. Actual data appear to have a downward and, hence, opposite temperature trend from front to back to that of the revised profile. In this case, when compared to the experimental data, the revised data is in equally poor agreement with the initial results.

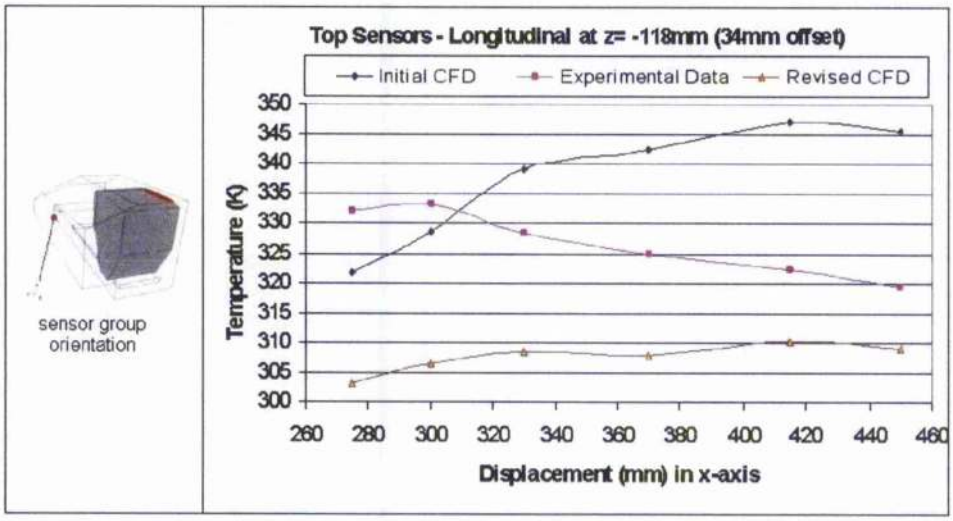

Figure 4-11 Measured and Simulated Data at Top (z34) at 5ms^{-1}

Again, data from both simulation have a similar trend but a significantly different range of values. All agreement is poor.

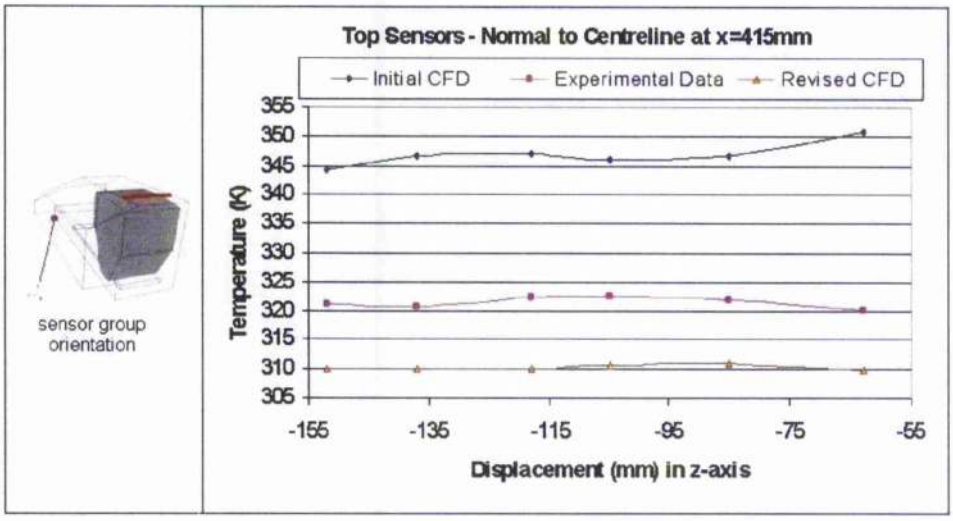

Figure 4-12 Measured and Simulated Data at Top (x415) at 5ms^{-1}

In this case, there is, at least a similar trend between revised and actual data although temperature ranges are still considerably different. Initial and revised, however, differ widely in both temperature range and trend.

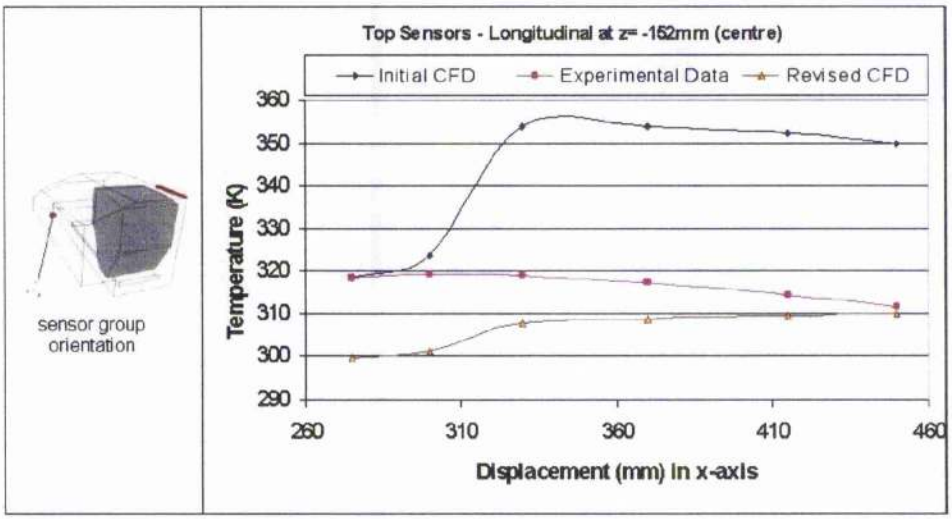

Figure 4-13 Measured and Simulated Data at Top (Centre) at 12.5ms^{-1}

Again, (figure 4-13) these are typical results for top of engine compartment. No particular correlation between observed and either revised or initial data, although there are slight similarities in trend between initial and revised simulations.

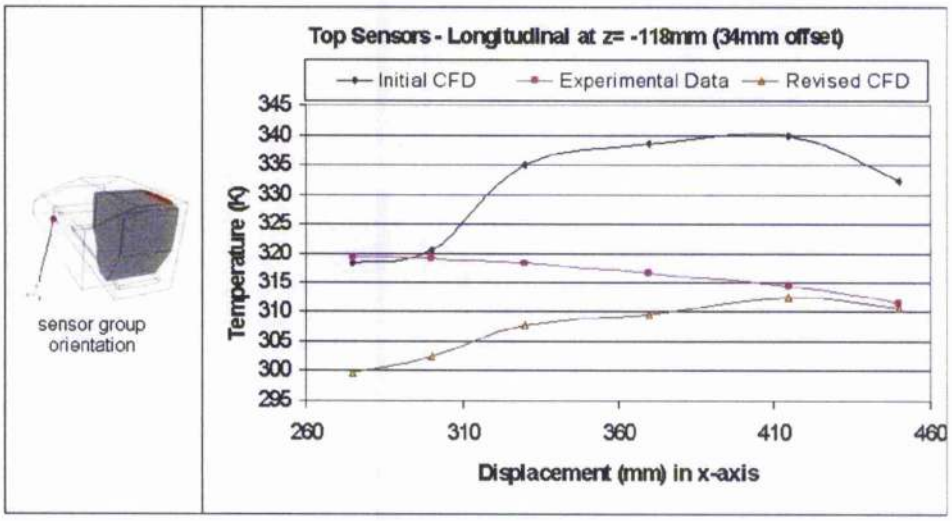

Figure 4-14 Measured and Simulated Data at Top (z34) at 12.5ms^{-1}

No discernible correlation between observed data and that from either case in figure 4-14. Similarities in trend are evident between the two simulations again, albeit the temperature ranges are very different.

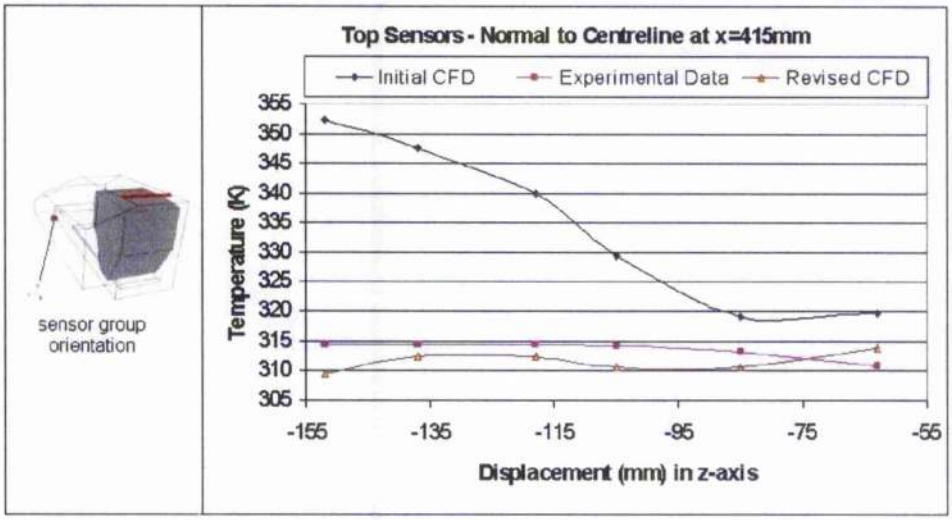

Figure 4-15 Measured and Simulated Data at Top (x415) at 12.5ms^{-1}

In figure 4-15, there is reasonable agreement between the revised and measured data. The temperature ranges for the measured and revised data, it should be noted, are much closer for the lateral sensor bank than for the longitudinal sensor banks. Nonetheless, FLUENT again displays large disparities between the initial and revised profile.

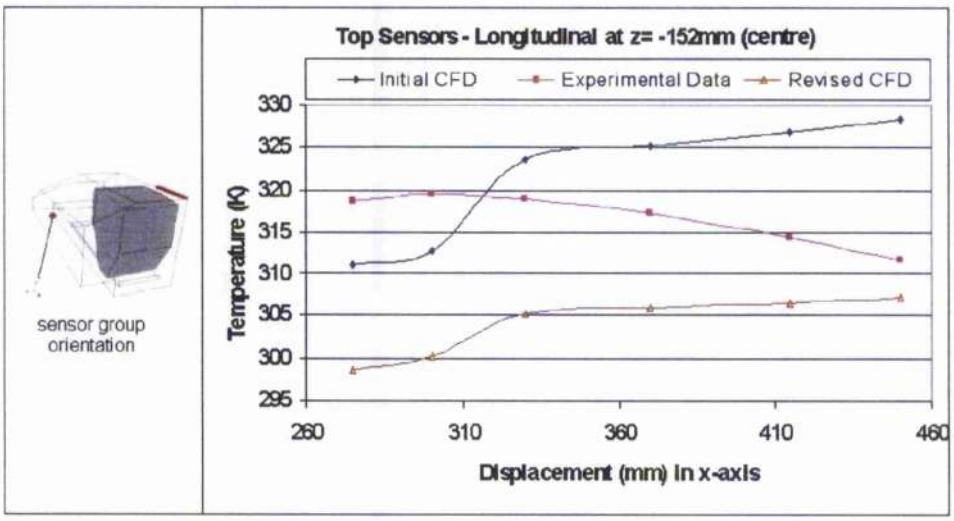

Figure 4-16 Revised Values at Top (Centre) at 20ms^{-1}

In figure 4-16, neither of the computed trends are akin to the measurements and are largely in poor agreement. Both simulations, however, exhibit similar trends but for very different temperature ranges.

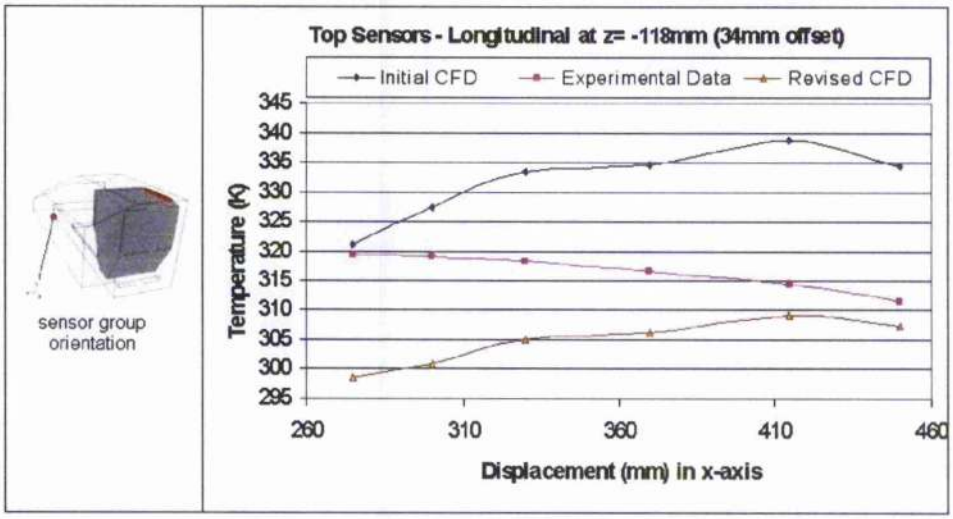

Figure 4-17 Measured and Simulated Data at Top (z34) at 20ms^{-1}

In figure 4-17, the comments of that for figure 4-16 are valid. both simulations exhibit similar trends but very different temperature ranges.

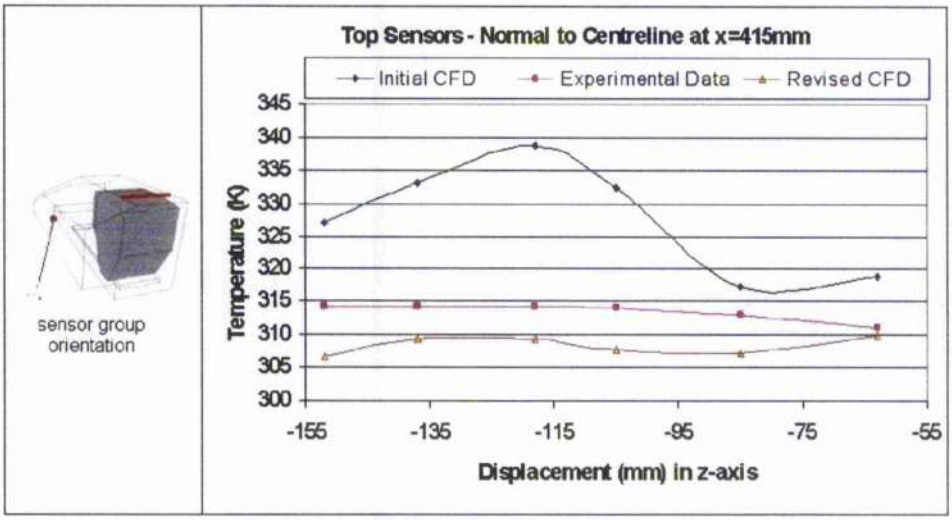

Figure 4-18 Measured and Simulated Data at Top (x415) at 20ms^{-1}

In figure 4-18, no particular correlation between simulations but the agreement between the revised and measured data is reasonable, but only just.

4.4. Discussion and Conclusions

The data from the rear panel sensors have, in general, been in reasonable agreement with the revised computed values. The same comparisons on the top of the compartment, however, were poor. So much so, that sensor numbering was re-examined thoroughly and found to be correct.

Whilst these top surface data show poor correlation, in terms of absolute temperature the differences are of the order of 5%. To highlight these differences in an alternative format, the actual values of the sensor output have been plotted on the simulation output in the appropriate and corresponding colours in figures 4-19 to 4-24. This gives a more compact visual appreciation of the resulting comparison.

Values at the rear bulkhead (figure 4-19 to 4-21), while not corresponding exactly, are broadly satisfactory and occasionally require the sensor data to be highlighted to distinguish it from the background colour. The comparison of data across several velocities (table 2-4 to 2-9), in the initial simulations, exhibited considerably different temperature contours to those measured experimentally. For the measured data, the trends at each sensor configuration were similar, whereas the initial simulated data exhibited a significant change between the lower and higher velocities.

Top sensor placement was based on a well-defined plume evident, at higher velocities, on initial simulations. Although there are similarities in trends between the revised data and initial data, the formation of the plume is not as pronounced in the revised simulations and the changes in temperature contour appear similar to those found in the lower speed initial simulations (table 2-4 to table 2-9). This suggests that although the cooling effect is regular in reality, it is considerably harder to model than first envisaged.

It should be noted that the values at the top of the engine compartment show, as expected, little or no correlation (figure 4-22 to 4-24). The reason for this is unknown at present but may be associated with the effect of the insulation which was added to allow for the absence of the car body. Also, the simulation was on an exact copy of the experiment.

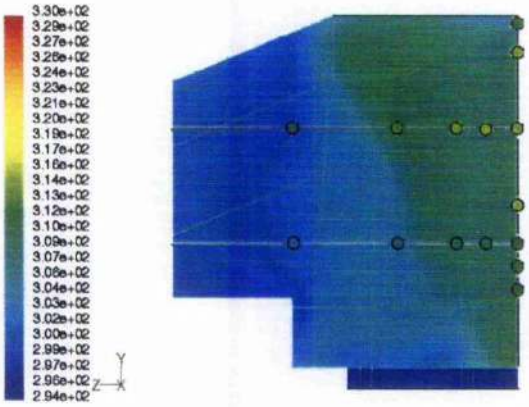

Figure 4-19 Simulated Temperature Contours at 5 ms^{-1} Back Panel

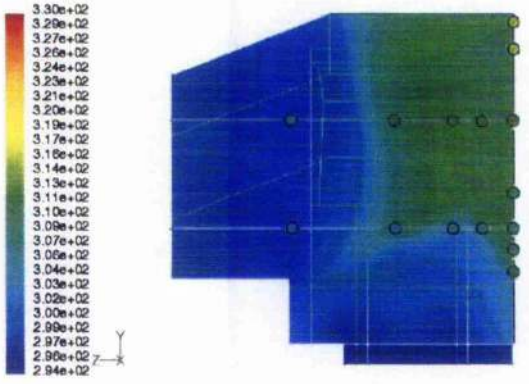

Figure 4-20 Simulated Temperature Contours at 12.5 ms^{-1} Back Panel

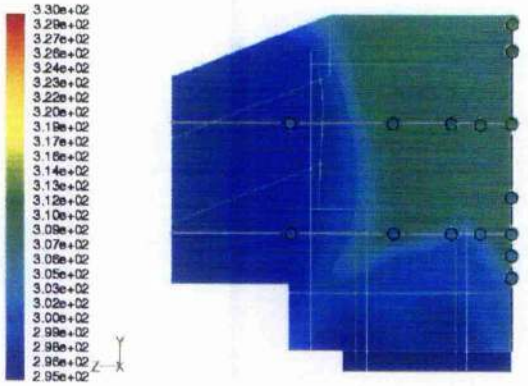

Figure 4-21 Simulated Temperature Contours at 20 ms^{-1} Back Panel

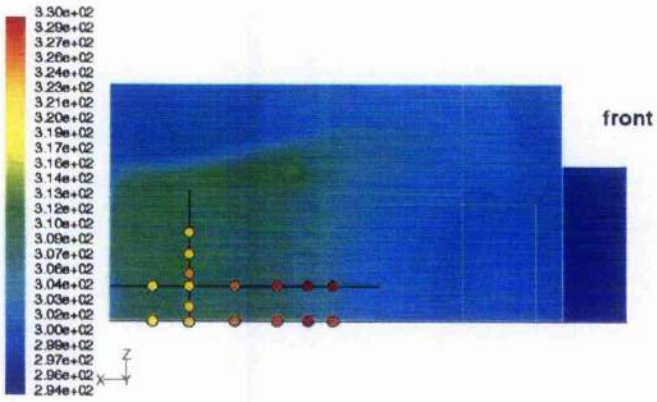

Figure 4-22 Simulated Temperature Contours at 5 ms^{-1} Top View

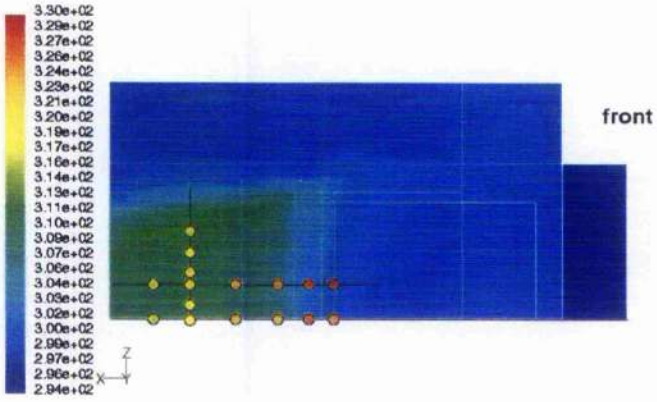

Figure 4-23 Simulated Temperature Contours at 12.5 ms^{-1} Top View

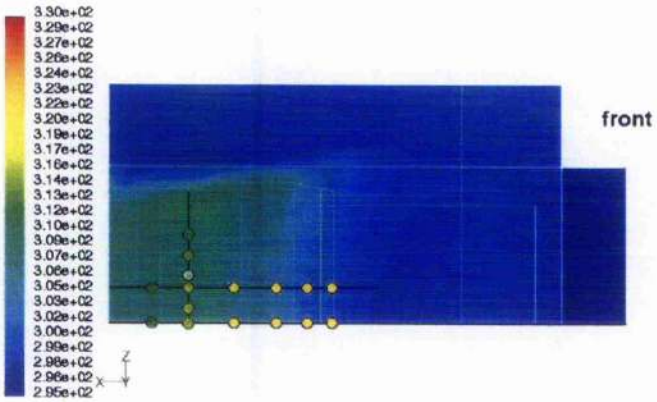

Figure 4-24 Simulated Temperature Contours at 20 ms^{-1} Top View

5. Conclusion and Further Work

5.1. Overall Main Conclusions

It appears from the comparisons of Chapter 4 that the assumptions for using the model engine compartment on the chassis but without the bodyshell may have been inappropriate and that the engine compartment, when placed in the wind tunnel may not have been suitable for direct comparison with CFD prediction and vice versa. This then suggests the CFD simulation should perhaps have included external flow as well as the internal volume considered. Further, had sufficient computing power been available, then the CFD simulation could have included the model and wind tunnel. This would have highlighted the true disparities between the data sets.

Accordingly, most evident from this work is the conclusion that isolating a complex geometry such as the engine compartment from its overall environment is not a particularly efficient methodology for tackling this type of problem. It is undoubtedly a better strategy to include as much of the surrounding geometry as is permissible by computing power, ideally a full body simulation. As noted in chapter 2, however, these tend to require several million mesh elements. The trend within the industry has been to exploit computer power as it becomes available rather than break down a problem into component parts. This research tends to confirm that this will remain the most valid strategy for numerical simulations for some time.

Adaption of the mesh also proved to be a problem in that adapted meshes in FLUENT could not be used with a number of radiation models. Most significantly, the S2S model could not be used when it became available without complete remeshing. It was decided not to incorporate this model. Additionally, running the associated simulations thereafter

would also take considerably longer than those without radiation modelling. In cases where radiation models are to be employed, therefore, the mesh quality has to be addressed at the outset. This may have to take place by considering the design of the mesh on the basis of a number of initial simulations.

Experimental results simply did not correlate with simulated data at the top of the compartment whereas those data at the rear of the engine compartment were, in many cases, very encouraging. This appears to show that the assumptions made were valid in some cases and not others. This certainly shows that an iterative approach to design using simulated and experimental data is a viable strategy.

CFD will no doubt become, as CAD has, a reasonably priced desktop tool for the engineer, but experimental methods remain the most tangible and, often, acceptable source of data. The combination of both methods, where the expense of experimental testing is alleviated by creating test models based on initial simulations and then enhancing the simulation by use of measured data is an idealised situation. A facility incorporating dedicated computing hardware and a wind tunnel facility where rapid turnaround of results is possible would certainly be desirable.

5.2. Design Considerations

As noted earlier, the design was affected greatly by changing commercial circumstances within the original sponsor company, KIS Ltd. This necessitated that the project became effectively independent within the university. It soon became apparent that a very complex geometry based on an actual production car would severely impinge on the computing facilities available and that a simplified generic solution would have to be adopted.

As the intention was to then integrate this work with the work of Sheng (2003), it also became apparent that modelling the engine compartment within the full car model would be limited by the available computer resources. Consequently, Sheng's work, to which the author contributed, comprised modelling the closed body car model within the working section of the Argyll wind tunnel, whilst this work concentrated on the airflow within the engine compartment itself.

5.2.1. Modelling

ACIS modelling was chosen, as noted previously, because of the ability to create models and alter them within a short space of time using a CAD package. The dedicated meshing program, GAMBIT, was not used for geometry generation because of the poor real-time response of the visual interface on the computing facilities available. This was a problem to such a degree that it was found that using the command line interface could be more efficient. As this requires the user to define all geometry and the operations on it manually, it is easy to appreciate how time-consuming the process could be. This is not an insurmountable problem where simple geometries are concerned but more complex ones require a great deal of attention.

Sheng's work was completed largely in GAMBIT but this involved modelling the fairly regular geometries of the working section and importing the car geometry in from IGES format. Additional geometries were, as with this work, created as ACIS models and imported.

With greater computing power, these deficiencies would be alleviated and all geometry could be directly created in GAMBIT. This would certainly be preferable, as the dedicated nature of the software would alleviate some of the problems encountered, such

as the creation of contiguous boundaries. The main advantage of the CAD package, the creation of engineering drawings, is not an issue, in this case, as ACIS models can be imported from GAMBIT for this purpose.

5.3. Experimental Considerations

It was decided to run the experiments without the car body for two reasons. As noted earlier, the originally proposed wind tunnel facility was not available and there was also a perceived fire risk. For safety reasons, this latter concern greatly influenced the decision.

Insulation was originally added to the engine compartment to protect the car body but, in the configuration that was eventually adopted, this was assumed to be an insignificant factor due to the airflow directly over the compartment. This, however, may have been one of the major factors affecting the results at the top of the compartment.

5.3.1. Viewing Panels

The panel at the top of the engine compartment was incorporated as the use of IR imaging, rather than direct sensing, was envisaged at the outset. In the final model, however, this was not possible and so sensors were mounted on an aluminium plate which was fitted in the same configuration as the viewing panel. As noted above, sensor position area was dictated by the position of this panel at the top of the engine compartment and restricted their placement to some extent. The detailed placement within this area was, of course, guided by the CFD.

The viewing panel at the side of the compartment was not used for sensors and was simply sealed with a blanking plate.

5.4. Further Development of Test Rig

5.4.1. Viewing Panel

It was considered that interchangeable panels would be useful for general experiments incorporating visualisation techniques and thermal studies using IR cameras but, as there is no facility for IR viewing becoming available, or could be borrowed within the department, it would be reasonable to reconstruct the top section of the model without the viewing panels. Ideally, if this work is to be continued in some form, two engine compartments could be created, one for visualisation and another for direct sensing. In this case, positioning of instrumentation would not be dependent on the need for transparent sections and the consequent problem with fouling would be negated.

5.4.2. Sensors

For temperature sensing within the ranges observed, the arrangement of thermistors performed well. The thermistors were calibrated to work within a given range and it was observed that they could go out of range when there was no airflow and before the engine block had cooled. It is not unreasonable, therefore, to suggest that for experiments which investigate wider temperature ranges that sensors could be arranged in discrete banks for different areas with wider variation in temperature gradients.

The positioning and density of the sensors can also be addressed. The linear positioning of banks of sensors was chosen due to the perceived time benefit in deriving simulation

data in this form rather than individual data points. In the final analysis, as the data points do not alter for different cases, there is no particular advantage to this method for as few as 32 sensors. The initial approach of targeting the areas with the most extreme gradients could be adopted more precisely (see section 3.5.4). The number of sensor positions, though, could be increased twofold or fourfold and the instrumentation extended to the front and sides of the model. In this case, the original decision to place the sensors in a linear arrangement would be justified but future work with a limited number of sensors should address them as individual points in space.

5.4.3. Additional Sensors

As sensor positioning at the top of the engine compartment was determined primarily by the removable panel, there was no consideration given to other types of sensors, which could be mounted. The addition of pressure sensors would be a welcome addition to the CFD validation process simulations. The original view that the engine compartment could be multifunctional militated against using a larger number of sensors than were actually used. If, as suggested above, a second engine compartment were constructed purely for non-visual experiments, this would allow the engine compartment to be fully instrumented with pressure and velocity sensing at appropriate points.

As noted earlier, there was some interest in using the engine compartment model for IR studies. This was deemed impractical due to the cost of sourcing the appropriate material for a viewing panel of this size. If, as suggested below, there could be a redesign of the front end of the car model to a more simplified configuration then it could incorporate a circular viewing panel in an IR transmissible glass or acrylic glass. In this case the IR camera could be mounted say within the instrument fairing in the Argyll tunnel. The instrumentation is shown below in figure 5-1 with the fairing removed.

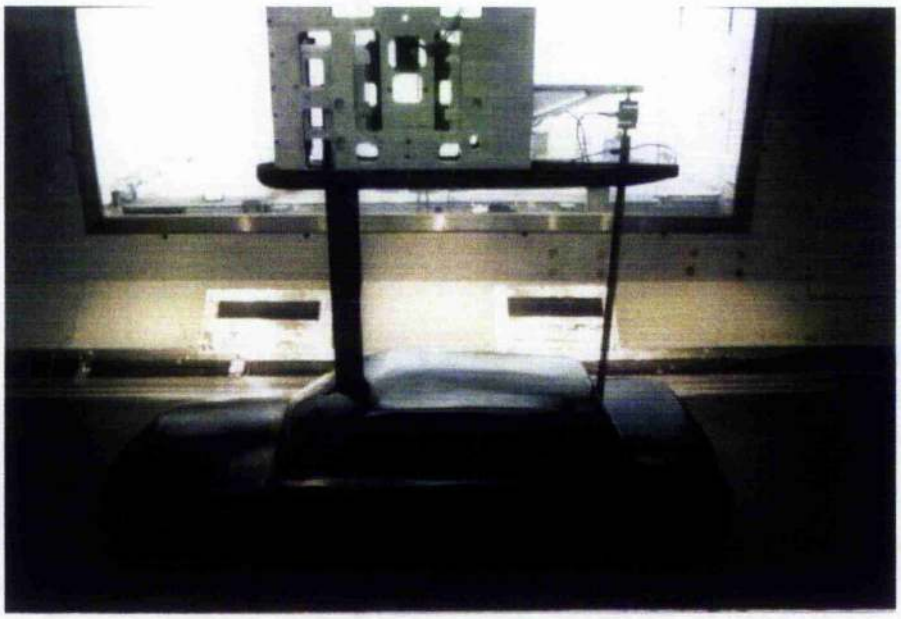

Figure 5-1 Car Model in Argyll Wind Tunnel

5.4.4. Heated Sections

It was originally envisaged that heating elements would be cast to the exact shape of the engine block. Again, this was deemed to be too expensive and the mixed medium solution was adopted. In the event of future research using this rig, this would be a desirable upgrade, as the power handling to the elements would be more controllable and the data available from the manufacturers would allow more accurate values to be incorporated into the simulations.

The surface temperatures in an actual vehicle would be less variable with airflow than those observed and controlling the elements to a given temperature and/ or a given power level would be welcomed. This would allow the use of the rig for temperature ranges which are not necessarily likely but which would allow general trends to be observed.

5.4.5. Insulation

It is to be hoped that the engine compartment will be incorporated into the full car body model at some stage but, as discussed in the previous chapter, much greater consideration has to be given in the modelling of insulated areas.

5.4.6. Simplifying Car Model

The motivation for creating a model around the car body shape, given in the FLUENT tutorial files, was to have a realistic model in the wind tunnel experiment. It would certainly be more convenient to construct a generic front end (up to A post) from aluminium for further experiments. The chassis extending from the back of this section should not adversely affect the experiment but flow visualisation should be used at an early stage in its development to confirm this. This arrangement would alleviate the problems caused by considering insulation materials in construction, test and simulation.

5.5. CFD Considerations

5.5.1. Mesh Generation

Ideally, when practical, the modelling should be completed entirely in GAMBIT rather than importing files from a CAD package. As greater computational facilities become available, all but the most complex geometries can be readily created in this manner.

Although care was taken to accommodate the properties of differing materials in and around the engine compartment, future work should address these in greater depth or, as noted in the previous section, incorporate a new generic front-end model.

Initial models of the simplified engine compartment based on actual car geometry (section 3.4.1) show clearly that the inner wings and fan were initially considered. Although the generic engine compartment itself is now complete, there is still scope for the inclusion of additional components geometry within it and it would be useful to model the fan. This would allow for the FLUENT fan model to be incorporated to some useful effect.

The assumption was made, on the basis of initial simulations, that the main area of interest would be in the immediate vicinity of the engine block. Results have shown that the area further forward in the engine compartment is of interest. This suggests that the meshing should have been finer throughout the engine compartment although this was not a realistic prospect at the time.

Initial tests with energy models showed no significant improvement on the basic cases other than smoother temperature gradients and broadly lower temperatures. This certainly suggests that the radiation model can be left to be incorporated at a later stage of development. The surface to surface (S2S) radiation model was made available late in the lifecycle of this project and would have required a very considerable effort to incorporate into the cases already completed but it would be hoped that it could be incorporated into future work given the claim that it is up to 4 times less processor intensive than the DTRM model.

5.5.2. Boundary Conditions

Although temperatures were measured at various positions around the engine block and engine compartment, the anomalies at the top of the engine compartment suggests that the airflow encountered in that area was not as predicted. In retrospect, the use of airflow

measurement should have been incorporated into the experimental model to provide feedback for modelling the inlet and outlet more accurately.

In addition the modelling of these areas, specifically the outlet, should, in future, be modelled as contiguous sections rather than as a single area.

5.5.3. Radiation Modelling

As noted in previous chapters, there were limitations in the use of radiation modelling due to the computing power available at the time. This has since been addressed and the S2S model should be incorporated.

5.6. Alternative Development Paths

As noted in the introductory chapter, this project was originally driven by the problem of positioning of electronic components in the underhood environment. To some extent, since the research was first undertaken, this has become less of an issue. However, if the other suggestions in this section are incorporated into future work, it would still be reasonable to include scaled component housings with one of the following properties either:

- Temperature sensing: using thermistors or thermocouples. This, however has the added problem of cabling;
- Pass / Fail test : including a grid of temperature sensitive materials within the housing and studying deformations after experiment.

Transient testing was discussed at the outset of the project and this was the basis of the chassis dynamometer testing. Although this was a crude tool for the type of experiments that would have been required there was some discussion of the use of engine dynamometers and environmental chambers and the combination of data from different series of experiments. This avenue of testing was effectively closed down by the company's liquidation but is still there to be explored. A more esoteric (and expensive) approach to this type of testing would be to mount an engine dynamometer within a modified car body shell and take measurements from the transmission rather than the wheels. The torque forces of the dynamometer and engine could be balanced within the rig by electro-rheological suspension units. This would allow the experimental rig to be tested in a full-scale wind tunnel. Of course, a project on this scale would be prohibitively expensive and would require the involvement of a manufacturer but, again, it is still a possible avenue for research and would be a single solution rather than requiring the integration of data from various experiments.

5.7. Commercial Exploitation

The project had its origins in the commercial automotive environment. That motivation is still there. The generic test model and the FLUENT simulation illustrate that the process is very complex and will require much skill in its proper interpretation. As such the importance of the work to commerce has increased over the original assessment.

A possible development path, which was briefly explored in the early work at KIS Ltd., was the integration of this type of work with 1D engine simulations. A method for exploring more realistic simulations of actual temperatures based on factors such as engine load under differing conditions would be welcome but may be prohibitively costly in terms of man/hours.

Another factor which impinges on the commercial worth of this work is the recent interest in alternative fuel vehicles and hybrid electric vehicles (HEVs). Due to comparatively greater engine compartment temperatures in HEVs, in particular, there has been a general trend to increase the temperature rating of electronic components. Similarly uprated components are, consequently, now being adopted in IC engines (BERGER 2002) and may affect the placement of components further still.

5.8. Conclusion

As shown in chapter 4, the data derived from the top of the model showed little correlation either in temperature range or trends. The possibility that the sensor numbers were in error was considered briefly but they are confirmed to be as *per* the design. This would tend to suggest that the shape of the entire car body is very much more significant to the underbody pressure than previously thought and that the flow at the top of the engine compartment may be considerably greater than suggested by initial simulations. It was also assumed that the insulation applied to the engine compartment would not be significant as it was applied mainly to protect the car body from the engine compartment. It was also assumed originally that there could be a problem with cooling due to insufficient insulation and this was certainly not the case, the area in question being considerably warmer than data derived from either the initial or revised simulations

Further simulations where heat generation terms were grossly overestimated made no significant difference to the simulated results. Use of the P1 radiation model also had little effect on the results. The simulations for the top of the engine compartment should therefore be attempted again with the engine compartment and car body geometry fully

integrated as the problem in this area has been too complex to decompose. Both the simulations and the experiments must be closely scrutinised and improved.

Full car body simulations show a very slight pressure differential below the car when it is at a comparable height to the ones used for this experiment. When these pressures were substituted into early cases they showed very slight differences, as might be expected, from the cases where a neutral pressure was incorporated. It was also assumed that the lack of a moving ground would also be insignificant, given the ground clearance of the model, but this may prove not to be the case. Without pressure sensors, it is difficult to tell but results suggest there is suction from the engine compartment at the front and that there may be a significant positive to negative pressure gradient rather than a neutral area, as assumed in the engine compartment simulation, or an overall negative pressure area, albeit a very slight one, as seen from the full car body simulations.

As noted above, the ability to model contiguous boundaries would prove useful in allowing an iterative approach to defining boundary conditions based on experiments. The poor results for the top of the engine compartment would appear to confirm the need for an iterative simulation and experimental approach.

The results show an acceptable correlation, however, between experimentally derived and simulated data at the rear of the engine compartment. This would also tend to suggest that the combined use of CFD and wind tunnel facilities in an iterative design strategy can be used to 'fine tune' a solution.

REFERENCES

Papers, Theses, Reports

Agarwal, R.K, Gschwend, K.,
1997
Thermal Analysis Of An Underhood Mounted Powertrain Control Module,
Automotive Engineering Nov 97,
23 -29

Aoki, K., Hanaoka, Y.; Hara, M.,
1990,
Numerical Simulation Of Three Dimensional Engine Compartment Air Flow In FWD Vehicles
Proceedings of the Society of Automotive Engineers
SAE Paper 900086

Ap, N.S., Golm, N. C,
1997
New Concept Of Engine Cooling System (Newcool),
Vehicle Thermal Management Systems 3
SAE 971775

Ashmawey,M., Berneburg, H.; Hartung, W.; Werner, F.,
1993
A Numerical Evaluation Of The New V6 Engine On The Underhood Environment Of The 1993 Opel Vectra ,
Proceedings of the Society of Automotive Engineers
SAE 930295,

Banerjee, P.,
1993
Automobile Underhood System Layout Design,
Proceedings of ISATA 26th International Symposium, Aachen, Germany,
93ME031
241 – 248

Bauer, W., Ehrenreich, H.;Reister, H.,
1995
Design Of Cooling Systems With Computer Simulation And Underhood Analysis Using CFD
Vehicle Thermal Management Systems 2,
IMechE C496/042/95,
499-511

Bauer, W., Reister, H.; Ross, F.; Robinson, D.,
1996
Parallel Computing For CFD Applications In The Automotive Industry - First Experiences
Lecture Notes in Computer Science No.1647
106-115

Bauer, W.,
2001
CFD As Part Of A CAE Driven Development Process : Experiences From The Automotive Industry,
STAR-CD DYNAMICS 16 (*Abridged Version*)

Berger, I,
2002
Can You Trust Your Car,
Institution of Electrical and Electronic Engineers Spectrum, April 2002
40-45

Berneburg, H., Cogotti,A.,
1993
Development And Use Of LDV And Other Airflow Measurement Techniques As A Basis For The Improvement Of Numerical Simulation Of Engine Compartment Airflows,
Society of Automotive Engineers Special Publication Pt-46 Vehicle Thermal Management
SAE 930294
349-364

Blisset, M.C., Austin, K.,
1999
Engine Thermal Management Comparison Between Predicted And Measured Results,
Vehicle Thermal Management Systems 4,
IMechE C543/087/99,

Brandt, R., Doorhy, B.;Sonday, S.,
1993
Thermal Analysis Of A Powertrain Control Module, ,
Vehicle Thermal Management Systems 1,
SAE 931090
181-185

Campbell, T., Galbraith, R.A.McD., Sheng, W., Fleming.A
2003
CFD Combining Wind Tunnel Data to Assess Aerodynamics of Road Vehicles
Proceedings of the Society of Automotive Engineers
SAE 2003-01-1250

Couetouse, H., Gentile, D,
1992
Cooling System Control In Automotive Engines
Proceedings of the Society of Automotive Engineers
SAE 920788
153-161

De Vos, G.W., Helton, D.E.,
1999
Migration Of Powertrain Electronics To On-Engine and On-Transmission,
Proceedings of the Society of Automotive Engineers
SAE 1999-01-0159
151-157

Dhaubhadel, M.N.,
1996
Review: CFD Applications In The Automotive Industry,
Journal of Fluids Engineering Vol.18,
647-653

Dhaubhadel, M.N., Shih, T. S.,
1996
Underhood Thermo-Fluids Simulation For A Simplified Car Model ,
American Society of Mechanical Engineers - Fluids Engineering Division Vol 238/3
249-254

Dohi, M., Sudou, Y.; Noguchi, H.; Kamada,N.,
1998
Airflow Simulation In Engine Compartment By CFD Analysis,
Proceedings of the Society of Automotive Engineers
SAE 982803,
1-7

Draper, E.J., Haidar,N.,
1999
CFD Investigation Into Effect Of Bumper Design On Flow Through A Van Cooling Pack,
Vehicle Thermal Management Systems 4,
IMechE C543/026/99

Emmelmann, H. J., Berneburg, H.,
1990
Aerodynamic Drag And Engine Cooling-Conflicting Goals?
Proceedings of the Society of Automotive Engineers
SAE 905128,
67-73

Ferguson, G.
2001
Private Correspondence

Frank, R., Krohn, N.; Shukman, H.,
1998
The Role Of Semiconductors In Automotive Powertrain And Engine Control,
Sensors Magazine Dec 98 (reproduced at www.sensorsmag.com)

Ghani, S.A.A.A, Aroussi, A.; Rice, E.,
2001
Simulation Of A Road Vehicle Natural Environment In A Climatic Wind Tunnel,
Simulation Practice and Theory 8,
359-375

Gilliéron, P., Samuel, S., Chometon, F.
1999
Potential of CFD Analysis Under-Bonnet Airflow Phenomena,
Proceedings of the Society of Automotive Engineers
SAE 1999-01-0802,
99-111

Gupta, R.K.,
1993
Materials Impact Of Automotive Thermal Management,
Vehicle Thermal Management Systems 1,
SAE 931078
83-92

Hajiloo, A., Williams, J.; Hackett, J.E.; Thompson, S.A.,
1990
Limited Mesh Refinement Study Of The Aerodynamic Flow Field Around A Car-Like Shape: Computational Versus Experimental Fluid Dynamics,
Society of Automotive Engineers Special Publication 1145: Vehicle Aerodynamics,
SAE 960677,
75-89

Han, T., Skynar, M.,
1992
Three-Dimensional Navier-Stokes Analysis Of Front End Air Flow For A Simplified Engine Compartment
Proceedings of the Society of Automotive Engineers
SAE 921091,
289-295

Han,T., Sunantran,V.; Harris,C.; Kuzmanov, T.; Huebler, M.; Zak, T.,
1996
Flow-Field Simulations Of Three Simplified Vehicle Shapes And Comparisons With Experimental Measurements,
Society of Automotive Engineers Special Publication 1145: Vehicle Aerodynamics,
SAE 960678,
75-89

Hartsock, D., Herman, J.; Fletcher, J.; Byrd,T.,
1997
Development Of A Test Procedure For Ranking Underhood And Underbody Heat Shield Materials And Designs,
Vehicle Thermal Management Systems 3,
SAE 971820,
387-397

Hyslop, S.M., Palmer, P.J.; Williams, D.J.,
1999
Tools For System Specific Packaging For Electro-Mechanical Systems,
Proceedings of the IEEE/CPMT International Electronics Manufacturing Technology (IEMT) Symposium,
395-401

Igarishi, I.,
1986
New Technological Of Sensors For Automotive Applications,
Sensors and Actuators 10 (1986)
181-193

Jung, J., Hur, N.; Kim, K.H.; Lee, C.S.,
1991
Analysis Of Engine Cooling System For A Passenger Vehicle,
Proceedings of the 6th International Pacific Conference On Automotive Engineering,
SAE 912505,
437-443

Kataoka, T., China, H.; Nakagawa, K.; Yanagimoto, K.; Yoshida, M.,
1991
Numerical Simulation Of Road Vehicle Aerodynamics And Effect Of Aerodynamic Devices,
Society of Automotive Engineers Publication Pt.46 Vehicle Thermal Management,
SAE 910597
151-163

Katoh, N., Ogawa, T.; Kuriyama, T.,
1991
Numerical Simulation On The Three Dimensional Flow And Heat Transfer In The Engine Compartment,
Proceedings of the Society of Automotive Engineers
Proceedings of the Society of Automotive Engineers
SAE 910306,

Kern, J., Ambros, P.,
1997
Concepts For A Controlled Optimized Vehicle Engine Cooling System,
Vehicle Thermal Management Systems 3,
SAE 971816,
357-363

Kobayashi, H.,
1996
Four Essential Points In Developing Automotive Sensors,
Sensors and Actuators A57
53-63

Krishna, A.,
1997
Computational And Experimental Studies For Radio Thermal Management,
Vehicle Thermal Management Systems 3,
SAE 971860,
749-756

Li, P., Chui, G.K.; Glidewell, J.M.; Chue, T.H.; Lai, M.C.,
1993
A Flow Network Approach To Vehicle Underhood Heat Transfer Problem,
Vehicle Thermal Management Systems 1,
SAE 931073,
39-47

Luettgen, M.,
1998
Transient Thermal Analysis Of Power Electronics,
Proceedings of the 1998 Society of Automotive Engineers International Congress & Exposition,
SAE 980346,
49-61

Matsuda, Y.,
1991
Recent Environmental Demands On Automotive Connectors,
Materials Issues for Advanced Electronic and Opto-Electronic Connectors (ed Crane et Al.)
17-28

Minegishi, T., Uematsu,Y.; Shimonosono,H.; Yoshikawa,Y.,
1993
A Study Of A Practical Numerical Analysis Method For Heat Flow Distribution In The Engine Compartment,
Vehicle Thermal Management Systems 1,
SAE 931081,

Morris, S.C., Foss, J.F.,
2001
An Aerodynamic Shroud For Automotive Cooling Fans,
Journal of Fluids Engineering Vol. 123
287-292
Ono, K., Himeno, R.; Fujitani, K.; Uematsu, Y.,
1992
Simultaneous Computation Of The External Flow Around A Car Body And The Internal Flow Through Its Engine Compartment,
Proceedings of the Society of Automotive Engineers
SAE 920342

Paschal, K., Yao,C.; Bartram,S.; Shack,D.; Shih,G.,
1996
Turbulence Measurements Of A Simplified Underhood Automotive Flow,
Available from http://techreports.larc.nasa.gov/ltrs/PDF/1997/tm/NASA-97-tm110305v1.pdf
[Accessed June 2000]

Pierson, J.R., Johnson, T.,
1993
Development Of Automotive Battery Systems Capable Of Surviving Modern Underhood Environments,
Journal of Power Sources
237-246

Reister, H., Ross, F.,
1997
Numerical Simulation Of An Axial Cooling Fan,
Vehicle Thermal Management Systems 3,
55-59

Rubin Z.J., Mumm, S.A.; Moskwa, J.J.,
1997
The Development Of Vehicular Powertrain System Modeling Methodologies: Philosophy And Implementation,
Proceedings of the Society of Automotive Engineers
SAE 971089,

Sakai, I.,
1993
The Overview Of Japanese Automotive Thermal Engineering Current Status,
Vehicle Thermal Management Systems 1,
SAE 931103,
277-284

Saunders, J.W., Udvary, T.P.,
1991
Car Radiator Transient Response: Front-End Air Management,
Proceedings of the 6th International Pacific Conference On Automotive Engineering,
SAE 912504,
1541-1549

Selow, J., Wallis, M.; Zoz,S.; Wiseman, M.,
1997
Towards A Virtual Vehicle For Thermal Analysis,
Vehicle Thermal Management Systems3,
SAE 971841,
563-572

Shack, D. H., Bernal, L.P.; Shih, C.S.,
1995
Experimental Investigation Of Underhood Flow In A Simplified Automobile Geometry ,
American Society of Mechanical Engineers - Fluids Engineering Division Vol 217 (1996) : Seperated and Complex Flows
239-248

Sheng, W
2003
CFD Simulations in Support of Wind Tunnel Testing
PhD Dissertation
University of Glasgow Faculty of Engineering

Shimonosono, H., Shibata, Y.; Fujitani, K.,
1993
Optimization Of The Heat Flow Distribution In The Engine Compartment,
Vehicle Thermal Management Systems 1,
SAE 930883,
183-192

Sidders, J.A., Tilley, D.G.,
1997
Optimising Cooling System Performance Using Computer Simulation,
Vehicle Thermal Management Systems 3,
SAE 971802,
219-230

Singh, V.
2001
Private Correspondence

Smith, W.S.,
1993
In Vehicle Cooling Module Performance Prediction - PC Program Features,
Vehicle Thermal Management Systems 1,
49-56

Stevens, S.P., Bancroft, T.G.; Sapsford, S.M.,
1999
Improving The Effectiveness Of Underhood Airflow Prediction,
Proceedings of the Institution of Mechanical Engineers
IMechE C543/058/99,

Taniguchi, N., Kobayashi, T.,
1991
Numerical Simulation For The Flow Around A Car-Like Bluff Body,
Proceedings of the 6th International Pacific Conference On Automotive Engineering,
SAE 912575,
1053-1060

Torossian, P., Lanphear, D.,
1990
EEC-IV Module Thermal Analysis Program,
Proceedings of the Society of Automotive Engineers
SAE 901719,

Williams, J.E., Hackett, J.E.; Oler, J.W.; Hammer, L.,
1991
Water Flow Simulation Of Automotive Underhood Airflow Phenomena,
Society of Automotive Engineers Special Publication 855: Aerodynamics Recent Progress,
SAE 910307,
13-37

Winnard, D., Venkateswaran, G.; Barry, R. E.,
1995
Underhood Thermal Management By Controlling Air Flow,
Proceedings of the Society of Automotive Engineers
SAE 951013,

Zhao, H., Collings, N.; Ma, T.,
1992
Warm-Up Characteristics Of Surface Temperatures In An I.C. Engine Measured By Thermal Imaging Technique,
Society of Automotive Engineers Publication Pt46: Vehicle Thermal Management,
SAE 920187,
31-41

FLUENT Documentation

- Fluent 5 Manual
- Fluent 6 Manual
- Gambit 2 Manual
- Fluent Teaching Materials

Further Reading

(No author credited)
Full Vehicle Simulations Using Fluent/UNS
Fluent Newsletter Spring 97

(No author credited)
On The Road with the Opel CFD Group
Fluent Newsletter Spring 01

Alkidas, A
1993
Bibliography,
Society of Automotive Engineers Special Publications Pt-46 Vehicle Thermal Management,
421-429

Ap, N.S.,
1999
A Simple Engine Cooling System Simulation Model ,
Proceedings of the Society of Automotive Engineers
SAE Paper 1999-01-0237

Bajaj,C.L, Coyle, E.J.; Lin, K.,
1996
Surface And 3D Triangular Meshes From Planar Cross Sections,
Proceedings of 5th International Meshing Roundtable,

Cai, X., Wang, G.; Cheng z.,
2001,
Environment Study of Automotive Electronics Module,
Chinese Journal of Mechanical Engineering,

Chang, X., Chiang, E.C.; Johnson, J.H.; Yang, S.L.,
1991
The Dimensionless Correlation Of Airflow For Vehicle Engine Cooling Systems,
Society of Automotive Engineers Special Publication Pt-46 Vehicle Thermal Management
301-317

Cogotti, A., Berneburg, H.,
1991
Engine Compartment Airflow Investigations Using A Laser-Doppler-Velocimeter,
Society of Automotive Engineers Special Publication Vehicle Aerodynamics Recent Progress Sp855
SAB 910308
33-49

Damodaran, V., Kaushik, S.,
2000
Simulation To Identify And Resolve Underhood/Underbody Vehical Thermal Issues,
Fluent News Article Ja118,
1-4

El-Awar, N.Y., Geer, D.J.; Krellner, T.J.; Straub, P.J.,
1999
Automotive Temperature Sensing,

El-Bourini, R., Chen, S.,
1993
Engine Cooling Module Development Using Air Flow Management Techniques,
Vehicle Thermal Management Systems 1
SAE 931115,
379-387

Free, J.A., Russel, R.; Louie, J..
1995
Recent Advances in Thermal/Flow Simulation: Integrating Thermal Analysis into the Mechanical Design Process,
Institution of Electrical and Electronic Engineers 11th Semi-Therm

Ghani, S.A.A.A, Aroussi, A.; Rice, E.,
1999
An Investigation Into Water Ingress Through Car HVAC System,
Vehicle Thermal Management Systems 4,
IMechE C543/005/99,

Grun, N.,
1996
Simulating External Aerodynamics With Carflow,
Society of Automotive Engineers Special Publication 1145: Vehicle Aerodynamics,
SAE 960679
91-108

Habchi, S. D., Ho, S.Y; Elder, J.; Singh. S,
1994
Airflow and Thermal Analysis of Underhood Engine Enclosures,
Institution of Electrical and Electronic Engineers 12th Semi-Therm
SAE 940316

Holmes, R.T.,
1993
Progress In Automated Calorimetry - The Development Of Equipment And Methods For Complex Automated Calorimetry,
Vehicle Thermal Management Systems1,
649-657

Ishikawa, T., Shiozawa, H.; Oshima M.; Ono, K.,
1999
Development Of Techniques For Identifying The Factors Determining The Temperatures Of Engine Compartment Components And For Predicting Their Temperatures,
Vehicle Thermal Management Systems 4,
IMechE C543/073/99,

Jasak, H., Et Al.(11),
1999
Rapid CFD Simulation Of Internal Combustion Engines,
Proceedings of the Society of Automotive Engineers
SAE-1999-01-1185,

Khartabil, H.F., Christensen, R.N.,
1993
An Experimental Investigation Of Factors That Affect The Accuracy Of Heat Transfer Resistances Obtained From Heat Exchanger Data,
Proceedings of the Society of Automotive Engineers
SAE 931127,
471-476

Lyu, M., Ku, Y.,
1996
Numerical And Experimental Study Of Three-Dimensional Flow In Engine Room,
Proceedings of the Society of Automotive Engineers
SAE 960270,
33-40

Martin, D., El-Bourini, R.,
1991
Engine Compartment Air Management For Engine Cooling And Air Conditioning System Performance,
Proceedings of the Society of Automotive Engineers
SAE 911933,

Mathur, S.R., Lim, C.K.; Nair, R.,
2000
Development Of Finite Volume Shell Conduction Model For Complex Geometries,
American Society of Mechanical Engineers International Mechanical Engineering Congress & Exposition,

Matsushima,Y., Takeuchi, T.;Kohri,I,
2000
Prediction Method Of Engine Compartment Air Flow Using CFD Analysis,
Japanese Society of Automotive Engineers Review 21
JSAE200004043,
197-203

Murthy, S.S., Joshi,Y.K.; Adams,V.H.;Ramakrishna,K.,
1999
Integrated Thermal Analysis Of An Automotive Electronic System, ,
EEP Vol26-1 Advances In Electronic Packaging,
979-985

Park, K.S., Lee,D.Y.; Kauh,S.; Ro,S.T.; Kim,E.S.,
1991
System Development For The Design Of Gasoline Engine ECU,
Proceedings of the 6th International Pacific Conference On Automotive Engineering.
SAE 912457,
805-811

Parrino, M., Dentis, L.; Parola, A.,
1993
Heat Transfer Augmentation Of Mechanically Assembled Heat Exchanger By Internally Finned Tubes,
Vehicle Thermal Management Systems 1,
SAE 931135,
555-563

Shayler, P.J., Chick, J.P.; Hayden, D.J.; Yuen, H.C.R; Ma,T.,
1997
Progress On Modelling Engine Thermal Management Behaviour For VTMS Applications,
Vehicle Thermal Management Systems 3,
SAE 971852,
679-690

Sherwin, K., Barrow, H.,
1993
Determination Of The Heat Transfer Performance Of Finned Surfaces Using A Transient Lumped-Capacity Method,
Vehicle Thermal Management Systems 1,
549-553

Shibata, Y., Shimonosono, H.; Yamai, Y.,
1993
New Design Of Cooling System With Computer Simulation And Engine Compartment Simulator,
Vehicle Thermal Management Systems 1,
SAE 931075,
57-66

Srinivasan, K., Yan,J.Y.;Sun,R.L.,Gleason,M.E.,
2000
Rapid Simulation Methodology For Under-Hood Aero/Thermal Management,
International Journal of Vehicle Design Vol 23 (Nos. 1&2)
109-123

Trauger, P.E.,
1993
Use Of Infrared Imaging Technology In Heat Exchanger Development And Evaluation,
Vehicle Thermal Management Systems 1,
625-631

Ueda, M., Nishigami, T.; Suzuki, K.,
1995
Development Of Simulation Method On Automatic Transmission Thermal Management,
Vehicle Thermal Management Systems 2,
IMechE C496/029/95,
323-327

Williams, J.E., Vemaganti, G.,
1998
CFD Quality - A Calibration Study For Front-End Cooling Airflow,
Proceedings of the Society of Automotive Engineers
SAE 980039,
133-142

Willoughby, D.A, Williams, J.; Carroll, G.W.; Sun,R.L.; Maxwell,T.T,
1985
A Quasi Three Dimensional Computational Procedure For Prediction Of Turbulent Flow Through The Front-End Of Vehicles,
Proceedings of the Society of Automotive Engineers International Congress and Exposition
SAE 850282

Willoughby, D.A, Carrol, G.W.; Greiner,C.M,
1996
A CFD Method With Cartesian Grids And Complex Geometries Defined By Cell Porosities,
Proceedings of the American Society of Mechanical Engineers Congress and Exposition : Automotive Applications of CFD Industry

Online Articles

AUTOGAS
(No author credited)
Technology To Anticipate Future Stringent Emission Standards
http://www.autogas.nl/autocom/Techref.htm

CRYPTON TECHNOLOGY
Anon
On Board Diagnostics
http://www.cryptontechnology.com/eodb.htm

CYCLONE
Krus,H.W.,
1998
An Evaluation Of The Simulated Flow Through The Engine Cooling System Of A Truck,
Cyclone Fluid Dynamics: Engine compartment
http://www.cyclone.nl/art/artengi.htm

DUPONT
Anon
Ceramic Solutions for Automotive
http://www.dupont.com/mcm/car-automotive.html

MIRA / ATALINK
Adams.R, Jones.M, Fletcher D.,
Virtual Instrumentation – A versatile Approach to Data Acquisition in Automotive Thermofluids
http://www.atalink.co.uk/mira2000/html/p116

(No author credited)
Linking Different Computer Simulations – A First Step Towards Considering Interacting Systems
http://www.atalink.co.uk/mira2000/html/p108

Bocas, S.,
The Use of CFD in Electronics Systems Design Within the Automotive Industry
http://www.atalink.co.uk/mira2000/html/p103

Sanatian, R.,
A Brief History of CFD in the Automotive Industry
http://www.atalink.co.uk/mira2000/html/p113

St.John, C.,
Simulation by Anyone, of Anything, Anywhere
http://www.atalink.co.uk/mira2000/html/p113

UNIVERSITY OF COVENTRY ZEFREDO PROJECT
(No author credited)
Study of Zero Failure Electrical Technology
http://www.coventry.ac.uk/zefredo/apfin.htm

Appendix 2. Initial Sketches of Chassis

The design for the model used in the experiment was derived from Gordon Bisset's Honours year final project (2002). The original sketches from which are reproduced here. All dimensions are in mm.

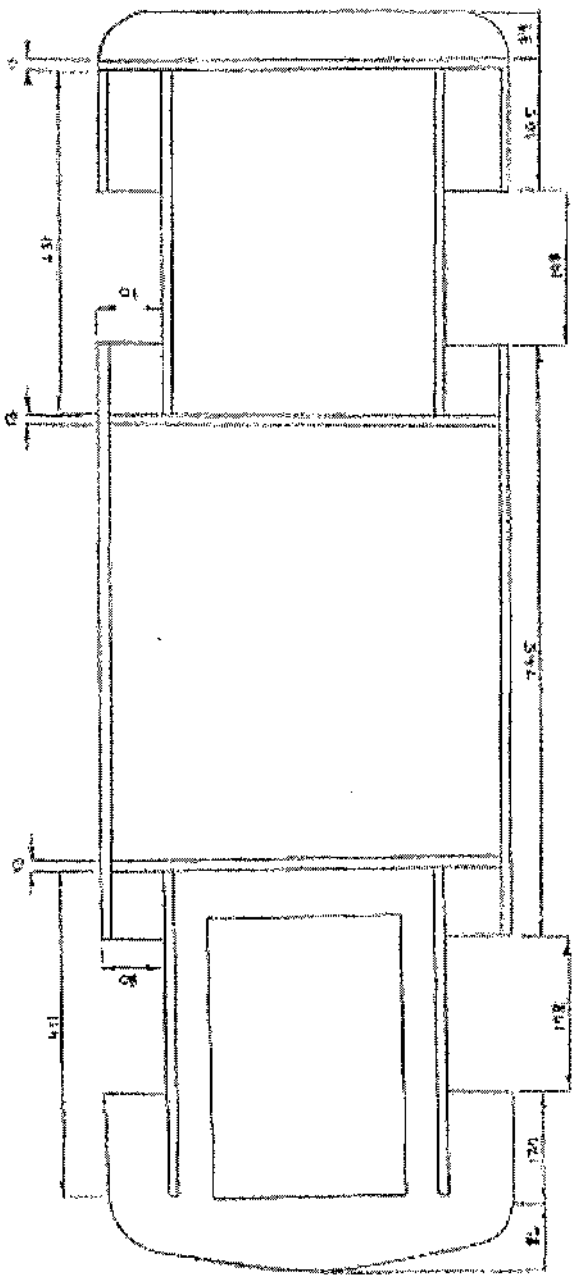

Figure Appendix 2-1 Plan View of Chassis

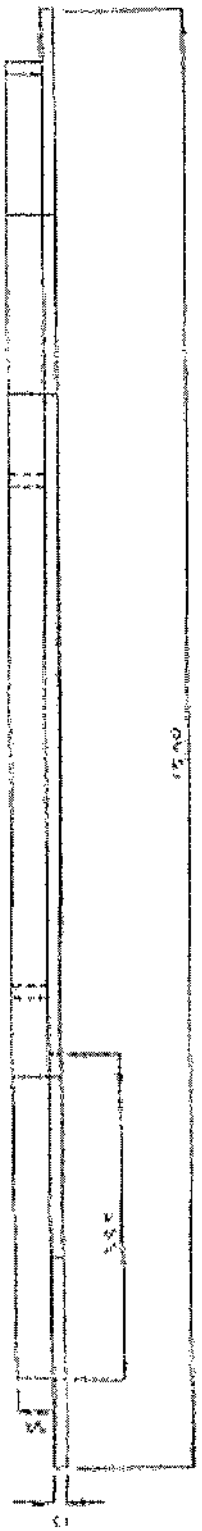

Figure Appendix 2-2 Side View of Chassis

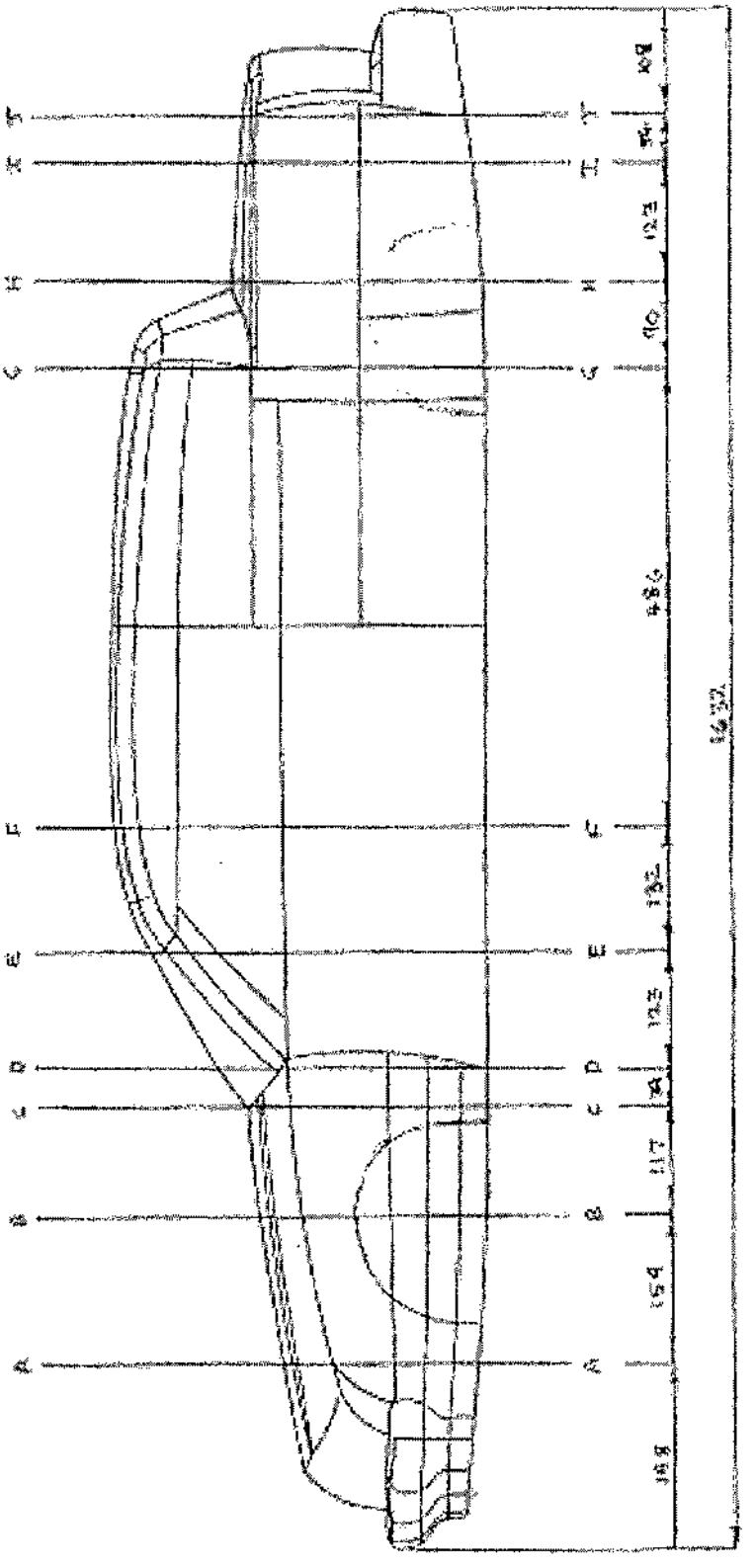

Figure Appendix 2 3 Sections Through Car Model

Figure Appendix 2-4 Front View of Chassis

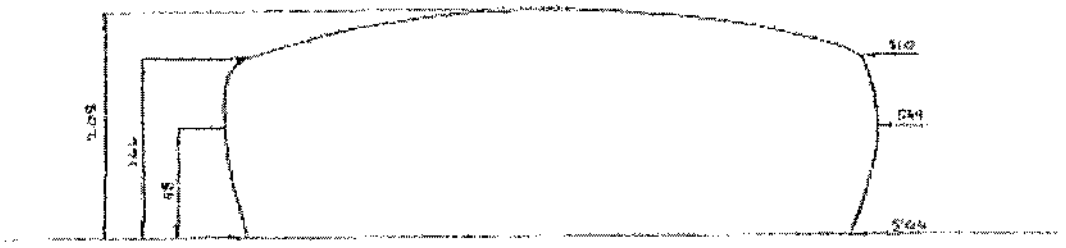

Figure Appendix 2-5 Section A-A

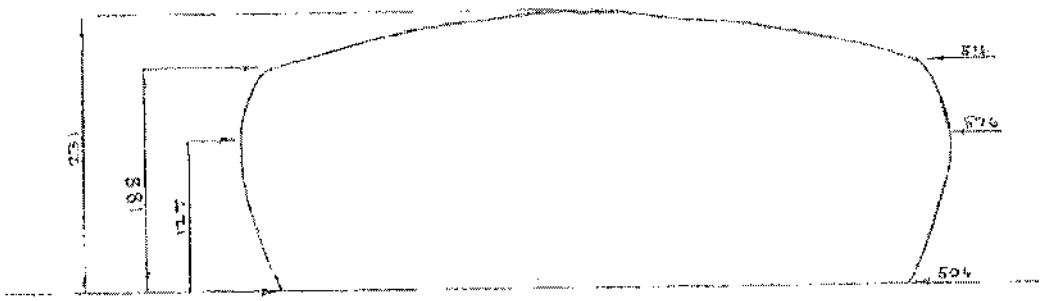

Figure Appendix 2-6 Section B-B

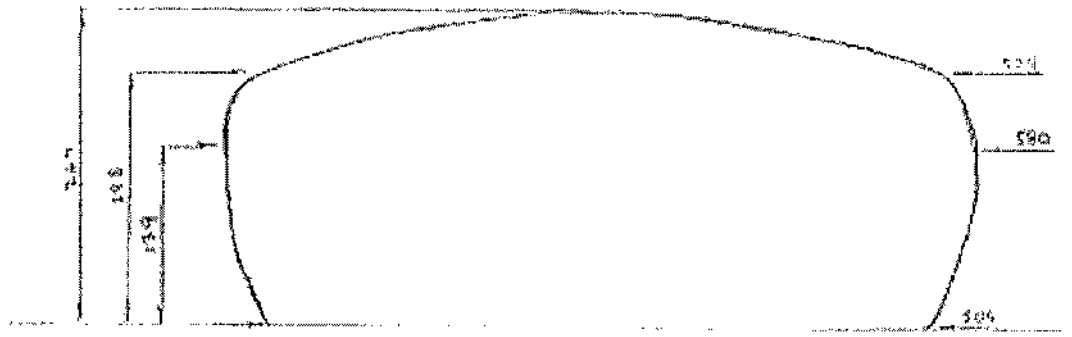

Figure Appendix 2-7 Section C-C

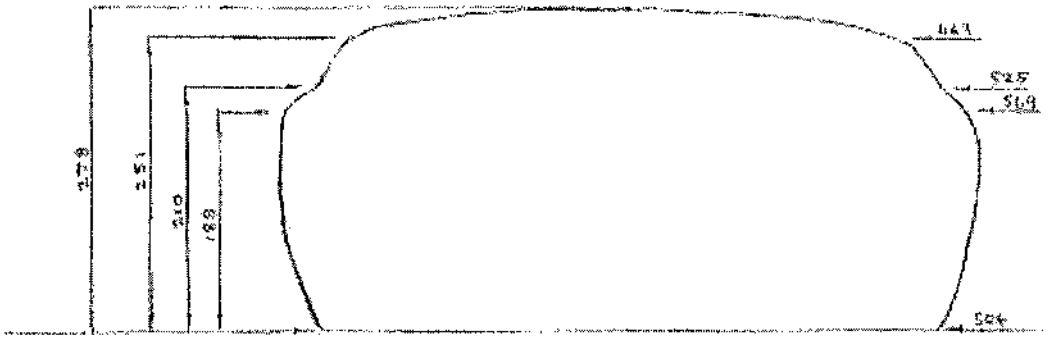

Figure Appendix 2-8 Section D-D

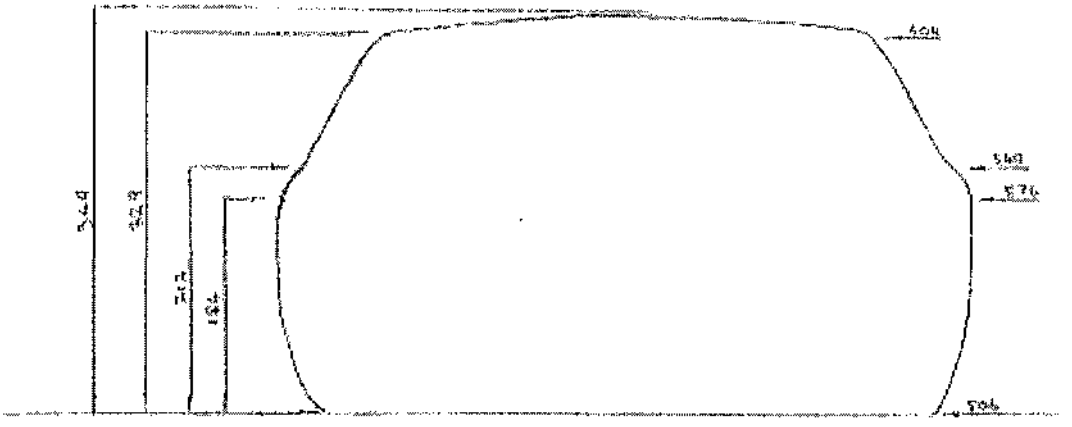

Figure Appendix 2-9 Section E-E

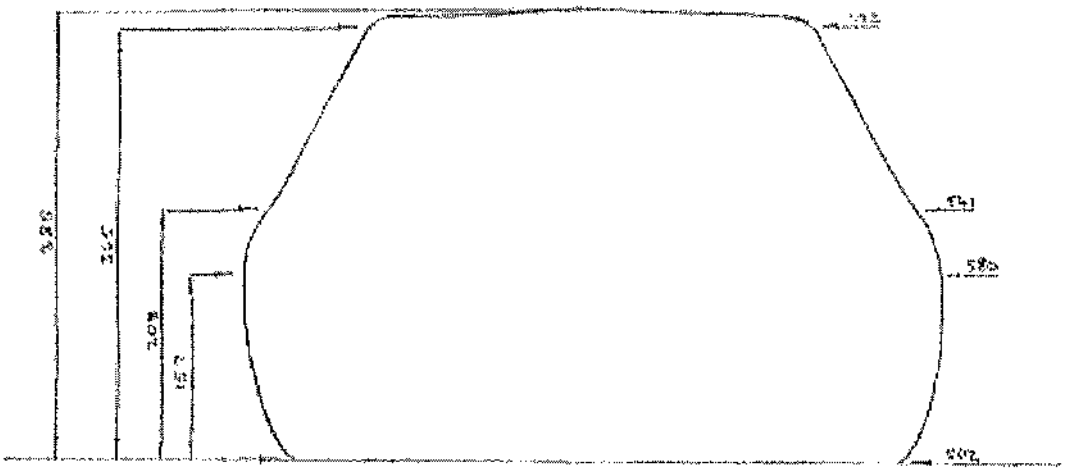

Figure Appendix 2-10 Section F-F

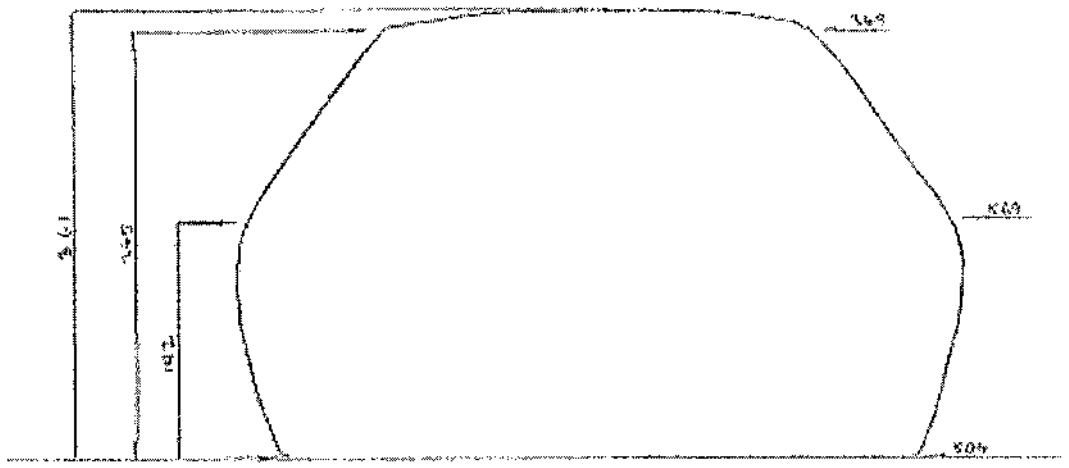

Figure Appendix 2-11 Section G-G

Figure Appendix 2-12 Section H-H

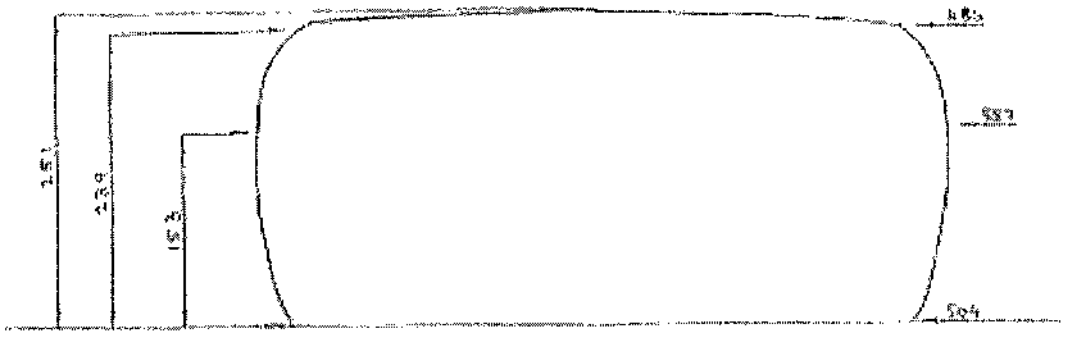

Figure Appendix 2-13 Section I-I

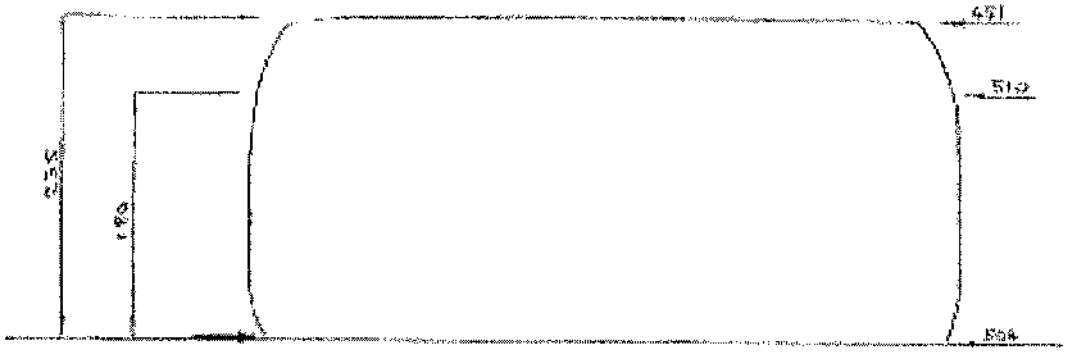

Figure Appendix 2-14 Section J-J

Appendix 3. CAD Drawings

The engine compartment referred to in the text was designed to abut onto the chassis created for carry the car body as used in the work of both Bissett (2002) and Sheng (2003). The original drawings are for the car body are shown in this appendix. The drawings herein concentrate specifically on the engine compartment.

Note that the rake on the downpipes as shown in figures 3-8 to 3-10 was reduced in the final model due to difficulties in meshing and also the possibility of fractures to the element.

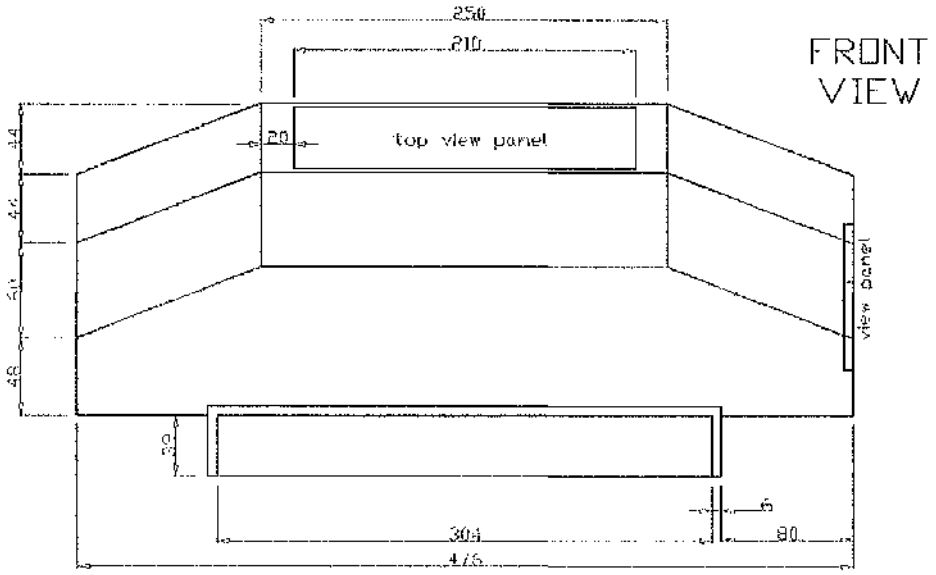

Figure Appendix 3-1 Front Elevation of Engine Compartment

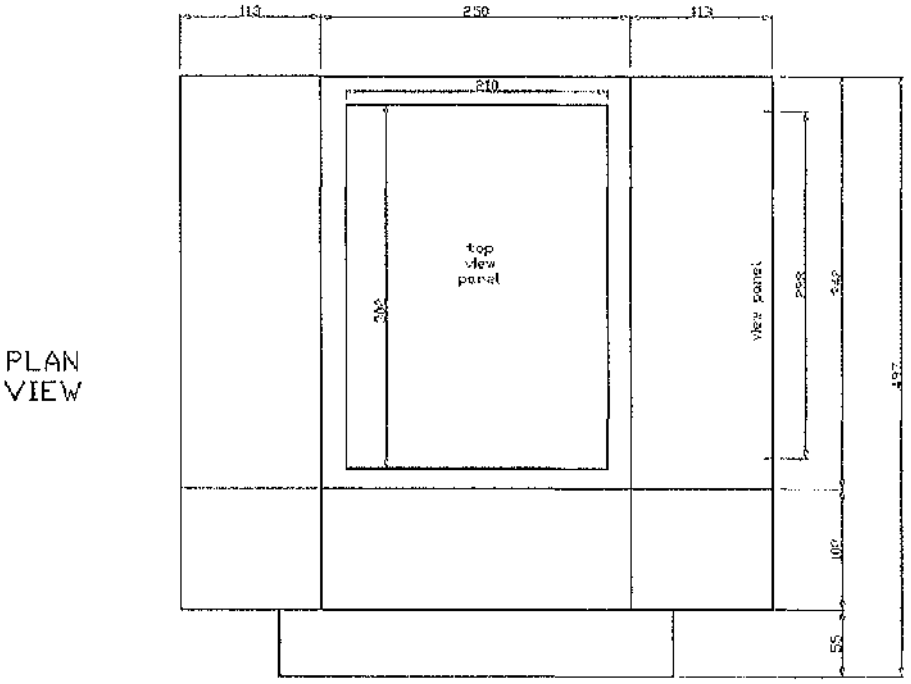

Figure Appendix 3-2 PlanView of Engine Compartment

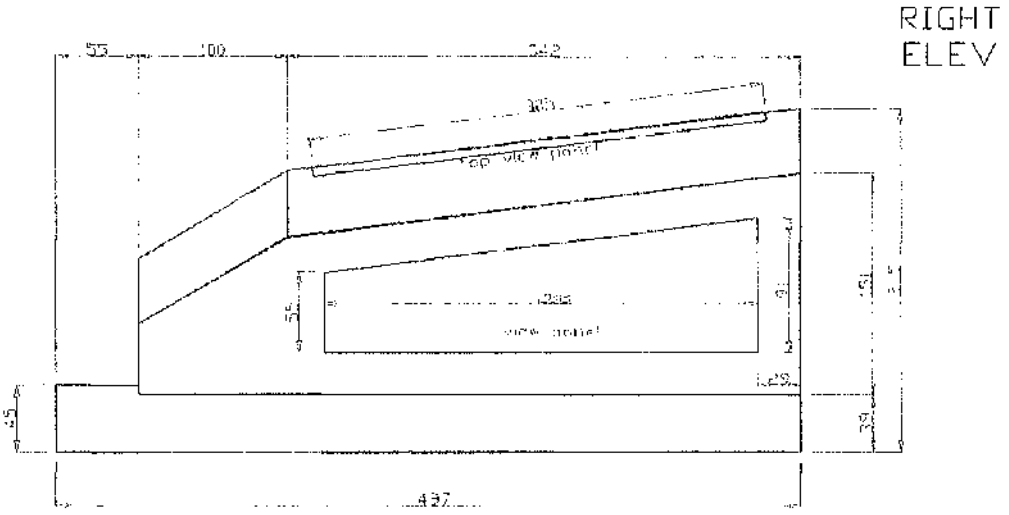

Figure Appendix 3 3 Right Elevation of Engine Compartment

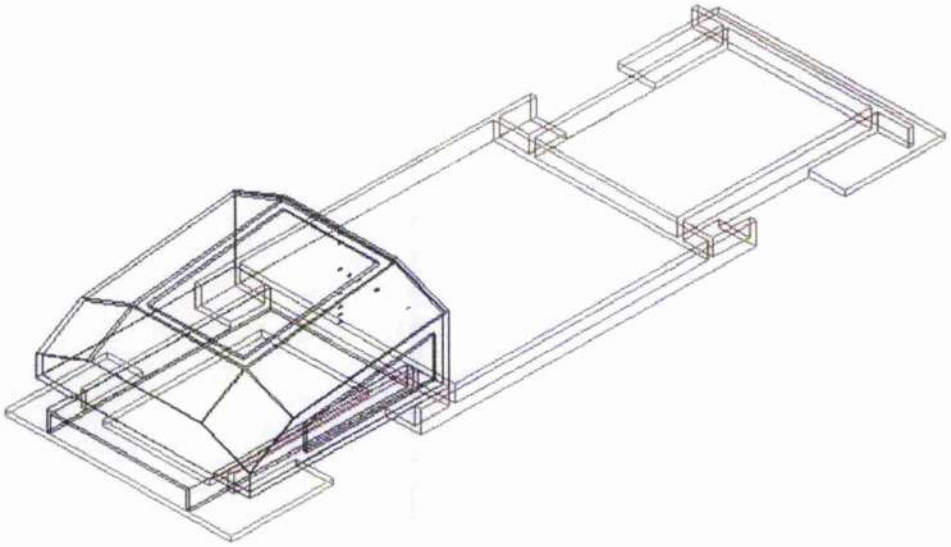

Figure Appendix 3-4 Wireframe CAD Model of Engine Compartment on Chassis (SE View)

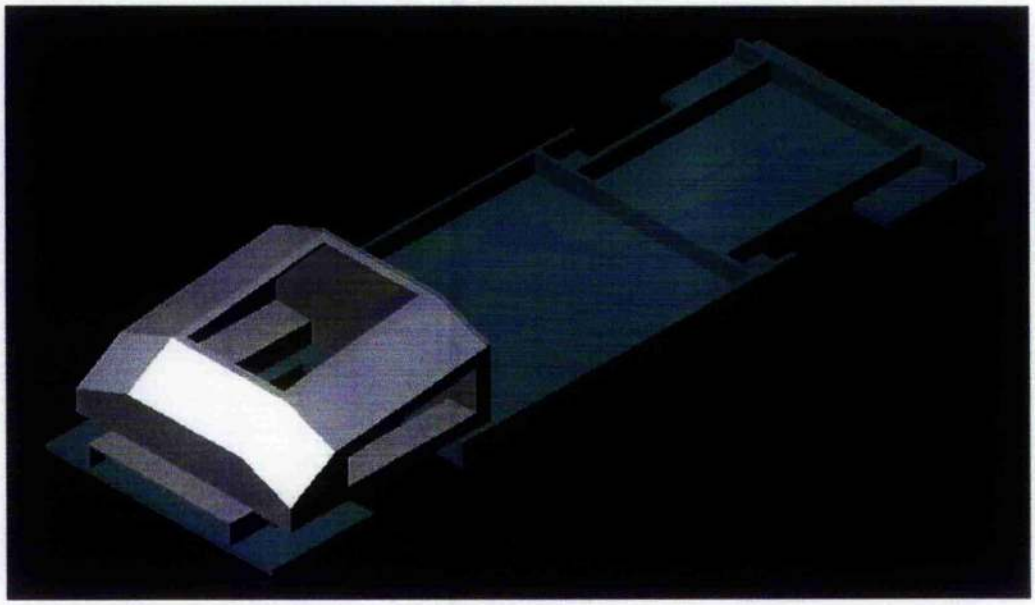

Figure Appendix 3-5 Shaded CAD Model of Engine Compartment on Chassis (SE View)

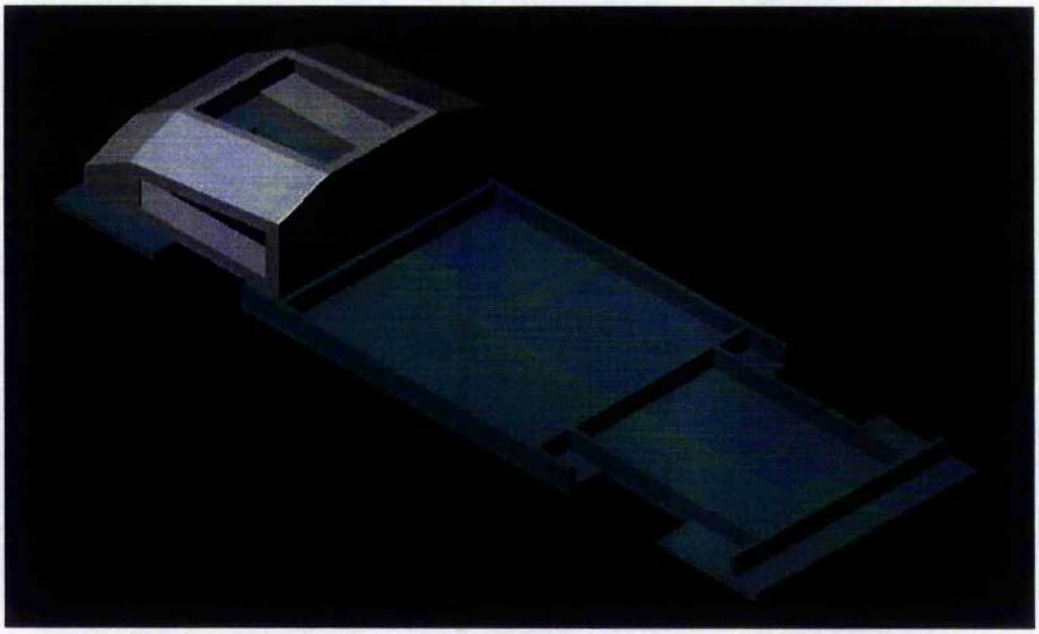

Figure Appendix 3-6 Shaded CAD Model of Engine Compartment on Chassis (NE View)

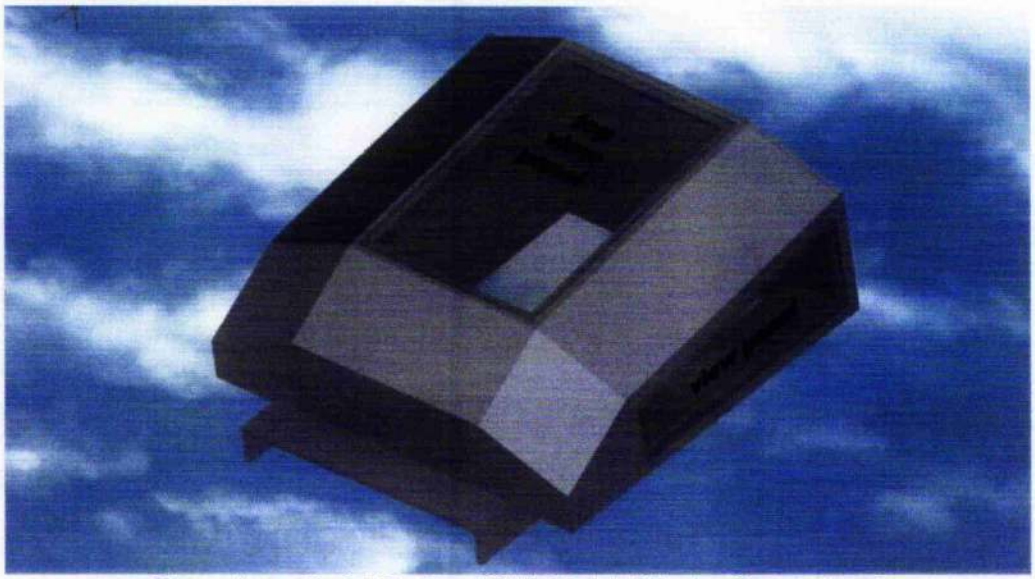

Figure Appendix 3-7 Rendered CAD Model of Engine Compartment

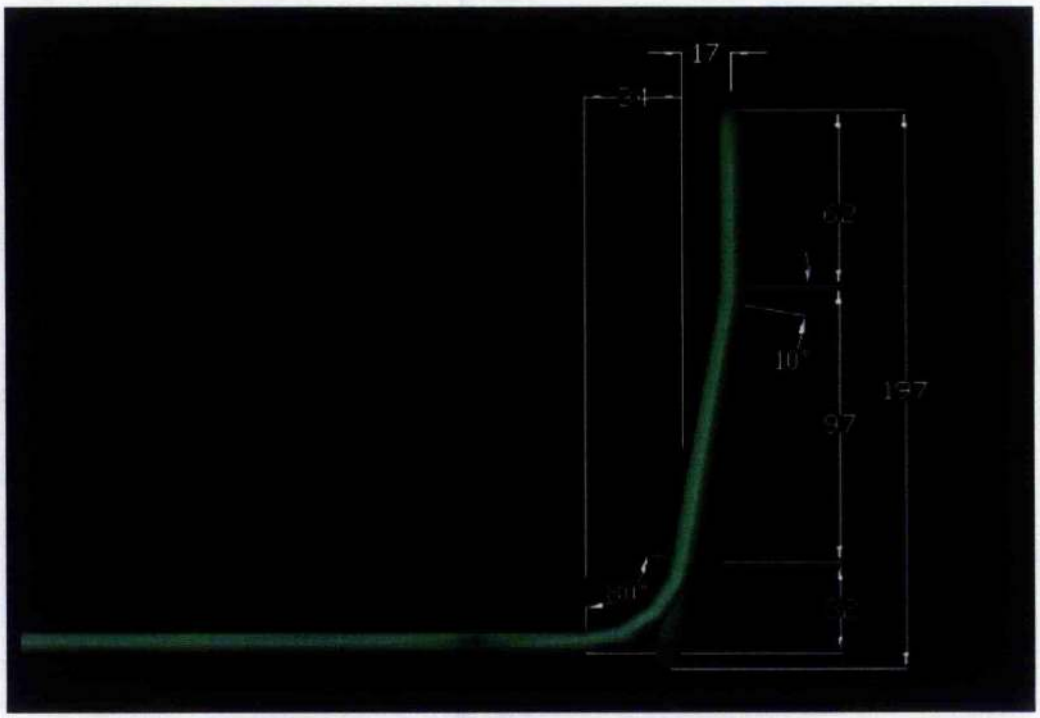

Figure Appendix 3-8 Downpipe (element) dimensions

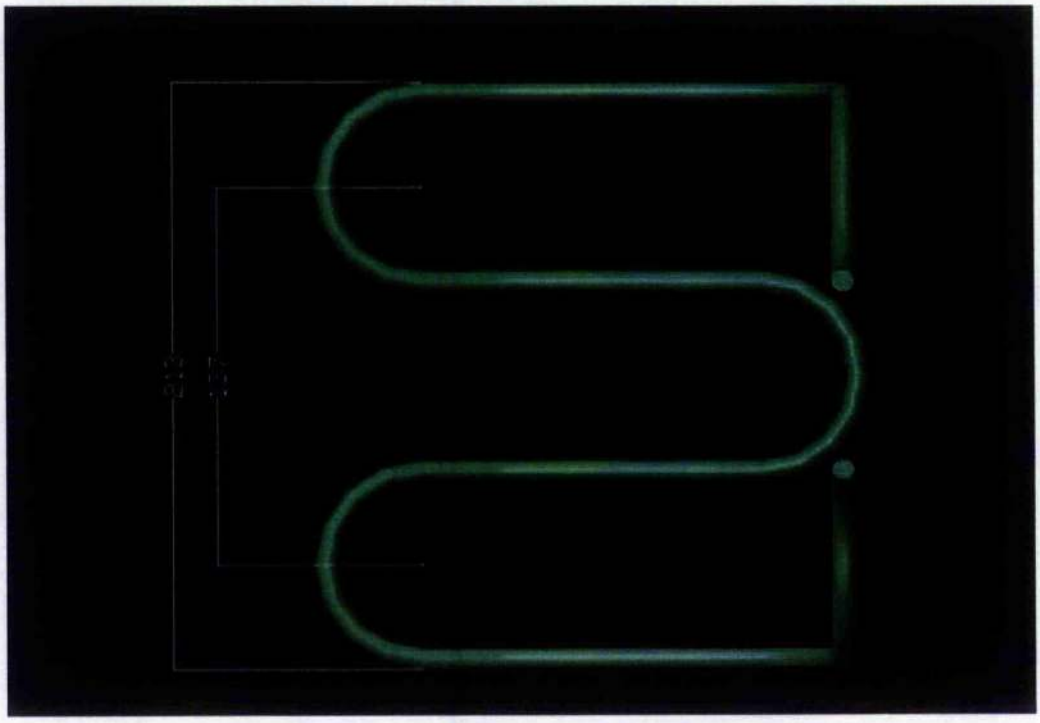

Figure Appendix 3-9 Downpipe (element) Dimensions

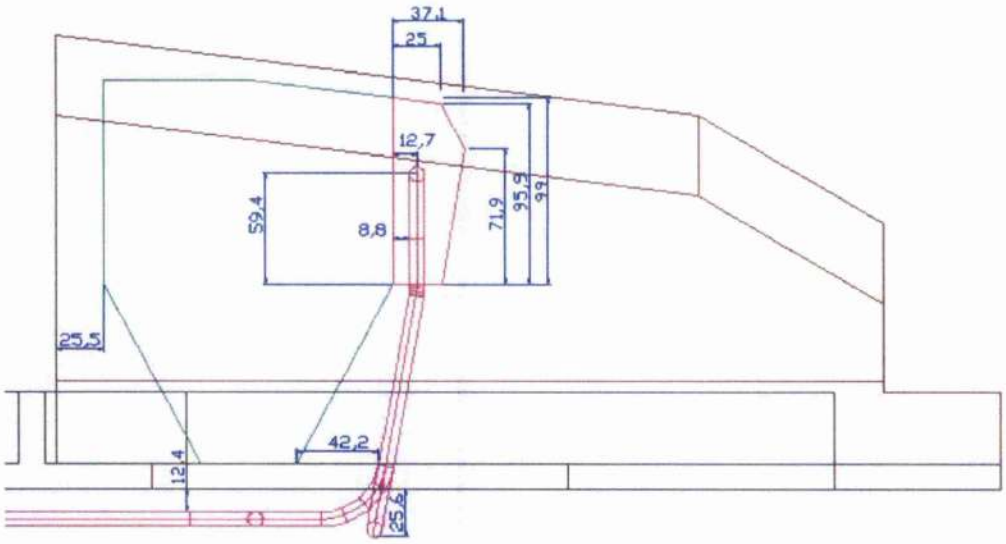

Figure Appendix 3-10 Downpipe and Engine Block within Compartment

Figure Appendix 3-11 Rendered CAD Model of Downpipes *in situ*

Appendix 4. Thermistor and Themocouple Data Sheets

MATERIAL TYPE: G

AVAILABLE PRODUCTS:

HM, C100, EC95, DC95, MC65, MF65, SC30, SC50

Data for material type : G

Temp Range (°C)	Ratio	Beta
0 to 50	10.48	4147
0 to 70	22.65	4178
25 to 50	2.97	4201
25 to 85	10.91	4252
25 to 100	17.80	4271
25 to 125	37.37	4298
37.8 to 104.4	11.48	4299

To calculate Rt/R25 at temperatures other than those listed in the table, use the following equation:

$Rt/R25 = \exp(A + B/T + C/T^2 + D/T^3)$

where T = temperature in K

where K = °C + 273.15

Temp Range (°C)	A	B	C	D
-50 to 0	-1.5617990E+01	5.0890089E+03	-9.8695494E+04	-7.7908099E+06
0 to 50	-1.5573763E+01	5.0310600E+03	-8.5956132E+04	-8.8322667E+06
50 to 100	-1.5358271E+01	4.7986321E+03	-3.1012401E+03	-1.8614904E+07
100 to 150	-1.8012530E+01	7.9402031E+03	-1.2428041E+06	1.4446457E+08

To calculate the actual thermistor temperature as a function of the thermistor resistance, use the following equation:

$1/T = a + b(\ln R/R25) + c(\ln R/R25)^2 + d(\ln R/R25)^3$

Rt/R25 range	a	b	c	d
85.730 to 3.5223	3.3537960E-03	2.4096581E-04	2.2453225E-06	1.1817106E-07
3.5223 to 0.33620	3.3540142E-03	2.4060636E-04	2.4402966E-06	8.0079806E-08
0.33620 to 0.05619	3.3541651E-03	2.4087966E-04	2.5742490E-06	8.8746970E-08
0.05619 to 0.01381	3.3357228E-03	2.2502940E-04	-1.9469544E-06	-2.4181662E-07

†The deviation resulting from the tolerance on the material constant, Beta. The deviation must be added to the resistance tolerance of the part as specified at 25°C.

Temperature (°C)	Rt/R25 nominal	Temp Coef (%/°C)	† Deviation (±%)
-50	85.73	7.50%	3.48%
-45	59.01	7.25%	3.27%
-40	41.54	7.01%	3.03%
-35	29.43	6.78%	2.77%
-30	21.09	6.56%	2.50%
-25	15.28	6.35%	2.23%
-20	11.18	6.15%	1.96%
-15	8.264	5.96%	1.70%
-10	6.162	5.77%	1.44%
-5	4.639	5.60%	1.19
0	3.522	5.43%	0.95%
5	2.697	5.26%	0.73%
10	2.081	5.11%	0.53%
15	1.618	4.96%	0.34%
20	1.268	4.82%	0.18%
25	1.000	4.68%	0.00%
30	0.7942	4.55%	0.14%
35	0.6348	4.42%	0.26%
40	0.5106	4.30%	0.37%
45	0.4131	4.18%	0.46%
50	0.3362	4.07%	0.54%
55	0.2751	3.96%	0.60%
60	0.2263	3.86%	0.65%
65	0.1871	3.75%	0.68%
70	0.1555	3.66%	0.70%
75	0.1298	3.56%	0.71%
80	0.1089	3.48%	0.71%
85	0.09170	3.39%	0.69%
90	0.07757	3.31%	0.66%
95	0.06589	3.23%	0.62%
100	0.05619	3.15%	0.57%
105	0.04810	3.07%	0.51
110	0.04133	3.00%	0.45%
115	0.03563	2.92%	0.39%
120	0.03083	2.87%	0.24%
125	0.02676	2.80%	0.15%
130	0.02330	2.73%	0.09%
135	0.02036	2.68%	0.05%
140	0.01784	2.61%	0.17%
145	0.01567	2.55%	0.26%
150	0.01381	2.50%	0.43%

Figure Appendix 4-1 Thermistor Data Sheet

Thermocouples

Data Sheet

General specification for RS thermocouple products

	Type J	Type K	Type N	Type T	Type R	Units
Minimum continuous temperature	-60	-200	-230	-200	-50	°C
Maximum continuous temperature	+850	+1300	+1300	+400	+1350	°C
Maximum spot reading	+1100	+1300	+1320	+500	+1400	°C

Tolerances (IEC 60584-3)

Accuracy - Class 2 (see note)		±2.5°C or 0.0075 x T	±2.5°C or 0.0075 x T	±2.5°C or 0.0075 x T	±1°C or 0.0075 x T	±1.5°C	°C
Temperature range - Class 2		-40 to +750	-40 to +1200	-40 to +1200	40 to +350	-40 to +1600	°C
BS specification number		4937 Part 4	4937 Part 4	4937 Part 8	4937 Part 5	4937 Part 2	
+ve arm		Iron	Nickel/Chromium	Nicrosil	Copper	13% Rhodium Platinum/Pt	
Composition	Cr	none	~10	14.2 ±0.2	unspecified		%
	Si	none	unspecified	1.4 ±0.2	unspecified		%
	Fe	100	unspecified	0.15 max	unspecified		%
	C	none	unspecified	0.05	unspecified		%
	Mg	none	unspecified	none	unspecified		%
	Ni	none	balance	balance	unspecified		%
	Cu	none	unspecified	none	balance		%
-ve arm		Nickel/Aluminum	Nickel/Aluminum	Nisil	Copper/Nickel	100% Platinum	
Composition	Cr	none	unspecified	0.02 max	unspecified		%
	Si	none	balance	4.4 ±0.2	unspecified		%
	Fe	0.3	unspecified	0.15 max	unspecified		%
	C	none	unspecified	0.05 max	unspecified		%
	Mg	none	unspecified	0.05 to 0.2	unspecified		%
	Ni	12	95	balance	40 to 45		%
	Cu	balance	unspecified	none	balance		%
	Mn	1.5	balance	none	unspecified		%
	Al	none	balance	none	unspecified		%

Colour codes BS 4937 pt.30, IEC (IEC 60584)

Thermocouple and extension wiring	+ve arm	black	green	pink	brown	orange	
	-ve arm	white	white	white	white	white	
	overall	black	green	pink	brown	orange	
Compensating cable and wiring	+ve arm	black	green	pink	brown	orange	
	-ve arm	white	white	white	white	white	
	overall	black	green	pink	brown	orange	

Note: T refers to measured temperature in °C

Figure Appendix 4-2 ThermocoupleData Sheet

Appendix 5. Drawings - Thermistor Placement

Thermistors were placed in areas of interest determined by initial results. Revised values were chosen for ease of manufacture.

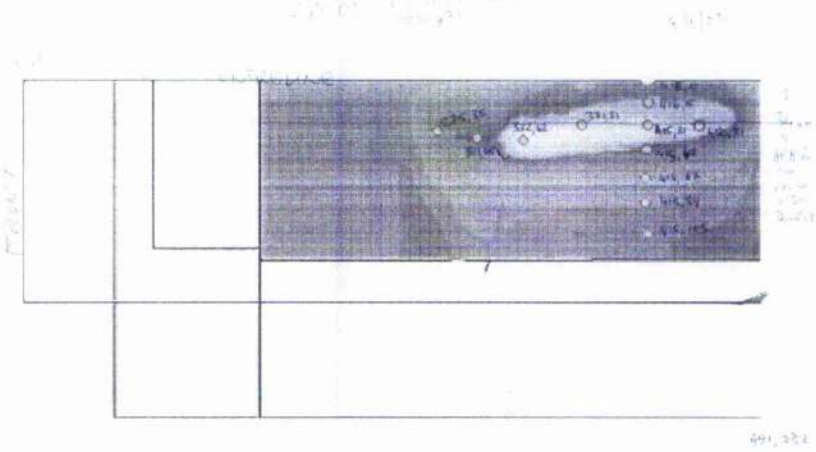

Figure Appendix 5-1 Original Sketch for Probe Positions in Top Panel

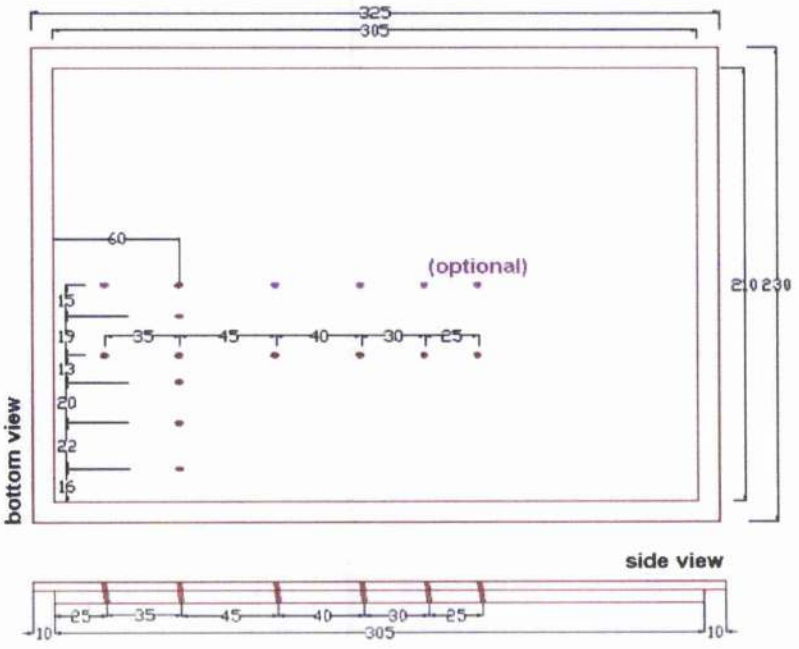

Figure Appendix 5-2 CAD Drawing for Revised Positions on Top Panel

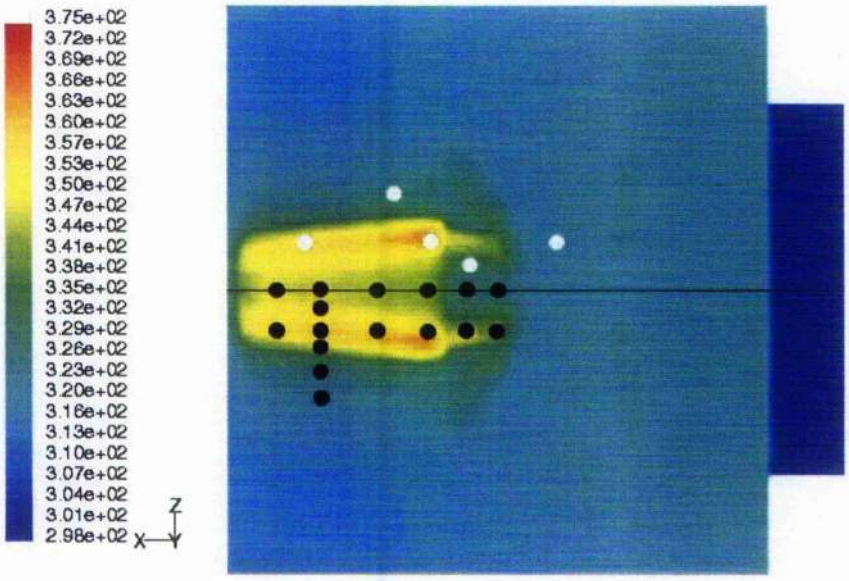

Figure Appendix 5-3 Comparison of Top Panel Original Positions with Revised Positions

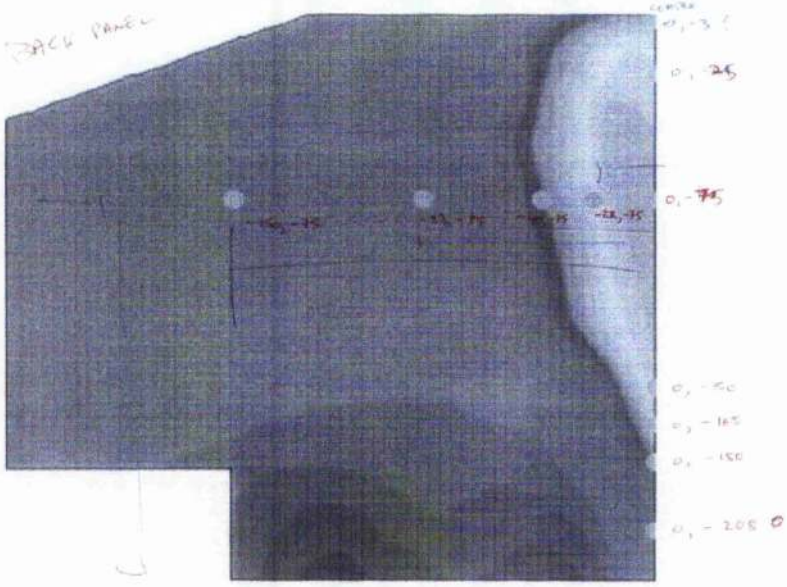

Figure Appendix 5-4 Original Sketch for Probe Positions on Rear Face

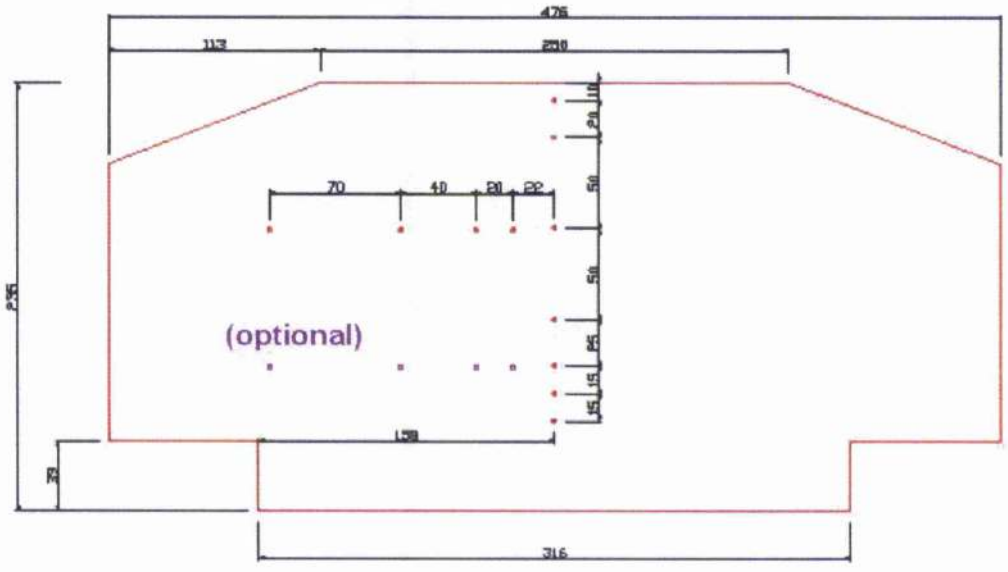

Figure Appendix 5-5 CAD Drawing for Revised Positions on Rear Face

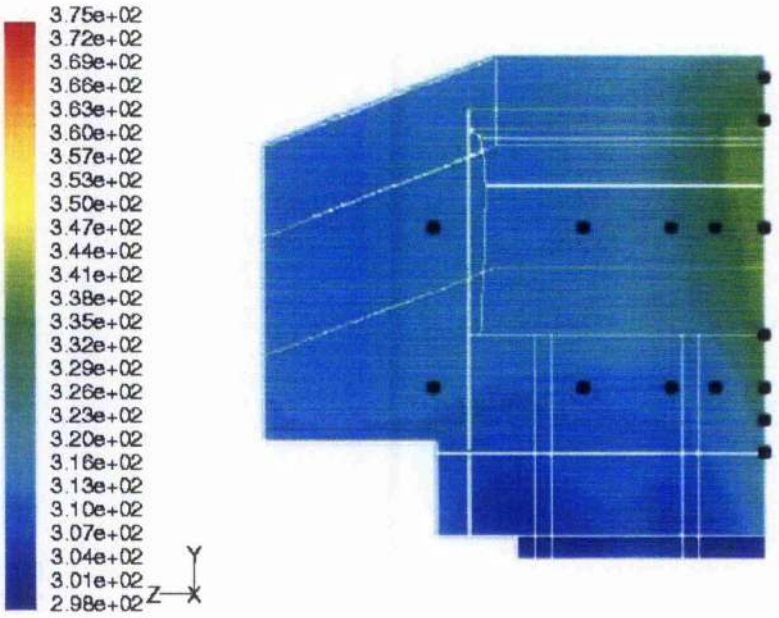

Figure Appendix 5-6 Rear Panel Revised Positions

Appendix 6. Data Acquisition

Data acquisition programs were written in Labview by the Aerospace Department's Research Technologist, Robert Gilmour. Figures 1 and 2 show the user interface for the two programs Datarun and Datasave. Datarun was used to verify the temperatures for the experiment and Datasave was used to capture sample data for analysis.

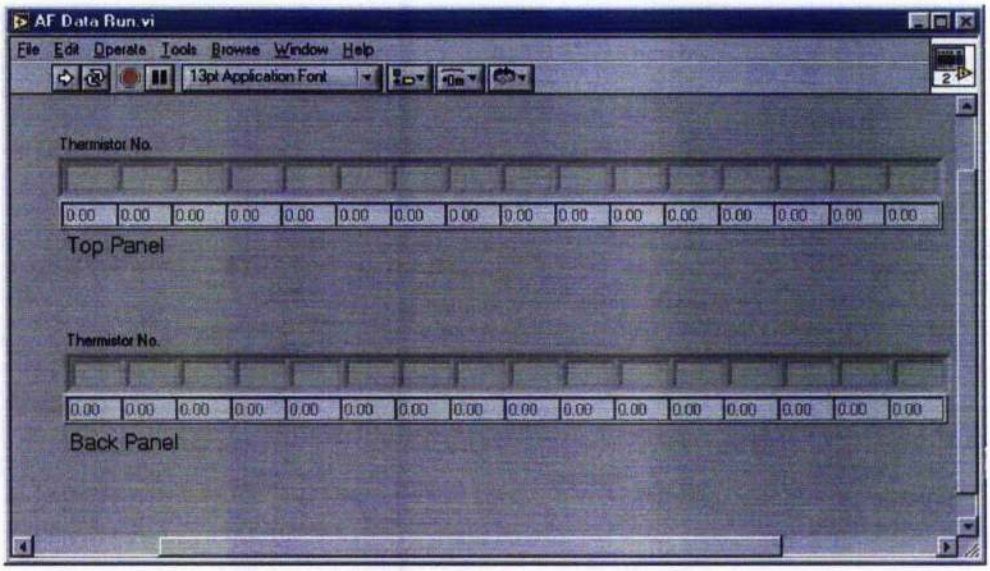

Figure Appendix 6-1 DataRun.vi User Interface

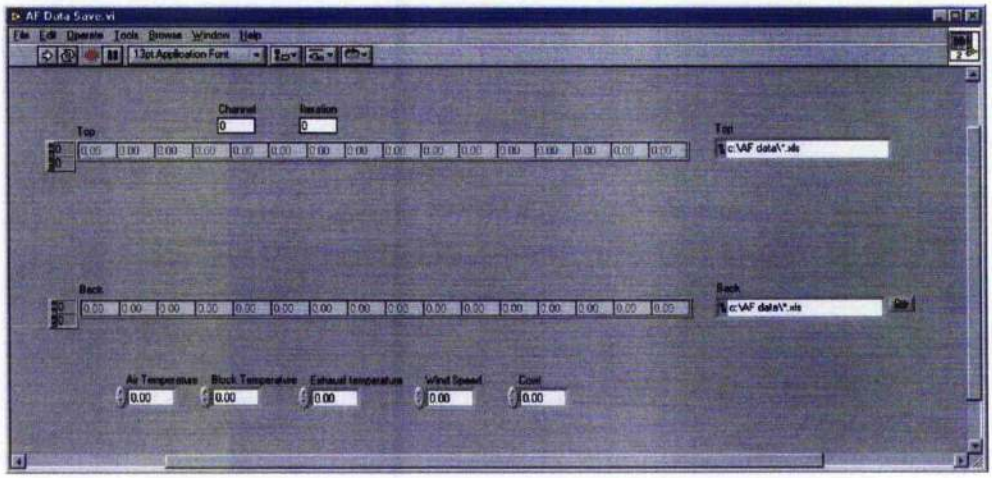

Figure Appendix 6-2 DataSave.vi User Interface

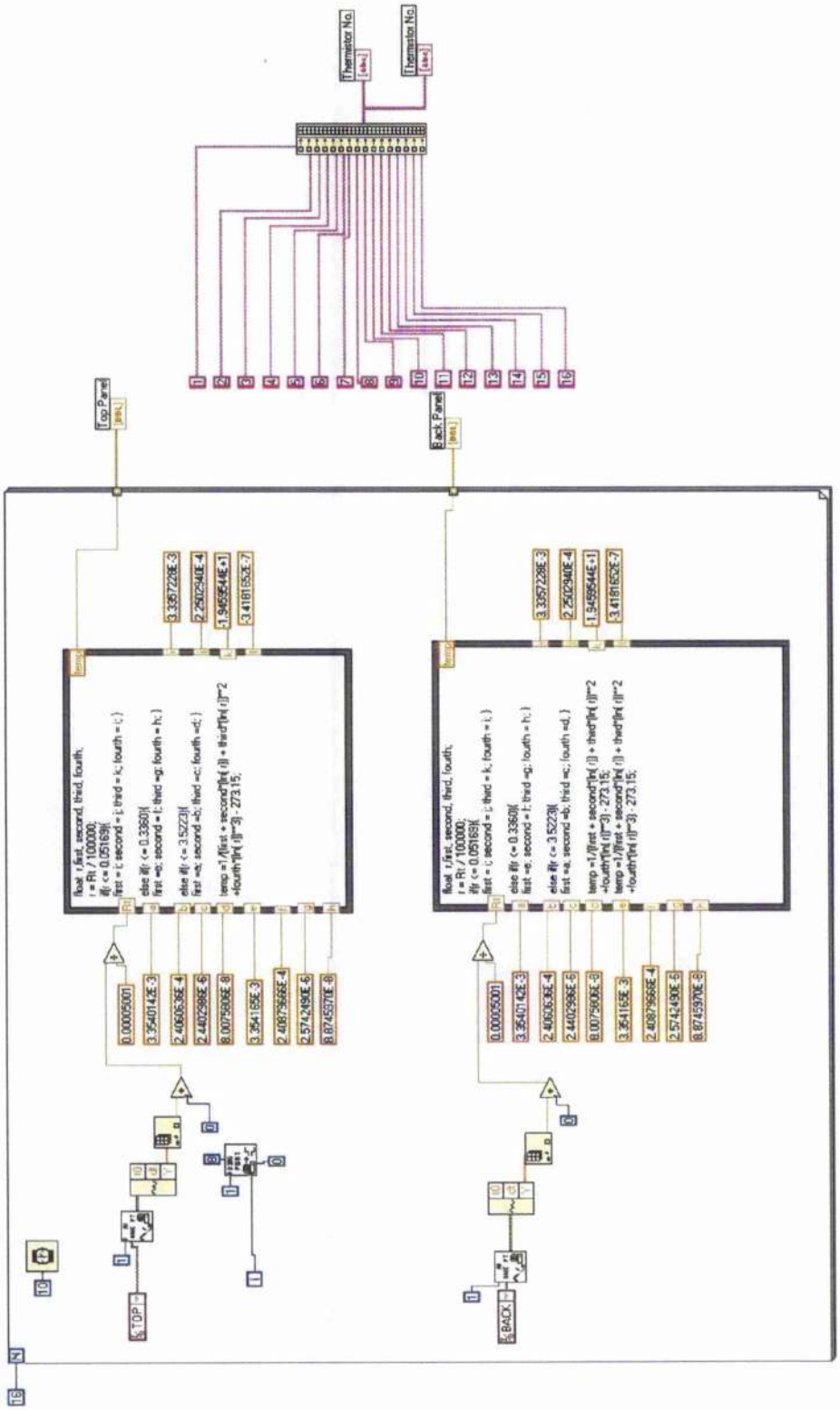

Figure Appendix 6-3 DataRun.vi Functional Schematic

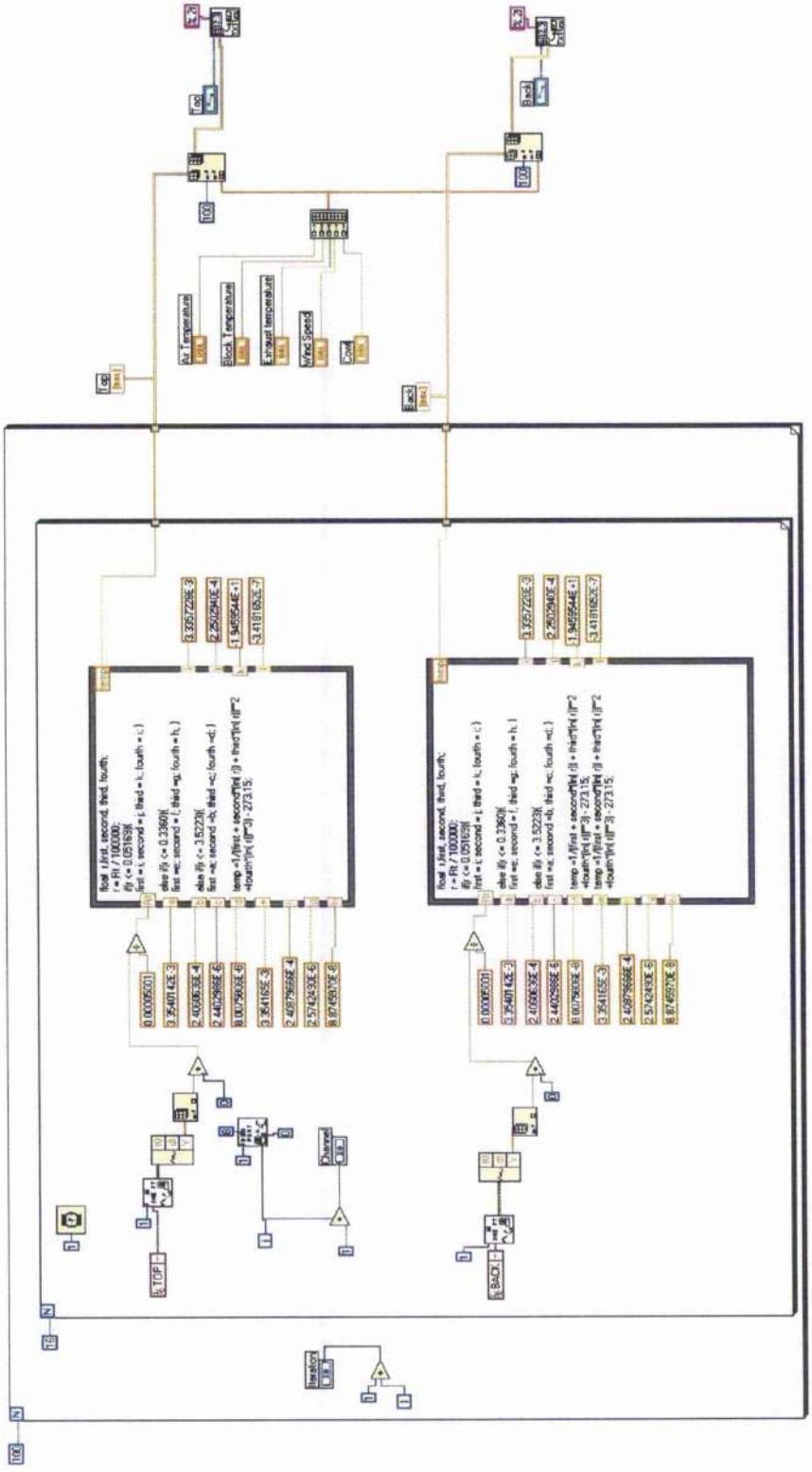

Figure Appendix 6-4 DataSave.vi Functional Schematic

Appendix 7. Fluent Setup

The typical parameters for the jobs carried out in this study were entered in the following manner

1. Solver selected. Segregated has lower computer overhead than coupled. Other parameters are default values.

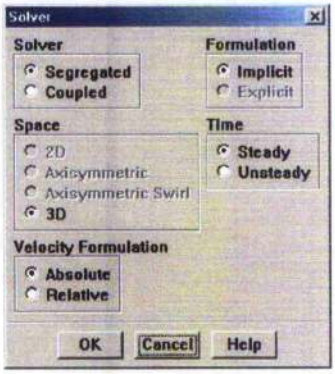

Figure Appendix 7-1

2. Viscous (turbulence) model selected. Standard k-epsilon model chosen as this is adequate for most industrial applications (FLUENT Training materials)

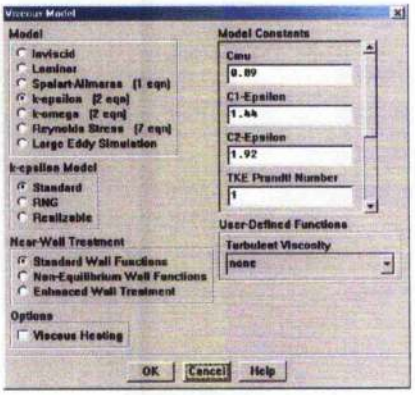

Figure Appendix 7-2

3. Energy equation enabled. Needed for simulations involving thermal solutions.

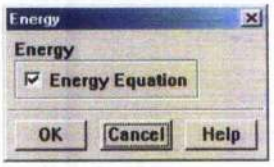

Figure Appendix 7-3

4. Radiation Model. In this case, the radiation model was turned off as the computer overhead for most models was too great for. This screen, reproduced from Fluent 6, shows S2S model is available. Future simulations should employ this model but the task of remeshing for the existing simulations would have been excessively time-consuming.

Figure Appendix 7-4

5. In this case solution has been computed from all zones and has a single velocity component. Other parameters have default values

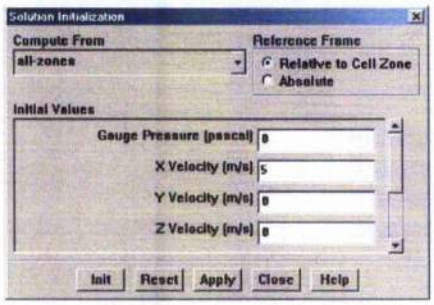

Figure Appendix 7-5

6. The case is ready to iterate. Here, only a single iteration has been set. This is so that case specific data can be saved for a job to be run in the background or overnight. This is achieved by creating a small script file which instructs Fluent to use data from one case file, iterate a number of times and save the results of the run in an updated file. Typically a value of around 400 iterations would be entered if a job was to be run overnight.

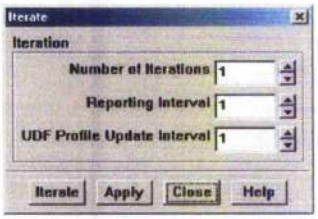

Figure Appendix 7-6

Appendix 8. Research Facilities

Details on the two wind tunnels referred to in the text are reproduced here from http://www.aero.gla.ac.uk/Research/LowSpeedAero/facilities.htm. This web location also provides details on additional departmental research facilities

A8.1. Argyll Wind Tunnel

Figure Appendix 8-1

The 2.65m * 2.04m 'Argyll' wind tunnel (Figure Appendix 8-1) is a closed-return wind tunnel with a maximum operating speed of 76 m/s.

Features include:

- Two interchangeable working sections.
- A 3.75m long by 1.9m wide moving ground that has been designed to operate at 60 m/s.
- A yawing capability of up to 10 degrees is included in the design.
- Rotary vortex generator for helicopter rotor wake simulation.
- Rig can be used for studies of tip vortex structure, interaction experiments and blade tip geometry effects.
- A mechanical six-component balance.

A8.2. Handley-Page Wind Tunnel

The 2.13m * 1.61m **'Handley-Page'** wind tunnel is a closed-return facility with a maximum operating speed of 60 m/s.

Features include:

- Three-strut hydraulic actuation system for dynamic testing of pitching wings and aircraft planforms
- Hydraulically actuated two dimensional dynamic stall testing rig. This rig can provide a wide range of motion types from high/low frequency, low amplitude to high/low frequency, high amplitude
- Helicopter main rotor blade vortex interaction test rig.